ABSTRACT

Title of Thesis: SHEAR STRESS RESPONSE AND BOND-BREAKING
                     UNDER MODERATE FREQUENCY SINUSOIDAL
                     TRANSLATIONAL SHEAR DEFORMATION OF
                     HETEROGENEOUS RAT CEREBRUM

                     Jenna Gipple, M.S. Mechanical Engineering, 2018

Directed By: Dr. Henry W. Haslach, Jr., Mechanical Engineering

Blast waves, which include sinusoidal shear waves, may cause mild traumatic brain injury (mTBI) in brain tissue. The experiments model repeated insults separated by a period of rest via application of translational sinusoidal shear waves to hydrated, heterogeneous rat cerebrum at six deformation frequencies between 25 Hz and 125 Hz and displacement amplitudes of 10% or 25%. Each deformation frequency produces transient and apparent steady shear stress states that frequency analysis describes by harmonic wavelet and Fourier frequency components. Sinusoidal shear deformation waves induce bond and synapse breaking at as little as 10% displacement amplitude. Even in vitro, some bonds reform during rest. An increase in deformation frequency increases drag force between the ECF and solid matter, probably due to increased fluid acceleration and inertia. Imaging and histology do not clearly detect mild damage due to bond breaking that underlies mTBI, which the analysis of the shear stress response captures.

SHEAR STRESS RESPONSE AND BOND-BREAKING UNDER MODERATE FREQUENCY SINUSOIDAL TRANSLATIONAL SHEAR DEFORMATION OF HETEROGENEOUS RAT CEREBRUM

By

Jenna Gipple

Thesis submitted to the Faculty of the Graduate School of the
University of Maryland, College Park in partial fulfillment
of the requirements for the degree of
Masters of Science
2018

Advisory Committee:
Dr. Henry W. Haslach, Jr., Chair
Dr. Balakumar Balachandran
Dr. Amr Baz

Contents

List of Tables

List of Figures

1 Introduction

Mild traumatic brain injuries (mTBI) can result from impact, acceleration, and high frequency blast waves. By definition, TBI is considered mild if medical imaging results are normal, loss of consciousness is under 30 minutes, and alteration of conciousness/mental state and post-traumatic amnesia does not exceed 24 hours [1]. The detrimental effects of mTBI on patients includes cognitive problems such as memory loss, disorientation, and sometimes seizures. Unlike severe traumatic brain injuries, mTBIs frequently are undetected by MRI or CT scans, causing the injured person to often go undiagnosed [2]. Loss of neuronal connectivity witihin the brain tissue is often associated with mTBI [3]. Therefore, the sinusoidal shear deformation that is produced by blast and impact waves must break bonds to induce the loss of connectivity. Understanding the mechanical response of damaged brain tissue could aid in the understanding of mTBI and provide a better characterization of brain tissue structural components response to mild damage.

Blast waves induce mTBI via a deformation wave that travels through the brain tissue. This deformation wave is composed of sinusoidal compressive and translational shear waves ([4], [5], [6]). Currently, blast wave effects are studied using rats that are subjected to a high pressure compressed air blast from a shock tube [7]. However, these blast tests using shock tubes are too uncontrolled to produce useful insight on the local behavior of the brain tissue under these induced deformation waves. It is necessary to perform controlled tests that apply translational shear waves to relate the form of the shear stress waves to the solid structure of heterogeneous brain tissue and to the extracellular fluid (ECF).

A translational sinusoidal shear deformation is applied to full length heterogenous cerebrum specimens from a rat brain. The normal in vivo frequency of the shear deformation of rat brain tissue is about 1 Hz. This deformation frequency of approximately 1 Hz naturally occurs in the brain due to the glymphatic system, which

consists of the cranial arteries pumping at a frequency of 1 Hz, to move extracellular fluid through the tissue [8]. To compare to the 1 Hz working frequency of the brain tissue, higher deformation frequencies are applied to capture the deformation rate dependence and assess potential damage indicators within the tissue as a result of a mechanical insult. The applied deformation frequencies range from 25 Hz to 125 Hz in 25 Hz increments; there is an exception of a 60 Hz deformation frequency that was completed based on the large change in stress response seen from 50 Hz to 75 Hz. The deformation frequencies are applied at both 10% and 25% displacement amplitude to assess the effects of larger strains commonly seen in injury. A set of 50 cycles at a certain deformation frequency and displacement amplitude is performed, followed by a relaxation period of 60 seconds, and then another set of 50 cycles at the same deformation frequency and displacement amplitude.

Signal analysis techniques are applied to the shear stress response induced by sinusoidal translational shear deformation. Characteristics of the signal may correlate with the behavior of structural components of the tissue and the ECF. Signal characteristics are analyzed by Fourier and harmonic wavelet analysis. In each set of 50 cycles, Fourier analysis captures the significant frequency components of the signal. The power and magnitude of significant frequency components are compared at varying deformation frequencies to measure the effect of deformation frequency on tissue stress response. Harmonic wavelet analysis is then used to determine the time in the set of cycles at which the significant frequency components are present. The use of harmonic wavelets allows one to separately find the frequency components of the transient region and apparent steady state region.

Analysis of the shear stress response characterizes mild damage in the tissue due to the applied deformation frequency. The shear stress offers insight into the strength of bonds in cell adhesion molecules and synapses between axons and glial processes, or of bonds between tissue layers. The tests are performed in deformation control, so a

higher shear stress is correlated with a higher force required to deform the tissue to the desired displacement. The hypothesis is that the experimental technique measures the presence of bond and synapse breaking due to the insult that causes reduced functional connectivity, often seen in mTBI patients. Analysis of shear stress response induced by translational sinusoidal deformation is able to capture bond breaking that conventional techniques such as histology and imaging are not able to detect.

2 Background

Brain tissue is a heterogenous and viscoelastic material. Viscoelastic materials are rate dependent and experience stress relaxation, which is characterized by a decrease in stress upon constant deformation after the initial deformation has already occurred. The large deformations (10% and 25%) used in the experiments make the stress response non-linear viscoelastic. The morphology of the shear stress response curve depends on whether large-scale structures such as the apparent steady states or transients are present. The configuration of any transient is determined by how the stress changes in the region. The apparent steady state region may be periodic or quasi-periodic, which is defined by oscillations that follow a regular pattern but undergo a slight change in period.

2.1 Signal Types

Appropriate analysis techniques are chosen based on the signal type that the shear stress response creates upon deformation. Important to the analysis of the experimental data is periodic versus non-periodic and transient versus steady state signals. The Fourier analysis is only valid for periodic functions, while there is no need for periodicity to apply harmonic wavelet analysis.

Transient and steady state regions of the signal are important in analysis of data. The transient section occurs at the time of application of an input signal. A transient signal can also occur with any sudden change in load being applied to the signal. In the experimental data, there is no sudden change in load applied and therefore the only transient region is during the initial deformation. A nearly steady state may occur after the transient region ends (i.e. when the initial excitation is complete and the system becomes settled). An apparent steady state region has minimal changes between cycles, whereas the transient region has considerable change. Figure 1 shows

the transient and steady state regions of an applied 25 Hz input signal to a brain tissue specimen. Fourier analysis gives no information on the time in which the frequency components occur, and therefore is not able to distinguish between which frequency components are contained in the transient region versus the steady state region. Harmonic wavelet analysis is able to distinguish the frequency components in the transient and steady state regions.
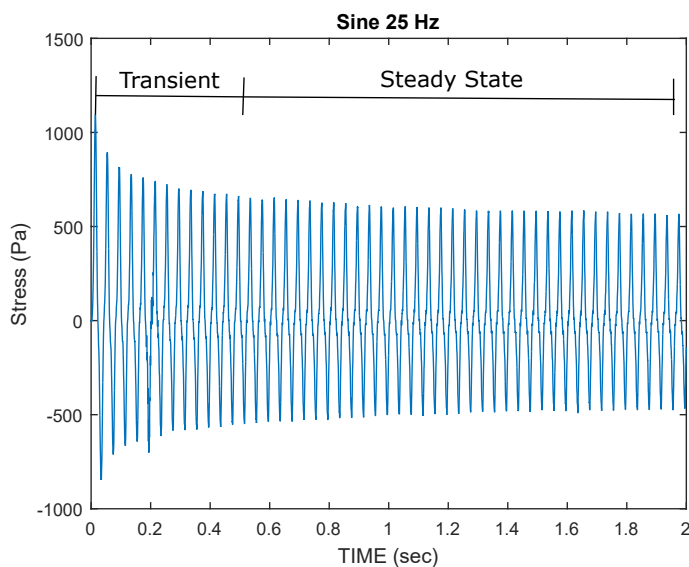
Figure 1: Transient and steady state regions in the shear stress response to translataional shear deformation at 25 Hz.

Signals can also be classified as periodic or non-periodic. A periodic signal is one in which it repeats itself over a specific interval of time. A sine or cosine wave is an example of a periodic signal. In contrast, a non-periodic signal does not repeat itself after a specific interval of time. Signals can also be quasi-periodic in which oscillations follow a regular pattern but have a slightly varying period. Quasi-periodic signals can often be considered periodic on a small scale.

2.2 Fourier Transform

The Fourier transform takes a continuous function or discrete time series signal and transforms it to the frequency domain. The Fourier transform equations (1) and (2) are used to transfer continuous functions in the time domain $h(t)$ to the frequency domain $H(f)$ (equation 1) and from the frequency domain to the time domain (equation 2).

$$H(f) = \int_{-\infty}^{\infty} h(t)e^{2\pi ift}\, \mathrm{d}t; \tag{1}$$

$$h(t) = \int_{-\infty}^{\infty} H(f)e^{-2\pi ift}\, \mathrm{d}f. \tag{2}$$

A simple example of the Fourier transform is shown in Appendix D. Similar to the continuous Fourier transform, the discrete Fourier transform is used for a finite set of discrete data and is

$$H_n = \sum_{k=0}^{N-1} h_k e^{2\pi ikn/N}, \tag{3}$$

where $h_k = h(t_k)$, and N is the number of data points.

The discrete Fourier transform is a monotonic function and can therefore be inverted. The discrete inverse Fourier transform is

$$h_k = \frac{1}{N} \sum_{n=0}^{N-1} H_n e^{-2\pi ikn/N}. \tag{4}$$

The time domain function has certain properties that can be translated to the frequency domain and are used in the Fourier transform computation. The time domain function $h(t)$ that is the original data is real-valued. The Fourier transform of a real function $h(t)$ has the property that $H(-f)$ is equal to the complex conjugate $H(f)^*$.

$$H(-f) = \int_{-\infty}^{\infty} h(t)e^{2\pi i(-f)t}\,\mathrm{d}t \tag{5}$$

$$= \int_{-\infty}^{\infty} h(t)[\cos(-2\pi ft) + i\sin(-2\pi ft)]\,\mathrm{d}t$$

$$= \int_{-\infty}^{\infty} h(t)[\cos(2\pi ft) - i\sin(2\pi ft)]\,\mathrm{d}t = H(f)^*.$$

This relation for the continuous Fourier transform is also true for the discrete Fourier transform function.

The power of frequency f measures the strength of the signal that is occupied by the frequency f. The power identifies significant frequencies and amplitudes in the signal [9].

$$P_{h(f)} = 2|H(f)|^2 \tag{6}$$

Parseval's theorem says the two ways of calculating total power of a signal, one in the time domain and one in the frequency domain are equal. The mean square value of a periodic function is equal to the sum of the squares of all its Fourier coefficients [9].

$$\int_{-\infty}^{\infty} |h(t)|^2\mathrm{d}t = \int_{-\infty}^{\infty} |H(f)|^2\mathrm{d}f \tag{7}$$

The discrete form of Parseval's theorem is

$$\sum_{k=0}^{N-1} |h_k|^2 = \frac{1}{N}\sum_{n=0}^{N-1} |H_n|^2. \tag{8}$$

The negative frequency domain function $H(-f)$ is equal to the complex conjugate $H(f)^*$. Since the negative values in the frequency domain are complex conjugates of the positive frequencies, the negative frequencies are neglected because they do not contain any new information. One application of the Fourier transform computation

is a power spectral density graph (PSD). We can find the power from 0 to the Nyquist frequency, N_f via the one-sided power spectrum, which shows how the power varies with frequency. Equation (5) means the power spectrum density looks the same from 0 to N_f, as it does 0 to $-N_f$, as in Figure 2. The one-sided power spectral density $P(f)$ is

$$P(f) = |H(f)|^2 + |H(-f)|^2 = 2|H(f)|^2 \quad \text{for} \quad 0 \le f \le N_f. \tag{9}$$
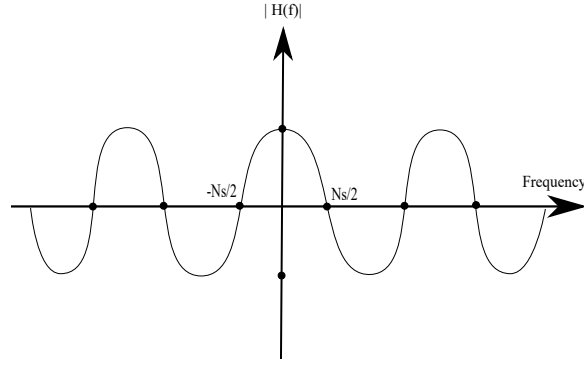
Figure 2: Frequency range between negative Nyquist frequency $(-N_s/2)$ to positive Nyquist frequency $(N_s/2)$ for the magnitude of H(f) plotted versus frequency f.

Intuitively, the power of a signal is analogous to the variation of the signal from zero. In the time domain, the power is defined as

$$P = \frac{1}{T} \int_0^T |h(t)|^2 \mathrm{d}t. \tag{10}$$

The variation of a signal is defined by

$$\sigma^2 = \int_0^T (h(t) - \mu)^2 f(t) \mathrm{d}t \tag{11}$$

where $f(t)$ is the probability distribution. By definition of probability distribution,

$$\int_0^T f(t) \mathrm{d}t = 1. \tag{12}$$

Making $\mu = 0$, Equation (11) simplifies to

$$\sigma^2 = \int_0^T (h(t))^2 f(t)\mathrm{d}t \tag{13}$$

where $f(t)$ must be equal to $1/T$ for $0 \le t \le T$.

The data for the shear response of rat brain is discretely sampled; a force is recorded over evenly spaced intervals of time. The inverse of the time interval determines the sampling rate which is the number of samples per second. The machine that is used for testing, the Bose-Electroforce Testbench, is programmed to collect data every 0.0002 seconds, making the sampling rate 5,000 points/second. The Nyquist frequency is half of the sampling frequency. In the case of our data, the Nyquist frequency is 2,500 Hertz. It is assumed that the frequency in the output stress will never be greater than the Nyquist frequency. Because of this, we do not have to worry about aliasing. Aliasing occurs when there are not enough data samples to properly describe the waveform, and therefore gives a false reading. If the value of n in equation (3) exceeds N-1, than H_n would falsely repeat itself. To ensure aliasing does not occur, n can only vary between 0 to $N/2$. Consider calculating H_n from (equation 3) with $n > N - 1$. For an example, use $n = N + l$ [10] for some l,

$$\begin{aligned} H_{N+l} &= \sum_{k=0}^{N-1} h_k e^{-i(2\pi k/N)(N+l)} \tag{14} \\ &= \sum_{k=0}^{N-1} h_k e^{-i(2\pi kl/N)} e^{-i2\pi k}. \tag{15} \end{aligned}$$

Since $e^{-i2\pi k}$ is always equal to 1, then $H_{N+l} = H_l$. To show that $e^{-i2\pi k}$ is equal to 1, refer to Figure 48 in Appendix E; $2\pi k$ is the angle between the real axis and the radius corresponding to the point on the circle that equals $e^{-i2\pi k}$. A rotation by 2π radians from the starting point, ends up where it started. Therefore, $e^{-i2\pi k}$ is at the

point (1,0) on the unit circle, so it is always equal to 1, no matter what the value of k is.

2.3   Comparing Fourier Transform to Wavelet Transform

The Fourier transform decomposes a signal into waves of infinite length, i.e. a combination of sine and cosine functions. The Fourier transform determines the frequencies within a signal, but not the instantaneous time at which the frequencies occur. Not knowing when a specific frequency occurs creates a problem of the resolution between the frequency domain and time domain. It is often necessary to represent a signal in the time and frequency domain at the same time.

To overcome this inability to determine the time location of a frequency, Denis Gabor elaborated on the Fourier transform and developed the short time Fourier transform (STFT), also called the Gabor transform [11]. In STFT, the signal is divided into small segments that are assumed to be stationary. This is done by sectioning the signal into narrow time intervals and then taking the Fourier transform of each interval. The short time Fourier transform of the time function $h(t)$ is

$$H(\tau, f) = \int_{-\infty}^{\infty} h(t) W(t - \tau) e^{2\pi i f t} \, \mathrm{d}t; \tag{16}$$

where $W(t)$ is the window function centered at $t = \tau$, where τ is a time parameter, f a frequency parameter, and $h(t)$ is the signal. Although the short time Fourier transform provides more information than the Fourier transform, there are still limitations based on the window size (i.e. how wide or narrow it is chosen to be). In STFT, time and frequency are both represented, but in limited precision that is determined by the size of the window. The chosen window must be narrow enough that the signal within the window can be considered stationary; however, making the window too narrow can diminish localization in the frequency domain. Another disadvantage of

the short time Fourier transform is that the length of the time window must be the same for all frequencies. The width of the window function is called the support of the window. If the window function is narrow, it is considered compactly supported (i.e. localized in time). Having limited flexibility in the window size for STFT drives the discovery and subsequent use of wavelets.

2.4 Wavelets

Wavelet analysis uses a scalable window that can be shifted along the signal; at each of these time positions that the window is shifted to, the frequency spectrum is analyzed to determine frequency components at that time position. The benefit of a scalable window is that wavelets cut up the data into different frequency components, and analyze each component with a resolution matched to its scale. Since this window can be scaled, it can provide gross and detailed features of the signal, with accuracy in both the frequency and time domain. Wavelets give information on the time within a signal that a frequency occurs. Unlike sine or cosine waves, wavelets are short bursts that quickly approach zero magnitude. Using a wavelet transform to decompose a signal produces better resolution in the time domain, as compared to the Fourier transform which has no resolution in the time domain. A wavelet transform deconstructs a signal using scaled versions of a mother wavelet, whereas the Fourier transform uses various sine or cosine waves at different frequencies. All window functions are dilated and/or time-shifted versions of the mother wavelet. Varying the size of the window allows one to determine either time or frequency information more accurately.

Applications of wavelet analysis are broad, but mainly used to analyze different classes of nonstationary (in time) signals. A stationary signal is one whose frequency content does not change in time. This means that one does not need to know at what time a frequency component exists, because all frequency components exist at

all times throughout the signal. Therefore, Fourier analysis is sufficient for stationary signals. In contrast, a nonstationary signal has a frequency that changes in time; different frequency components exist at different times, which the Fourier transform cannot capture.

To analyze a signal, the corresponding set of basis functions must first be determined. For nonstationary signals, the basis should have compact support [12]. A wavelet has compact support if it is zero outside of some finite interval [a,b] [13]. The choice of the wavelet function depends on the problem to be solved [12]. Wavelets are very diverse in their properties, some of the main characteristics are different degrees of smoothness, support, symmetry, and regularity. The smoothness of wavelets is dependent on the number of vanishing moments of the scaling and wavelet functions. A wavelet with n vanishing moments means that the wavelet coefficients for the nth order polynomial is zero. More vanishing moments means that the scaling function can represent more complex signals accurately [14]. However, more vanishing moments also means longer computation time. As with computation time, there is a trade off between number of vanishing moments and the length of the support. The wavelet function should be smooth and concentrated in both the frequency and time domain; there needs to be a balance between the length of the support and the number of vanishing moments.

2.4.1   Harmonic Wavelet

Harmonic wavelets were originally formulated by Newland who was searching for a wavelet whose Fourier transform is compact and could be constructed from simple functions [10]. In discrete wavelet transforms with real coefficients, as the number of coefficients increases, the wavelets Fourier transform becomes increasingly compact. However, the underlying frequency spectrum of the wavelet becomes more box-like as

the number of wavelet coefficients increases. This led Newland to seek a wavelet $w(x)$ whose frequency spectrum is a box so that the magnitude of its Fourier transform $W(\omega)$ is zero except for an octave band of frequencies. The Harmonic wavelet is a complex wavelet with real and imaginary parts. The introduction of a complex function allows the two parts to be represented by a single expression. This strategy is similar to in Fourier analysis how $e^{i2\pi kt}$ represents both an even and odd function, $\cos(2\pi kt)$ and $\sin(2\pi kt)$, respectively. The harmonic wavelet has the form

$$w(2^j x - k) = (e^{i4\pi(2^j x - k)} - e^{i2\pi(2^j x - k)})/i2\pi(2^j x - k) \tag{17}$$

where j indicates the level and k is the translation and is used to capture dominant frequencies (j-level) and the times (k-level) at which the frequencies occur within the signal.

The harmonic wavelet transform breaks the signal into local wavelets that have significant amplitudes in a finite time. The computation of the harmonic wavelet transform is based on FFT, which greatly reduces the computational cost as compared to other wavelets such as Daubechies [17]. The harmonic wavelet has a frequency spectrum which is confined exactly to an octave band so that it is compact in the frequency domain rather than the time domain. A signal can be decomposed as a series expansion of the harmonic wavelet and its dilations and translations. Each one of these functions belongs to the same family of wavelets and has its own particular octave band in the frequency domain. As a consequence, the dilations and translations are all orthogonal in the frequency domain (because none of them share frequency components along the whole frequency spectra). Orthogonality in the frequency domain allows for a unique set of wavelets in a given signal [10]. Wavelets of different levels (different j values) are always orthogonal; wavelets at the same level (same j value) are orthogonal if one is translated with respect to the other by a unit

interval (different k). Each wavelet is concentrated locally around $t = k/2^j$ because its horizontal scale is compressed by the factor 2^j and its position is translated k units at the new scale. A large advantage of harmonic wavelets is the ease of computation by the fast Fourier transform. The harmonic wavelet transform uses FFT and IFFT to analyze discrete experimental data, which does not need to be periodic or sinusoidal.

2.5 Rat Brain Structure

Rat brain tissue is a heterogenous tissue that is composed of various regions that are made up of white and grey matter as well as blood vessels. The rat brain can be divided into three main regions. These regions consist of the right and left cerebral hemispheres, that are composed of a mixture of grey and white matter; the cerebellum, which is composed of primarily grey matter; and the brainstem that is composed primarily of white matter. A schematic of a rat brain is shown in Figure 3. The corpus callosum is a band of white matter that connects the left and right hemispheres and is a major site of damage in mTBI [18]. The hippocampus is believed to be a significant area of disconnections caused by mTBI.

Brain tissue is composed of two main types of cells: neurons and glial cells (neuroglia). The primary function of neurons is to transmit communication signals. One of the major functions of glial cells is to provide mechanical support of the neurons (along with many other functions). The neurons are made up of a cell body, an axon, and dendrites that extend from the cell body. The grey matter consists of mostly neuron cell bodies, dendrites and unmyelinated axons, whereas the white matter contains myelinated axons. The white matter axons are covered in a myelin sheath which is about 70-85% lipid and 15-30% protein [19].
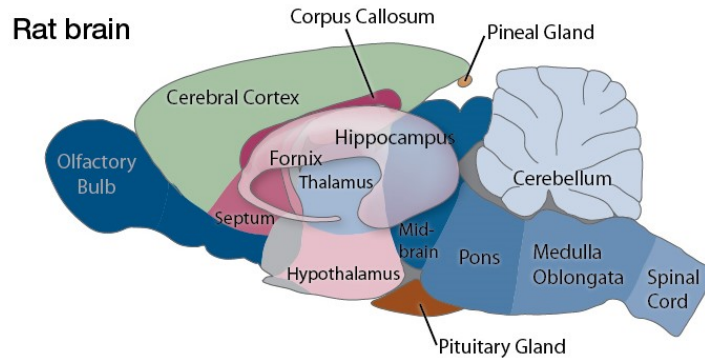
Figure 3: Sub structures in rat brain [20].

2.5.1 Neurons

Neurons have three basic parts: the cell body, the axon, and the dendrites. The cell body contains the nucleus and other organelles (endoplasmic reticulum, ribosomes, etc.). The axon is a long projection that carries an electrochemical message from the cell body to the dendrites. The dendrites are the nerve endings, which are small projections of the cell that make connections to other cells via synapses to communicate with other cells and the environment. Within the axon is a network of microtubules, microfilaments, and neurofilaments that provide a framework for axonal transport (Figure 4). Microtubules contribute significantly to the mechanical stiffness of axons [21]. The cytoskeletal framework allows applied stresses to the cell be distributed throughout a larger area.

Synapses are crucial in the conduction of information from neuron to neuron. Synapses have often been thought of as bipartite, containing only the presynaptic nerve terminal and postsynaptic nerve terminal, as shown in Figure 4. However, as more focus has been put on glial cells, there is a growing consensus that synapses may also be tripartite, that include the presynaptic and postsynaptic nerves and also glial cells that surround the synapse [23]. Figure 5 shows the complex interconnection of neurons and glial processes
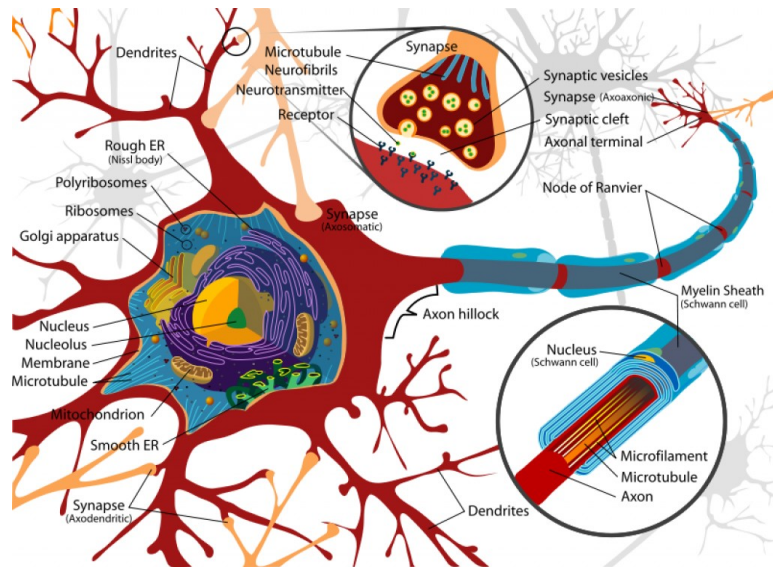
Figure 4: Anatomical structure of a neuron [22].
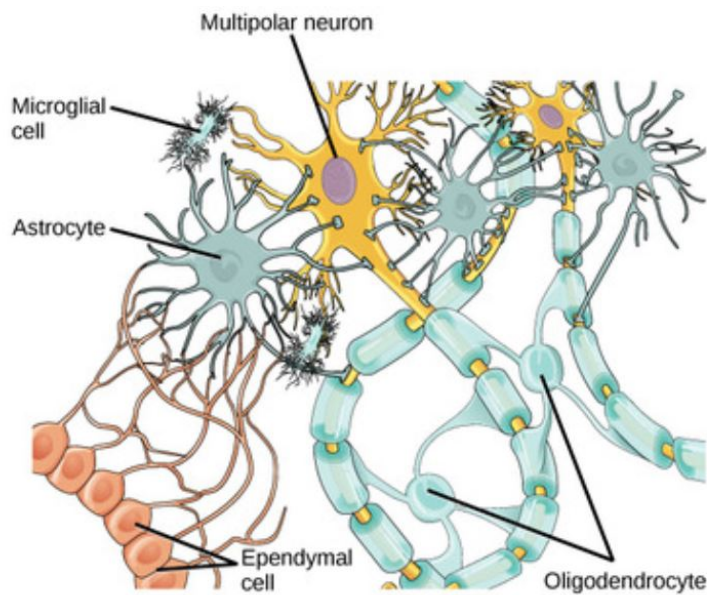
Figure 5: Anatomical structure of a neuron [22].

2.5.2 Neuroglia

Neuroglia consist of several types of cells that all primarily function in supporting neurons. Neuroglia cells had previously been thought to exceed the number of neurons in the nervous system by at least 10 to 1, however, new information suggests that it is closer to a 1:1 ratio [24]. Neuroglia retain their ability to divide throughout

their life span, as opposed to neurons which are unable to divide. There are four main types of neuroglia found in the central nervous system. Astrocytes maintain the blood brain barrier and preserve the chemical environment by recycling ions and neurotransmitters (chemical messengers). The blood brain barrier is a highly selective, semi-permeable membrane that separates the brain and extracellular fluid within the brain from circulating blood. Astrocytes are the most numerous cells in the central nervous system and cover the entire outer surface of the brain to form the glial pia (connective tissue meninx). Astrocytes react to neural tissue damage by forming scar tissue in the damaged space. Oligodendrocytes myelinate axons in the central nervous system (similar to how Schwann cells myelinate axons in the peripheral nervous system) and provide structural framework. Oligodendrocytes reach out to axons of nearby neurons and wrap around them forming a high resistance sheath called myelin. Myelin insulates a small region of the axon, which prevents ions from leaking into the extracellular fluid, to facilitate signal propagation down the axon towards the synaptic terminal. Processes from many different oligodendrocytes contribute to the myelin sheath of a single neuron's axon. Ependymal cells line ventricles in the brain and are involved in the production of cerebrospinal fluid. Microglia remove cell debris, waste, and pathogens via phagocytosis [24]. More recent research has also shown that glial cells, specifically astrocytes, function as signaling cells and form a complex neuron-glia communication network [25].

3   Methods

The methodology of the experimental design is to model the response of brain tissue subjected to shear waves under an external insult, such as a blast or impact waves. When subjected to an external insult, brain tissue experiences deformation waves that consist of translational shear and compressive waves. Symptoms of mTBI are associated with loss of neuronal connectivity. The sinusoidal shear deformation that is produced by blast waves must break bonds to induce the loss of connectivity seen in mTBI patients. The experiment is designed to model two insults each produced by sinusoidal cycles, at various fixed frequencies and fixed moderate deformation amplitudes, in order to investigate whether bond breaking occurs in both the first and second insults. The two insults are separated by a period of rest in which no deformation is applied to represent the treatment of mTBI by rest.

3.1   Specimen Preparation

The whole brain of a euthanized Sprague Dawley rat must be removed without damage to perform mechanical testing on the tissue. Any damage to the tissue results in that part of the tissue being discarded and not used for testing. The planes of dissection are shown in Figure 6 and used as a reference for following the procedure for removal of the brain.

The euthanized Sprague Dawley rat is placed on a surgical mat dorsal surface up with the anterior side facing pointing away from the researcher. A longitudinal incision at the mid-line is made on the dorsal surface by the nape of the neck with a No. 11 blade scalpel. The scalpel is inserted under the surface of the skin and used to extend the incision longitudinally to the right and left side of the upper neck. A scalpel is used to make transverse cuts into the muscle tissue at the base of the skull. Forceps are used to separate the tissue as the cuts become more medial. Once the
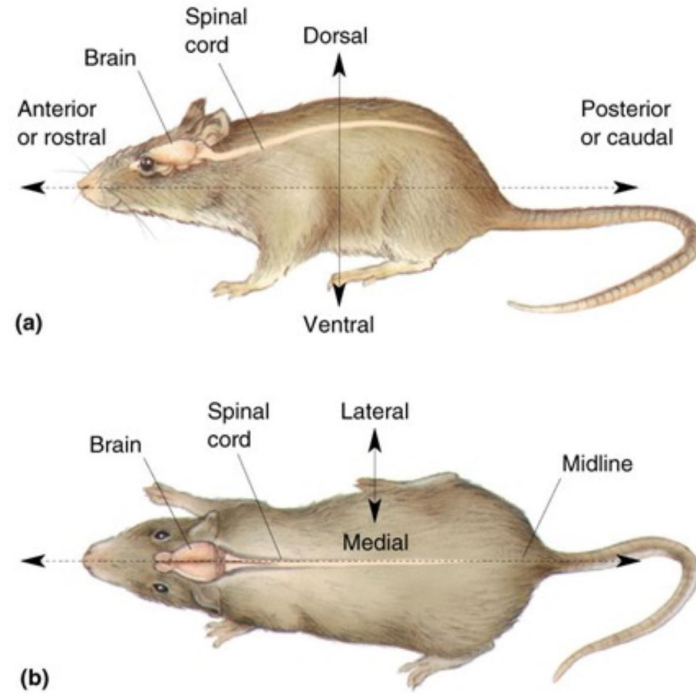
Figure 6: Anatomical planes of rat [26]. The coronal plane refers to the vertical plane that divides the body into ventral and dorsal sections. The sagittal plane (also called the medial plane) divides the body into the left and right.

muscle is separated on the posterior and lateral sides of the neck, the jaws of the bone cutters (FineScience Tools # 16107-14) are inserted on either side of the spine where the muscle tissue was separated distal to the skull. The bone cutters are used to cut through the spine. Once the spine has separated, a scalpel is used to cut the remaining connecting tissue to complete the decapitation. After decapitation, the brain is ready to be removed from the skull (refer to Figure 7 for bones of a rat skull).
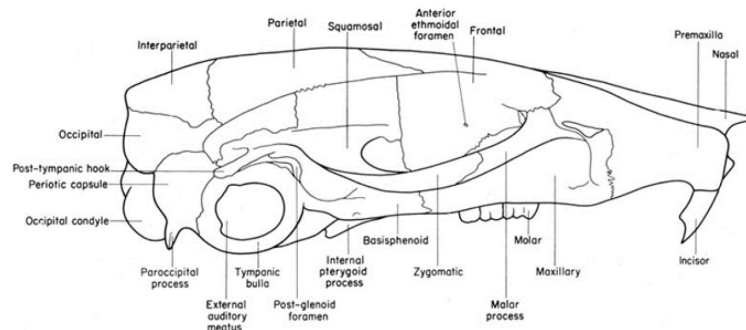
Figure 7: Rat skull diagram [27].

A sagittal incision is made down the center line of the head from between the eyes to the furthest posterior position. Superficial cuts are made along the medial of the skin to separate the skin from the muscle tissue on both the right and left sides to fully expose the muscles on the sides of the skull. The skin is flipped over the eyes so the skull is fully exposed. The bone cutters are used to pull the muscle tissue from the posterior occipital. Once most of the muscle tissue is cleared from the occipital, place the bone cutters with the blade proximal to the skull on the superior edge of the occipital and scrape against the bone to remove any remaining muscle tissue. The bone cutters are then inserted from the posterior side through the occipital hole with the rounded edge of the bone cutters facing medially and the sharp edge of the jaw faced inside of the skull so that the tip of the jaw blade points toward the dorsal, lateral corner of the occipital. Cut the occipital on both the right and left sides. Putting the bone cutters in the sagittal plane with the rounded edge of the bone cutters facing toward the occipital, insert the lower cutter jaw under the flap of the occipital that was created from the previous angled cuts. Rest the upper jaw on the back of the interparietal and rotate the occipital flap away from the brain in the posterior and dorsal directions.

Place the curved edge of the bone cutters facing the medial direction and directed in the sagittal plane pointing toward the rostral direction, make small cuts along dorsal surface of the skull. Gradually remove all parts of skull until the most anterior region of the skull is reached. Once the brain is exposed, the dura mater must be removed. The dura mater is visible along the interface of the left and right hemispheres of the cerebrum. Use the bone cutters to snip the dura matter between the right and eft hemispheres and along the interface between the cerebellum and cerebrum.

At this point, the top of the brain is fully exposed and unrestrained by the dura mater. However, there are still bones holding the brain in place between the interface of the cerebrum and cerebellum. Bring the bone cutters in the coronal plane with

the rounded edges facing the posterior side of the skull and slightly in the medial direction. Clamp the bone cutters and twist along the lateral-medial axis in the lateral direction. Perform this on both sides of the skull. The twisting ensures that the acoustic meatus, which retrains the brain from being lifted from the skull, is removed and does not damage the underlying brain tissue. The brain can now be fully removed from the skull by flipping the skull upside down over a tray filled with PBS. A surgical elevator is inserted between the ventral side of the brain and the skull to gently move the brain into the tray.

Once the rat brains are harvested from freshly euthanized Sprague Dawley rats, the brains are stored in a phosphate buffered saline (PBS) solution at room temperature until testing within two hours of harvest in order to minimize tissue degradation. After excising the brain from the rat, an incision parallel to the frontal plane separates the cerebellum from the cerebrum and an incision along the center line of the cerebrum separates the cerebral hemispheres (Figure 8). To produce specimens from each rat brain cerebrum that are nearly the same length of the cerebrum, a scalpel guided by grooves properly spaced in a metal fixture slices four sagittal planar slabs of thickness 3 mm, two from each hemisphere. The sagittal slab closest to the joint between the hemispheres is called an inner cerebrum specimen and the other is called an outer. Each slab contains an unknown proportion of white and grey matter, but the inner specimen contains white matter from the corpus callosum. The specimens are trimmed at the anterior and posterior ends to create a 10 by 6 mm surface and a thickness of 3 mm.

3.2   Apparatus

A shear fixture (Figure 9) was designed and built to apply translational shear from 25 mm long flat grips to flat rectangular plate specimens excised from the rat brain. The specimen is glued between two parallel test plates. The top plate is attached on the

Figure 8: Two hemispheres of rat brain cerebrum separated from cerebellum (grey matter) and brain stem (white matter).

Bose Electroforce Test Bench 200 N test machine that uses a linear magnetic motor design. The bottom plate is mounted to a Bose 250 gram load cell that measures the reaction force and rests on top of a linear bearing (Del-tron M-1 linear ball slide) with manufactured specified 0.003 coefficient of friction. The other end of the load cell is secured to a support bracket to fix one end of the load cell so it deflects due to the applied force. The support bracket is connected to a spring-loaded displacement stage (ThorLabs T12X) that enables the bottom plate and load cell to move up and down as a unit. This assembly is fastened to a mounting bracket that is screwed into a stationary stand.

The Bose machine contains a magnet that is suspended in an electromagnetic field. The magnet produces translational motion as the electromagnetic field changed. The shear sinusoidal deformation is applied in deformation control by a Bose-Electroforce Testbench 250N machine that can produce a maximum 100G acceleration, linear rate of deformation of up to 3.2 m/s, and 125 Hz sinusoidal frequency. The Bose software, WinTest 4.1, is used to program the Bose for desired settings for a given test.
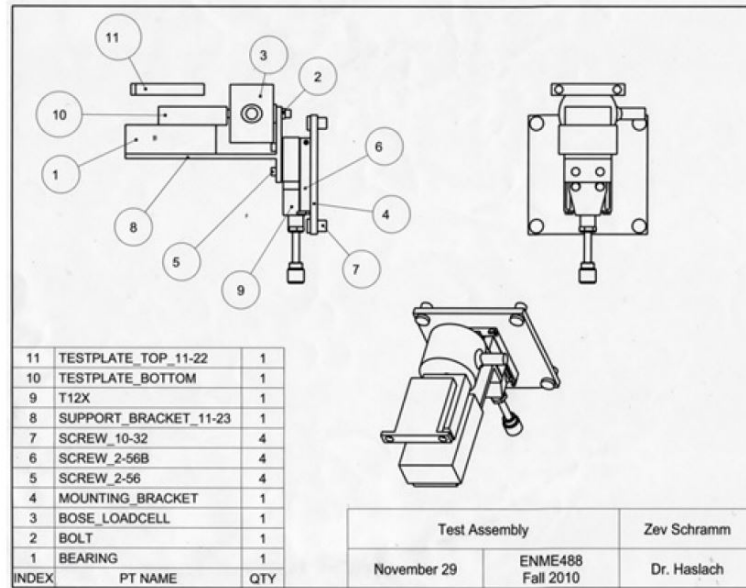
Figure 9: Apparatus for translational shear testing.

3.3 Protocol

At the beginning of testing, the Bose stationary stand is moved away from the top grip so that the specimen can be secured to the bottom plate. The shear specimens are attached to the grips 90 seconds prior to deformation by Vetbond (3M: 1469SB) which has a setting time of 15 seconds and shear strength on metal of about 16.55 MPa to prevent slip of the specimen on the grip. The specimen is placed on the bottom grip in the desired alignment, with the 6 mm side of specimen perpendicular to the mover and the 10 mm parallel with the mover. Another drop of glue is placed on the top of the specimen. The stationary stand is then readjusted to realign the top and bottom plate. The bottom plate is raised so that the top of the specimen is touching the top plate, with no compression on the specimen. The WinTest 4.1 records the elapsed time, displacement and load induced in the load cell. The force measured by the load cell on the lower grip accounts for the specimen thickness because the shear is driven by motion of the upper grip. The program outputs the recorded force at each specified time interval. The machine is programmed to take a data point every 0.0002 seconds. The translational shear stress is calculated from the load detected

from the bottom grip of the apparatus by

$$\sigma = 10^{-3}\frac{gF}{A} \tag{18}$$

where g is the gravitational constant, F is the load (g), and A is the cross sectional area of the specimen (m^2). The translational shear strain is then calculated from the displacement measured from the mover by

$$\epsilon = \frac{d}{L} \tag{19}$$

where d is the displacement (mm) and L is the length of the specimen (mm) in the direction parallel to the displacement direction.

3.3.1   Sinusoidal Translational Shear

Brain tissue is exposed to sinusoidal translational shear stresses after exposure to blast waves. The sinusoidal translational shear frequency range was chosen to be from 25 Hz to 125 Hz, to understand the effect that higher deformation frequencies have on stress response of heterogeneous rat brain tissue. Table 1 provides a summary of the number of specimens for each test type (deformation frequency, displacement amplitude) at 0% compression. At each deformation frequency, tests are completed at a displacement amplitude (strain) of 10% or 25% of their original length. These displacement amplitudes were chosen because it is expected that injury would have a substantial deformation, but not large enough that the injury would be considered severe. All specimens are 6x10x3 mm, so that a deformation amplitude of 1 mm is equivalent to 10% deformation. Likewise, a deformation amplitude of 2.5 mm is equivalent to 25% deformation. At a deformation frequency of 125 Hz, the Bose machine is unable to reach an amplitude of 25%; for this reason, only an amplitude of 10% were completed on the 125 Hz tests.

Table 1: Summary of completed sinusoidal shear tests on rat brain Cerebrum under 0% compression.

Frequency (Hz)	Deformation Amplitude (mm)	Number of Specimens
25	2.5	13
25	1.0	10
50	2.5	13
50	1.0	10
60	2.5	16
60	1.0	15
75	2.5	10
75	1.0	14
100	2.5	10
100	1.0	10
125	1.0	10

At each deformation frequency and displacement, a set of 50 cycles is completed followed by relaxation for 60 seconds and then another set of 50 cycles at the same deformation frequency and displacement amplitude. This is done to analyze redistribution of fluid within the tissue during the relaxation period and assess damage indicators upon a second insult to the brain tissue.

3.4 Method of Analysis

Frequency components and their location within each set of 50 cycles at all deformation frequencies and displacement amplitudes are analyzed. The frequency content and shear stress response to deformation is compared at increasing deformation frequencies, between sets of 50 cycles, and between 10% and 25% displacement amplitudes to gain insight on damage occurring within the tissue.

3.4.1 Detection of Frequency Components within Signal

The custom MATLAB fftsine program uses the Fast Fourier Transform to detect frequency components within a signal. The input signal is discrete experimental data that is imported into MATLAB from excel. Two objectives of this MATLAB program

are to determine significant components of frequency and then to compute the power and magnitude of those components. The power of the frequency components are based on the experimental data throughout the entire set of 50 cycles, while the magnitude of the frequency components are computed based on one cycle (cycle 20) in the apparent steady state region.

The required parameters include the deformation frequency, w, the number n of harmonics to be included in the frequency range examined, the period T of a cycle, the cycle number ncy to analyze, and the number of points in one input cycle. It is necessary to define the cycle number to be analyzed because the Fourier series coefficient calculation requires that the function or data be periodic. The shear stress is not periodic over the full 50 deformation cycles, but after about cycle 10-15, it approaches a steady state. Any cycle in the steady state can be analyzed, and is arbitrarily chosen as cycle 20. The number of points in one deformation cycle is determined by taking the period of one cycle (1/frequency) and dividing by the sampling rate (0.0002 seconds for the Wintest 4.1 program). The sampling frequency Fs is the inverse of the sampling rate.

Once the parameters are defined, the program computes the vector of significant frequencies in the stress response. The first step is to modify the length of the stress signal, which is denoted as $NFFT$, required by the MATLAB program fft. $NFFT$ equals the smallest power of two that is greater than or equal to the length of the stress data vector. The maximum frequency component, or Nyquist Frequency, for a signal sampled is one half of the sampling frequency, which is $Fs/2$, or $1/2\Delta$ where Δ is the sampling rate. The frequency vector goes from zero to the maximum frequency ($Fs/2$) with linearly spaced points that are $Fs/NFFT$ apart.

To locate where the maximums of the output frequencies occur in the power spectrum for the stress response data, the frequency range is broken up into sections. In each section, fftsine finds the maximum frequency. These sections are the unit

frequency point number for scanning, with the length defined by the term uf in fft-sine. These sections are then scanned to find the maximum magnitude within each section. Originally, uf was supposed to be the distance (in number of points) between harmonics. However, as seen in Figure 10, the spikes at the harmonics are too wide, which creates problems in finding the real maximum points. For example, this window would often give a double harmonic because it picked up values at the base of the spike, rather than the next true harmonic, or the same harmonic could be the maximum value in adjacent windows. To fix this issue, the start of the scanning point was shifted so it would begin scanning halfway through the first original uf section and extend halfway through the second original uf section. These sections are found by taking $(NFFT/Fs)$ which divides the sampling frequency Fs into the length of the frequency vector that is used in the fft program. $(NFFT/Fs)$ is the number of points between each Hertz in the frequency domain and was determined by dividing the Nyquist frequency, $Fs/2$ into the number of points leading up to the Nyquist frequency, $NFFT/2$. $(NFFT/Fs)$ is then multiplied by the input deformation frequency, to yield the number of points between harmonics in the frequency domain.

3.4.2 Fourier Series Coefficients

The Fourier series decomposes any periodic signal, $h(t)$, into a sum of sine and cosine basis functions

$$h(t) = 0.5a_0 + \sum_{n=1}^{\infty} \left(a_n \cos(2\pi f_n t) + b_n \sin(2\pi f_n t) \right), \tag{20}$$

where a_0 is the average value of $h(t)$ and f_n is the frequency at the nth harmonic, with f_1 being the original deformation frequency. The Fourier coefficients, a_n and b_n,
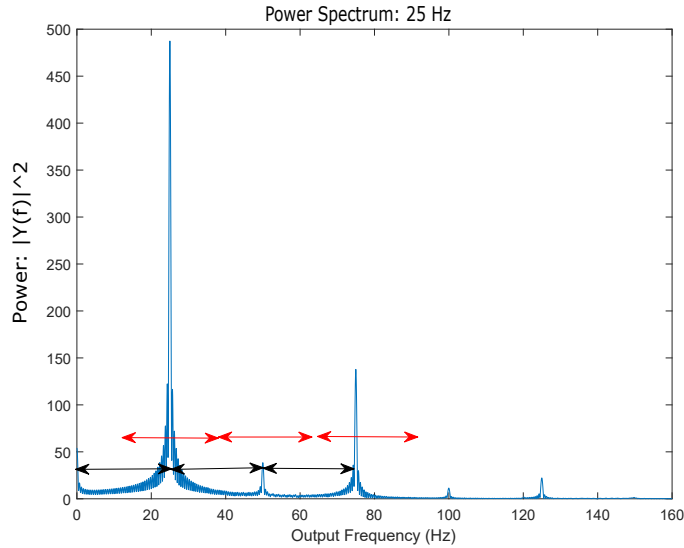
Figure 10: Graph showing power of harmonics and the original uf sections (in black) compared to the corrected uf sections (in red).

are found by evaluating the integrals

$$a_0 = \frac{2}{T} \int_0^T h(t)\mathrm{d}t; \tag{21}$$

$$a_n = \frac{2}{T} \int_0^T h(t)\cos(w2\pi t)\mathrm{d}t; \tag{22}$$

$$b_n = \frac{2}{T} \int_0^T h(t)\sin(w2\pi t)\mathrm{d}t; \tag{23}$$

To evaluate the integrals in (21) to (23), the MATLAB command trapz is used, where T is the period. This command computes the approximate integral of the function represented by a MATLAB vector that defines points on the curve to be integrated. The vector contains the stress values through one cycle. The coefficient a_0 is the average of the function. To find the average of the function, the time step is multiplied by the input frequency and then multiplied by the integral of the stress over one period. A for loop then creates a vector of all the Fourier coefficients for the specified number of harmonics, n. The Fourier coefficients are then used in Equation (20) to obtain a reconstructed equation that is plotted against the original stress

response curve.

3.4.3 Power and Magnitude Calculations

Using the fast Fourier transform, the power spectrum of a time series describes the distribution of power into frequency components composing the signal. The peaks correspond to harmonics of the deformation frequency. The power spectrum graph is based on the entire set of 50 cycles, and therefore gives the significant frequency components within both the transient and apparent steady state regions.

The magnitudes are calculated within a single cycle of the steady state region. The magnitude calculation does not use Fast Fourier Transform, but uses the Fourier series decomposition as discussed in Equations (22) and (23). After obtaining the Fourier coefficients, the magnitude is calculated as $\sqrt{a_n^2 + b_n^2}$. The magnitude gives the strength of frequency components within a cycle confined to the steady state region. This calculation is done on a single cycle, but it is noted that this cycle is chosen to represent the entirety of the steady state region. However Fourier series decomposition can only accurately fit periodic functions, therefore harmonic wavelet analysis is used in conjunction with Fourier analysis to provide a complete description of the frequency components within the signal.

3.4.4 Harmonic Wavelet to Determine Time Location of Frequency Components

The fast Fourier transform and the Fourier series decomposition provide information about the dominant frequencies that make up each stress response, but do not give information on where those frequencies occur in the signal. Harmonic wavelet analysis provides information about the location in time of the frequency components. Rather than having significant frequencies over the entire time period, harmonic wavelets have a significant magnitude over a finite time interval, which creates a local wavelet that is

characterized by a frequency level (j) and a time level (k). The fast Fourier transform is used in conjunction with the harmonic wavelet analysis to provide information on exact frequencies and time at which those frequencies occur.

Harmonic wavelet analysis is used because the signal does not need to be periodic and the analysis gives information on the location in time of frequency components. As discussed in section 2.4.1, harmonic wavelet analysis involves orthogonal wavelets that are confined exactly to an octave frequency band which is convenient in interpreting frequency content because the levels are interchangeable with the frequency band (Equation (26)) [16]. The harmonic wavelet captures dominant frequencies (j-level) and the times (k-level) at which the frequencies occur within the signal and has the form

$$w(2^j x - k) = (e^{i4\pi(2^j x - k)} - e^{i2\pi(2^j x - k)})/i2\pi(2^j x - k) \tag{24}$$

where j is the frequency level, k is the translation, $x = t/T$ is the normalized time, and T is the time of the signal. Given a signal that is 2^n points and a sampling interval Δ, T is the total time it takes to reach 2^n data points and is determined by $T = 2^n \Delta$, where n is chosen to be the highest integer value so that 2^n is less than the original total time.

The equation for the frequency range at any j level is

$$\frac{(2\pi)2^j}{T} \leq f < \frac{(2\pi)2^{j+1}}{T}. \tag{25}$$

Equation (25) is modified to convert its units from radians per second to Hertz for the j-levels by dividing by 2π to yield

$$\frac{2^j}{T} \leq f < \frac{2^{j+1}}{T}. \tag{26}$$

Equation (26) produces the upper and lower bound frequencies in Hertz at specific

j-levels. A substitution of $T = 2^n\Delta$ into Equation 26 produces

$$\frac{2^j}{T} = \frac{2^j}{2^{n-1}2\Delta} = \frac{2^j}{2^{n-1}}\frac{1}{2\Delta} \tag{27}$$

which shows that the j-levels break the signal up from 0 to the Nyquist frequency, where the Nyquist frequency is determined by $1/2\Delta$. The number of j-levels ranges between 0 to $n-1$. Equation (27) shows that the j-level range is determined by Δ and is independent of the deformation frequency frequency. For all deformation frequencies, Δ is the same, so n is the only variable that changes with the deformation frequency.

The times required for 2^n points at various deformation frequencies are summarized in Table 2. For example, at a deformation frequency of 25 Hz, the harmonic wavelet analysis with a time step of 0.0002 seconds (determined by Bose settings) between sample points over 2^n points requires a total time of $T = 1.6382$ s.

Table 2: Value of T used in calculating j-level ranges at specified deformation frequency.

Frequency	N	n	2^n	points per cycle	Number of Cycles in 2^n	T
25	10,000	13	8,192	200	40.9	1.6382
50	5,000	12	4,096	100	40.9	0.8191
60	4,167	12	4,096	83.3	49.2	0.8191
75	3,333	11	2,048	66.7	30.7	0.4096
100	2,500	11	2,048	50	40.9	0.4096
125	2,000	10	1,024	40	25.6	0.2048

In addition to the j-level which provides frequency information within the signal, the harmonic wavelet decomposition also provides the k-level at a specific j-level. The k-level says where in time the wavelet is located, and ranges from 0 to $2^j - 1$. The k range for specific j-levels is summarized in Table 3. The (j,k)-wavelet has its peak (of magnitude 1) centered at $2^j x - k = 0$ (Equation 24). Recalling that $x = t/T$, the time at which the wavelet peak occurs is $t = kT/2^j$, centered at 0. The definition of

$T = 2^n \Delta$ is used and the time at which the wavelet peak occurs is rewritten as

$$t = 2^{n-j} k \Delta. \tag{28}$$

This calculation finds the range of k values within the transient region for a specific j-level. For example, at a deformation frequency of 25 Hz, if the transient region ends after 3 cycles, the number of data points within the transient region is computed by $(5000 \frac{points}{sec})(\frac{1sec}{25Hz})(3\text{cycles}) = 600$ data points to complete 3 cycles. The value of k for the $j{=}5$ level is then found by $(600)/2^{13-5} = 2.3$. This pair of j, k values produces the wavelet whose center is nearest to the end of the transient region. This means that at a deformation frequency of 25 Hz, at the $j = 5$ level, the transient region approximately spans from $k{=}0$ to $k = 3$, noting that the entire k range is from 0 to 31. Low k values correspond to wavelets at the beginning of the signal (in time), so an increase in k level is associated with a shift in time.

Table 3: Ranges of k at specified j-levels found by using $2^j - 1$.

j-level	k range
1	0 to 1
2	0 to 3
3	0 to 7
4	0 to 15
5	0 to 31
6	0 to 63
7	0 to 127
8	0 to 255

The wavelets are organized into bins which depend on the amplitude of the wavelet and the (j, k)- wavelets are assigned to a specific bin number. The bins are separated by a step size of $\frac{max-min}{20}$ where max is the maximum wavelet magnitude and min is the minimum wavelet magnitude. Organizing the bins in this way results in 20 bins that range from large magnitude wavelets (bin 1) to small magnitude wavelets (bin

20). A higher bin number corresponds to a lower wavelet amplitude. For example, the wavelets in bin 1 are dominant in the signal, whereas wavelets in bin 19 are less dominant. The last bin (bin 20), contains many wavelets all with the bottom 5% magnitudes. A bin containing more than 50 wavelets often happens in higher bins (19 and 20) with the smallest amplitude wavelets and therefore is not considered for analysis.

3.4.5   Shear Stress Response Analysis

The shear stress response curve for each set of 50 cycles is made at each deformation frequency and displacement amplitude. The shear stress response curve may contain both a transient region and apparent steady state region. In the transient region, the initial peak stress value is recorded, which is the magnitude of the first cycle, in both the first set of 50 cycles and second set of 50 cycles. The length of the transient region is also recorded. The end of the transient region occurs at the cycle that has a small ($< 10\%$) change in magnitude between subsequent deformation cycles. Lastly, from the shear stress response graph, the shear stress magnitude of cycle 20 in the apparent steady state is taken. Figure 11 shows an example of the values taken from each shear stress response curve.
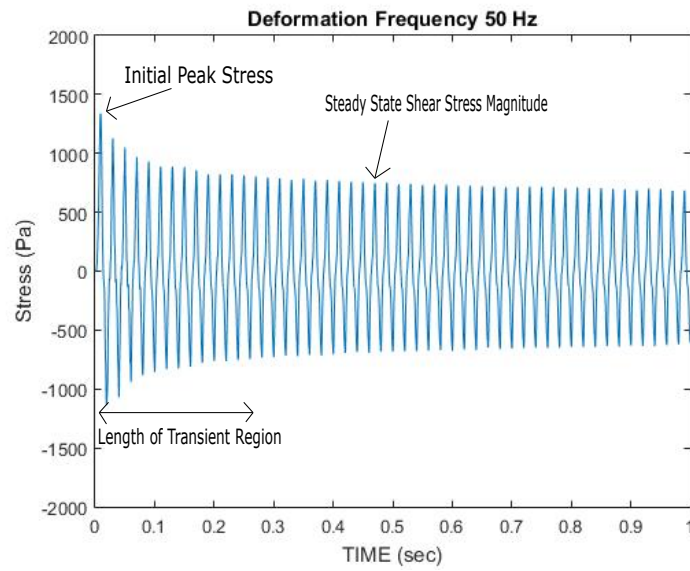
Figure 11: Shear stress response of a single specimen at 50 Hz deformation frequency showing the initial peak stress value in the transient region, approximate length of the transient region, and the apparent steady state shear stress magnitude.

4   Results

Brain tissue is tested under sinusoidal translational shear at varying deformation frequencies and displacement amplitudes to give insight on brain tissue response to damage. The brain tissue is subjected to a set of 50 cycles of sinusoidal translational shear at a given frequency followed by a 60 second period of stress relaxation, and then another set of 50 cycles of sinusoidal translational shear. The results are aimed at characterizing the dependence of the shear stress response to sinusoidal deformation at various frequencies and to determine whether damage can be identified in the shear stress response. The stress response at each deformation frequency in increasing order (i.e. 25 Hz to 125 Hz) is described.

In analyzing the shear stress response to sinusoidal deformation at various frequencies, the power throughout the signal and the location in time of significant frequency components are compared at all deformation frequencies and displacements, and between the first and second set of 50 cycles. The power of the signal over the set of 50 cycles is displayed in a power spectral density graph. The power spectrum is used in conjunction with harmonic wavelet decomposition to determine where the significant frequency components occur within the signal. Harmonic wavelet decomposition is able to capture both transient and apparent steady state regions, whereas Fourier analysis only captures steady state regions. An example of harmonic wavelet decomposition in a 25 Hz response is shown in Figure 12, and an example of the 125 Hz response is shown in 13. The transition from a deformation of 25 Hz to 125 Hz will be described throughout the results. The power spectrum and wavelet analysis are completed on all 50 cycles within the set, and therefore includes both the transient and apparent steady state regions.

The apparent steady state region is also examined to determine any difference in stress response after the initial deformation occurred. Decomposition of frequency components is performed on a single cycle within the apparent steady state region,

which is chosen to be cycle 20, based on the small change in amplitude of adjacent cycles. The decomposition of frequency components offers insight to the meaning of the separate harmonics and their influence on the stress response. The shape of the stress response curve gives information about the response to damage of brain structures. Each frequency component contributes to the overall shape of the stress response curve. For example, the third harmonic component adds a shoulder on the stress response curve and is attributed to interstitial fluid induced drag forces [32]. The Fourier fit graph shows how well an experimental data set matches with a specified Fourier fit equation. This gives information on which frequency components are present and the symmetry of the signal. It is used as a visualization of how each individual harmonic component contributes to the shape of the stress response curve. The magnitudes of significant harmonics within a single cycle in the apparent steady state are analyzed at all deformation frequencies.

As well as characterizing the stress response of brain tissue with increasing deformation frequency, the results also demonstrate damage that is occurring in the tissue. There are various indicators of possible damage in the shear stress response. Within the transient and apparent steady state regions, the power ratio of significant frequency components of the first and second set of 50 cycles are compared at each deformation frequency and displacement amplitude. The purpose of examining the power ratios are to determine any differences in the power of significant harmonics within the first set of 50 cycles compared to the second set of 50 cycles at a certain frequency and displacement. In the transient region, the initial peak stress value and the length of the transient region is recorded for each deformation frequency and displacement amplitude. The morphology of stress versus strain curves at each deformation frequency are compared to visualize the change in stress response from 25 Hz through 125 Hz. The stress versus strain graphs are completed over the entre set of 50 cycles. Lastly, to characterize damage that is occurring in the apparent steady state,

a comparison of the ratio of magnitudes of significant harmonics in cycle 20, after the initial damage has already occurred is completed at each deformation frequency and displacement amplitude. A ratio of the magnitudes at significant harmonics between the set of first 50 cycles and last 50 cycles are compared to determine if there are any significant differences after a relaxation period of 60 seconds.
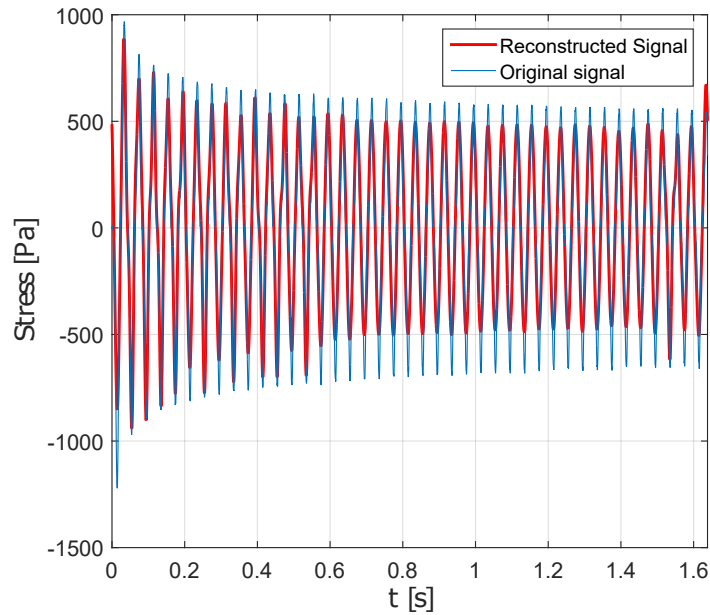
Figure 12: Harmonic wavelet decomposition curve and original stress curve for first 50 cycles of 25 Hz deformation frequency and 10% displacement for a single specimen.
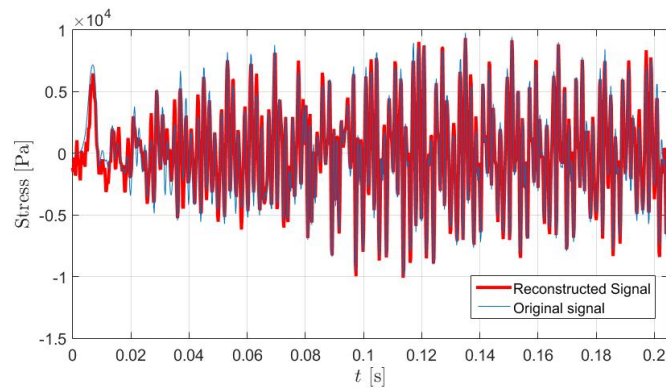
Figure 13: Harmonic wavelet decomposition curve and original stress curve for first 50 cycles of 125 Hz deformation frequency and 10% displacement for a single specimen.

4.1 Rate Dependence

The stress response due to increasing deformation frequencies is analyzed to determine effects of rate dependence on heterogeneous rat brain tissue. At deformation frequencies of 25 Hz through 125 Hz, the significant frequency components in the transient and apparent steady state regions are determined. The location of the significant frequency components are also determined via harmonic wavelet analysis, as demonstrated in Figures 12 and 13.

4.1.1 Frequency Analysis of 25 Hz

Analysis of Transient and Steady State Regions in set of 50 Cycles

Power Spectrum Analysis

The power of the signal is calculated over the entire set of 50 cycles (both first and last sets) for each specimen. Since it is calculated over the entire signal, it includes both the transient and apparent steady state regions. An example showing the power throughout the first 50 cycles at a deformation frequency of 25 Hz and 10% displacement is shown in Figure 14 for a single specimen. Although Figure 14 is only for one specimen, it is a typical response for all specimen at the specified deformation frequency and displacement. From Figure 14, the significant frequency components are the first and third harmonics. The significant frequency components are consistent for both the first and second set of 50 cycles and at 10% and 25% displacements. For this reason, only one power spectral density graph is provided. As expected, the power of the first and third harmonics are larger at a displacement of 25% as compared to 10%. Although the power is larger at 25% displacement, the same frequency components are present in both displacements. Tables 59 through 62 in Appendix A provide the power of significant harmonics throughout each set of 50 cycles at 10% and 25% displacement for each individual test at 25 Hz.
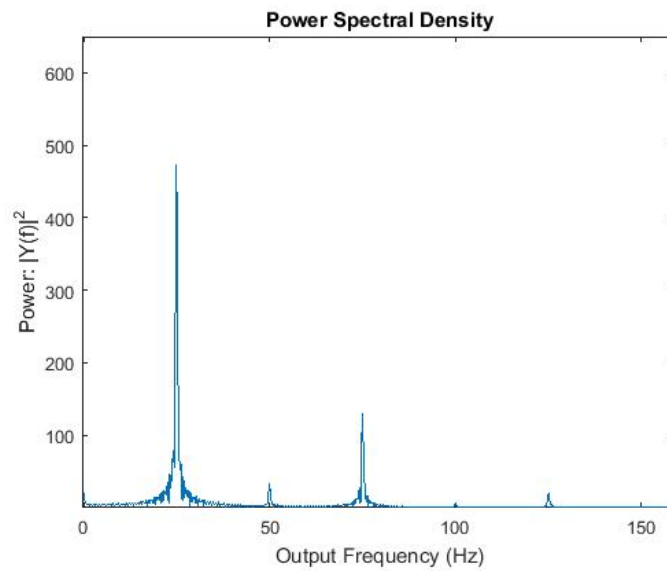
Figure 14: Power of frequency components throughout first 50 cycles with a deformation frequency of 25 Hz and 10% displacement for a single specimen.

As seen from the power spectrum of 25 Hz, the significant frequency components are the first and third harmonics. However, since the power spectrum is over the entire 50 cycles, it does not distinguish between the transient or apparent steady state regions, and does not give information on where the significant frequency components occurr in time. Harmonic wavelet analysis provides information on where the significant frequency components occur within the signal. Table 4 shows the j levels and their corresponding frequency range at a deformation frequency of 25 Hz. The j-level of 5 corresponds to a frequency range of 19.5 Hz to 39.1 Hz. This frequency range in conjunction with the Fourier analysis determines that the j-level of 5 corresponds to a frequency of 25 Hz, which is the first harmonic. There are also j-levels of 6 present, which correspond to a frequency range of 39.1 to 78.1 Hz. For the same reasoning, the $j=6$ level corresponds to a 75 Hz frequency, which represents the third harmonic. Tables 5 through 8 provide the j and k levels in specified bins for a deformation frequency of 25 Hz at the specified displacement and set of 50 cycles. These results are for a single specimen, but are typical of all specimen.

Table 4: Frequency ranges for j levels at a deformation frequency of 25 Hz.

j level	Lower Frequency Bound (Hz)	Upper Frequency Bound (Hz)
0	0.6	1.2
1	1.2	2.4
2	2.4	4.9
3	4.9	9.8
4	9.8	19.5
5	19.5	39.1
6	39.1	78.1
7	78.1	156.3
8	156.3	312.5
9	312.5	625.1
10	625.1	1250.2
11	1250.2	2500.3

Table 5 provides the j and k levels within each bin throughout the first 50 cycles of a deformation frequency of 25 Hz and 10% displacement. As mentioned in Section 3.4.4, for the $j = 5$ level, k spans from 0 to 31, and for the $j = 6$ level, k spans from 0 to 63. The $j = 5$ level (first harmonic) is present through all k levels, indicating that it is both in the transient and steady state response of the signal. The first harmonic is present in both low and high number bins, indicating that the wavelet amplitudes range from large amplitude to small amplitude, respectively. In contrast, the $j = 6$ level (third harmonic) is only present in high numbered bins, meaning the wavelets that make up the third harmonic have small amplitude. The third harmonic is also present throughout the entire signal, as indicated by the k levels ranging from 2 to 60.

Table 6 provides the j and k levels within each bin throughout the second set of 50 cycles at a deformation frequency of 25 Hz and 10% displacement. The first harmonic ($j = 5$ level) has a similar pattern as in the first 50 cycles. However, in contrast to the first set of 50 cycles, the third harmonic ($j = 6$ level), in the second set of 50 cycles is only present at very low k levels. Although similarly to the first set of 50 cycles, the third harmonic is only in the higher bin number with low amplitude wavelets.

Table 7 shows the j and k levels within each bin throughout the first 50 cycles of a deformation frequency of 25 Hz and 25% displacement. The first harmonic ($j = 5$ level) is present through all k levels, indicating that it is both in the transient and apparent steady state response of the signal. It is also present in low and high bins, showing that the wavelets have high and low amplitudes, respectively. In contrast, the third harmonic ($j = 6$ level) is only present in high numbered bins, meaning the wavelets have very small amplitude. The third harmonic is also present throughout quarter of the signal, as indicated by the k levels ranging from 0 to 18.

Table 8 shows the j and k levels within each bin throughout the second set of

Table 5: First 50 cycles at a deformation frequency of 25 Hz and 10% displacement for a single specimen (zshearsine60716a).

Bin Number	j level	k level
1	5	1
4	5, 5	0, 2
8	5	3
9	5, 5	4, 5
10	5, 5	6, 8
11	5, 5, 5, 5, 5	7, 9, 10, 11, 12
12	5, 5, 5, 5, 5, 5, 5, 5, 5	13, 14, 15, 16, 17, 18, 19, 22, 29
13	5, 5, 5, 5, 5, 5, 5, 5	20, 21, 23, 24, 25, 26, 27, 28
14	5, 5	30, 31
19	6, 6, 6, 6, 6, 6, 6, 6, 6, 6	2, 4, 5, 7, 10, 13, 16, 18, 21, 60

Table 6: Last 50 cycles at a deformation frequency of 25 Hz and 10% displacement for a single specimen(zshearsine60716a).

Bin Number	j level	k level
1	5, 5	1, 2
2	5	0
3	5, 5, 5	3, 4, 5
4	5	6
5	5, 5, 5, 5	7, 8, 9, 10
6	5, 5, 5, 5	11, 12, 13, 15
7	5, 5, 5, 5, 5, 5, 5, 5	14, 16, 17, 18, 19, 20, 22, 23
8	5, 5, 5, 5, 5, 5, 5, 5	21, 24, 25, 26, 27, 28, 29, 30
9	5	31
18	6, 6	2, 5

50 cycles of a deformation frequency of 25 Hz and 25% displacement. The first harmonic ($j = 5$ level) has a similar pattern as in the first 50 cycles. Similarly to the first set of 50 cycles, the third harmonic ($j = 6$ level) in the second set of 50 cycles is present throughout k levels of 0 through 17, throughout the transient and steady state response. The third harmonic contains wavelets only in higher bin numbers,

which are low amplitude wavelets.

Table 7: First 50 cycles at a deformation frequency of 25 Hz and 25% displacement for a single specimen (zshearsine60716g).

Bin Number	j level	k level
1	5	1
4	5	0
8	5	2
13	5, 5, 5	3, 4, 5
14	5, 5	6, 8
15	5, 5, 5, 5	7, 9, 11, 12
16	5, 5, 5, 5, 5, 5, 5, 5, 5, 5, 5	10, 13, 14 ,15, 16, 17, 18, 19, 22, 25, 29
17	5, 5, 5, 5, 5, 5, 5	20, 21, 23, 24, 26, 27, 28
18	5, 5, 6, 6, 6	30, 31, 2, 3, 4
19	6, 6, 6, 6, 6, 6, 6, 6, 6, 6	1, 5, 6, 7, 8, 10, 13, 15, 16, 18

Table 8: Last 50 cycles at a deformation frequency of 25 Hz and 25% displacement for a single specimen (zshearsine60716g).

Bin Number	j level	k level
1	5, 5	1, 2
4	5	3
5	5, 5, 5	0, 4, 5
6	5	6
7	5, 5	7,8
8	5	9
9	5, 5, 5, 5	10, 11, 12, 13
10	5, 5, 5, 5, 5, 5	14, 15, 16, 17, 18, 19
11	5, 5, 5, 5, 5, 5, 5, 5, 5	20, 21, 22, 23, 24, 25, 26, 28, 29
12	5, 5	27, 30
13	5	31
17	6, 6	2, 4
18	6, 6, 6, 6, 6, 6, 6, 6	1, 3, 5, 6, 7, 8, 9, 17

Analysis of Apparent Steady State

After the initial deformation occurs, the response reaches an apparent steady state that is marked by small change in amplitude of adjacent cycles. The magnitudes of significant harmonics are analyzed at cycle 20 for a deformation frequency of 25 Hz.

Significant Harmonics of Steady State Cycle and Fourier Decomposition

The magnitudes of significant harmonics within a single cycle in the apparent steady state are analyzed at 25 Hz. Cycle 20 is used in all magnitude calculations and is representative of the apparent steady state. However, any cycle within the apparent steady state is sufficient to use for magnitude calculations representing the apparent steady state. Within the apparent steady state at a deformation frequency of 25 Hz, the significant frequency components are the first and third harmonics. Magnitudes for each individual test at 25 Hz are found in Appendix B in Tables 91 through 94.

Figure 15 shows the frequency decomposition in cycle 20 containing the first and third harmonics and the original stress response for an individual specimen. From Figure 15, it is clear that the addition of a third harmonic creates a shoulder seen on the original stress response curve. The shoulder seen in the stress response is closely related to the third harmonic and fluid induced drag forces [32]. Figure 15 also demonstrates the symmetry in the stress response upon loading versus unloading. The addition of the first and third harmonics producing the original stress response curve is shown in Figure 16, where the shoulder effect due to the third harmonic is very clear.
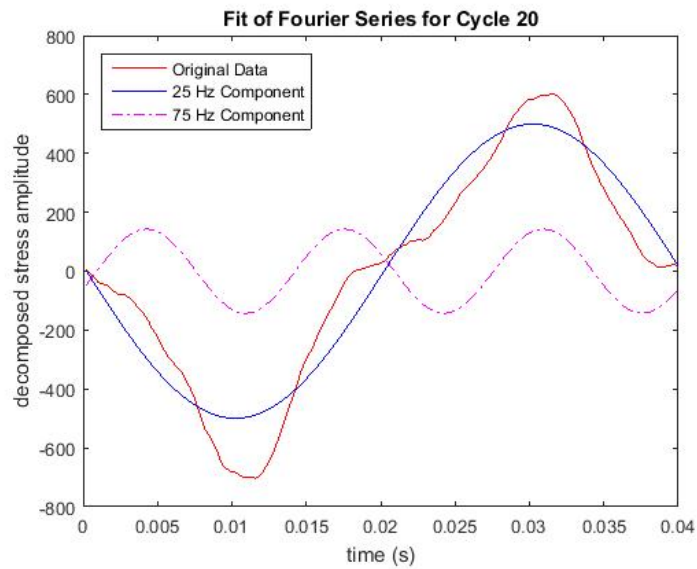
Figure 15: Frequency decomposition of the first and third harmonic components of the original data set at a deformation frequency of 25 Hz.
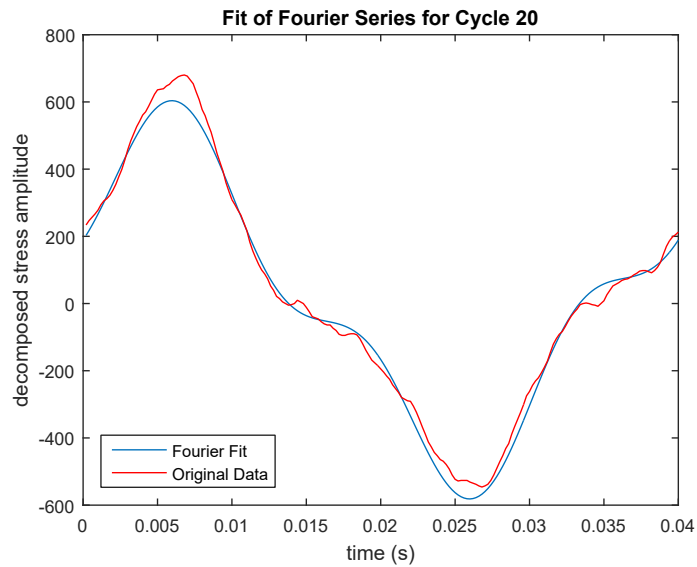
Figure 16: Example of Fourier fit function containing the first and third harmonics to the original data set with a deformation frequency of 25 Hz.

4.1.2 Frequency Analysis of 50 Hz

Analysis of Transient and Steady State Regions in set of 50 Cycles

Power Spectrum Analysis

Similarly to the 25 Hz response, at a deformation frequency of 50 Hz, the major frequency components are the first and third harmonics at both deformation amplitudes and both sets of cycles. Figure 17 displays the power spectral density graph over the first 50 cycles at 10% deformation. The power spectral density graph shows a large frequency component of 50 Hz (first harmonic) and 150 Hz (third harmonic). Similarly to 25 Hz, at a deformation frequency of 50 Hz, the frequency components in both the first and second set of 50 cycles and at 10% and 25% displacement were the same, therefore an example of only one power spectral density graph is provided. Tables 63 through 76 in Appendix A provide the power of the significant harmonics for each specimen at a deformation frequency of 50 Hz.
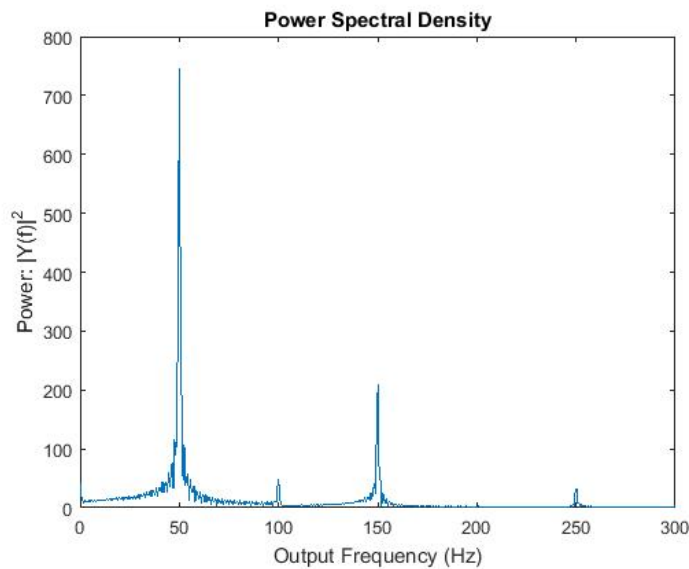
Figure 17: Power of frequency components throughout first 50 cycles (including transient and apparent steady state regions) with a deformation frequency of 50 Hz and 10% deformation for a single specimen.

Harmonic Wavelets

In reference to Table 9 and in conjunction with the Fourier analysis, the $j = 5$ level corresponds to the first harmonic (50 Hz) and the $j = 6$ level corresponds to the third harmonic (150 Hz). Tables 10 through 13 provide the j and k levels and bin numbers at the specified displacement amplitude and set of cycles.

Table 9: Frequency ranges for j levels at a deformation frequency of 50 Hz (T = 0.819).

j level	Lower Frequency Bound (Hz)	Upper Frequency Bound (Hz)
0	1.2	2.4
1	2.4	4.9
2	4.9	9.8
3	9.8	19.5
4	19.5	39.1
5	39.1	78.1
6	78.1	156.3
7	156.3	312.6
8	312.6	625.2
9	625.2	1250.3
10	1250.3	2500.6

Tables 10 and 11 provide the j and k levels at specific bins for the first and second set of 50 cycles at 10% displacement. In both the first and second set of 50 cycles, the first harmonic ($j = 5$) is present throughout the transient and apparent steady state regions, as marked by the k level ranging from 0 through 31. The first harmonic is also the only frequency component in the low bin levels (large amplitude wavelets). This is similar to what was seen at a deformation frequency of 25 Hz. The third harmonic ($j = 6$ level), is present throughout the beginning half of the signal in the first set of 50 cycles, but spans throughout the entire k range in the second set of 50 cycles. The $j = 6$ level is also still confined to the higher bin numbers, indicating it is composed of low amplitude wavelets.

Tables 12 and 13 provide the j and k levels at specific bins for the first and second set of 50 cycles at 25% displacement. At a deformation frequency of 50 Hz

Table 10: First 50 cycles at a deformation frequency of 50 HZ and 10% displacement for a single specimen (zshearsine60916b).

Bin Number	j level	k level
1	5	1
3	5	2
7	5	0
8	5	5
9	5, 5	3, 4
10	5	6
11	5, 5, 5	7, 8, 9
12	5, 5, 5, 5, 5	10, 11, 12, 13, 15
13	5, 5, 5, 5, 5, 5, 5, 5, 5, 5, 5	14, 16, 17, 18, 19, 20, 21, 22, 25, 26, 29
14	5, 5, 5, 5	23, 24, 27, 28
15	5, 5	30, 31
18	6, 6	1, 2
19	6, 6, 6, 6, 6, 6, 6, 6, 6, 6, 6, 6	3, 4, 5, 7, 10, 12, 13, 15, 18, 21, 29, 32

Table 11: Last 50 cycles at a deformation frequency of 50 Hz and 10% displacement for a single specimen (zshearsine60916b).

Bin Number	j level	k level
1	5, 5	1, 2
2	5, 5, 5	0, 3, 4
3	5, 5	5, 6
4	5, 5, 5, 5	7, 8, 9, 10
5	5, 5, 5, 5, 5	11, 12, 13, 14, 15
6	5, 5, 5, 5, 5, 5, 5	16, 17, 18, 19, 20, 21, 22
7	5, 5, 5, 5, 5, 5, 5, 5	23, 24, 25, 26, 27, 28, 29, 30
8	5	31
18	6, 6, 6, 6, 6, 6, 6, 6, 6, 6, 6, 6, 6, 6, 6, 6, 6, 6, 6, 6	0, 2, 3, 5, 6, 8, 11, 14, 16, 19, 22, 25, 30, 33, 36, 44, 47, 58, 61

and 25% displacement, the harmonic wavelet decomposition shows a $j = 5$ level (first harmonic) throughout all values of k, indicating the first harmonic is present in the transient and steady state regions within the first and second set of 50 cycles. In both

sets of 50 cycles, the first harmonic is also present in the low number bins and high numbered bins, meaning the wavelets associated with the first harmonic range from high amplitude to low amplitude. The third harmonic ($j = 6$ level) is present only at lower values of k (does not span the whole k region). This occurs in both the first and second set of 50 cycles. However, in the first set of 50 cycles, the third harmonic is in some of the low numbered bins, meaning those wavelets have a high amplitude. In the second set of 50 cycles, the third harmonic is only in the high numbered bins (low amplitude wavelets).

Table 12: First 50 cycles at a deformation frequency of 50 Hz and 25% displacement for a single specimen (zshearsine31016h).

Bin Number	j level	k level
1	5, 5	0, 1
8	5	2
12	6	1
13	5	5
14	5, 5, 5	3, 4, 6
15	5, 5, 6	8, 9, 2
16	5, 5, 5, 5, 5, 5, 5, 5, 5	7, 10, 11, 12, 13, 15, 16, 19, 29
17	5, 5, 5, 5, 5, 5, 5, 5, 5, 6	14, 17, 18, 20, 21, 22, 23, 25, 26, 28, 3
18	5, 5, 5	24, 27, 30
19	5, 6, 6, 6, 6, 6, 6	31, 0, 4, 5, 13, 14, 16

Table 13: Last 50 cycles at a deformation frequency of 50 Hz and 25% displacement for a single specimen (zshearsine31016h).

Bin Number	j level	k level
1	5, 5	1, 2
3	5	3
5	5, 5, 5, 5	0, 4, 5, 6
6	5, 5	7, 8
7	5, 5, 5	9, 10, 12
8	5, 5, 5, 5, 5	11, 13, 14, 15, 16
9	5, 5, 5, 5, 5	17, 18, 19, 20, 22
10	5, 5, 5, 5, 5, 5, 5, 5, 5	21, 23, 24, 25, 26, 27, 28, 29, 30
12	5	31
17	6, 6, 6, 6	3, 4, 6, 9

Analysis of Apparent Steady State

After the initial deformation occurs, the response reaches an apparent steady state that is marked by small change in amplitude of adjacent cycles. The magnitudes of significant harmonics are analyzed at cycle 20 for a deformation frequency of 50 Hz.

Significant Harmonics of Steady State Cycle and Fourier Decomposition

The magnitudes of significant harmonics at a deformation frequency of 50 Hz within cycle 20 are provided in Tables 95 through 98 in Appendix B. Similarly to 25 Hz, the significant harmonics seen in cycle 20 are the first and third harmonics. For this reason, the Fourier fit function contains only the first and third harmonics.

Figure 18 shows the Fourier fit curve containing the first and third harmonics with the original stress response curve. Similarly to the deformation frequency of 25 Hz, the 50 Hz response also has a clear shoulder in its stress response and demonstrates symmetry in loading and unloading.
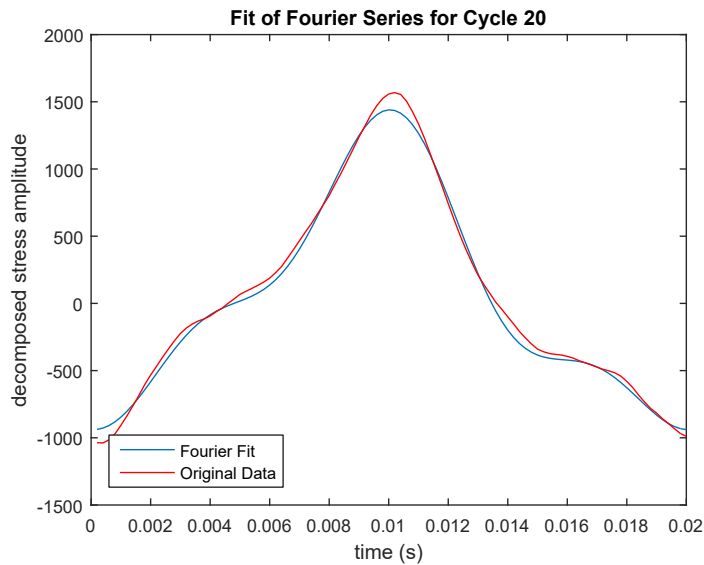
Figure 18: Example of Fourier fit function containing the first and third harmonics to the original data set with a deformation frequency of 50 Hz.

4.1.3 Frequency Analysis of 60 Hz

Analysis of Transient and Steady State Regions in set of 50 Cycles

Power Spectrum Analysis

Similarly to 25 Hz and 50 Hz, at a deformation frequency of 60 Hz and 10% displacement, the major frequency components are the first and third harmonics. However, at 25% displacement, there is also a significant ninth harmonic in addition to the significant first and third harmonics. Figure 19 shows the power spectral density graph over the first 50 cycles at 10% deformation. Figure 20 shows the power spectral density graph over the first 50 cycles at 25% deformation which shows the significant ninth harmonic. Although these power spectral density graphs are for a single specimen, they are typical responses for their respective displacements. Tables 77 through 80 in Appendix A provide the power of the significant harmonic components at a deformation frequency of 60 Hz for individual specimens.
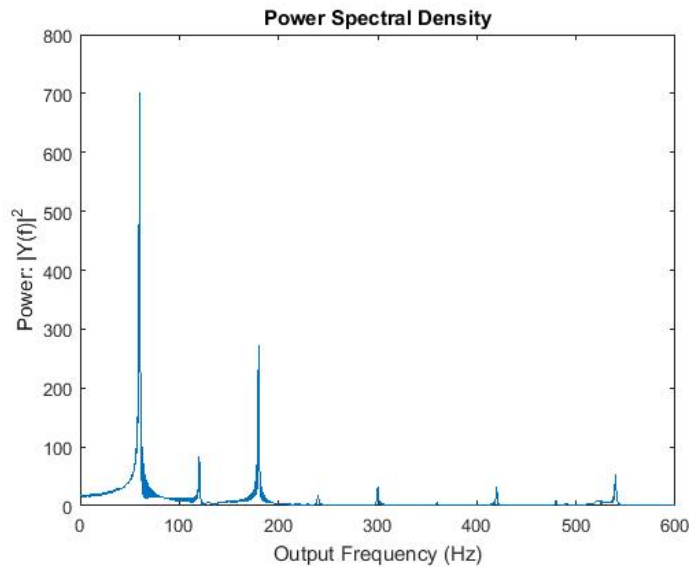
Figure 19: Power of frequency components throughout first 50 cycles (including transient and apparent steady state regions) with a deformation frequency of 60 Hz and 10% deformation for a single specimen.
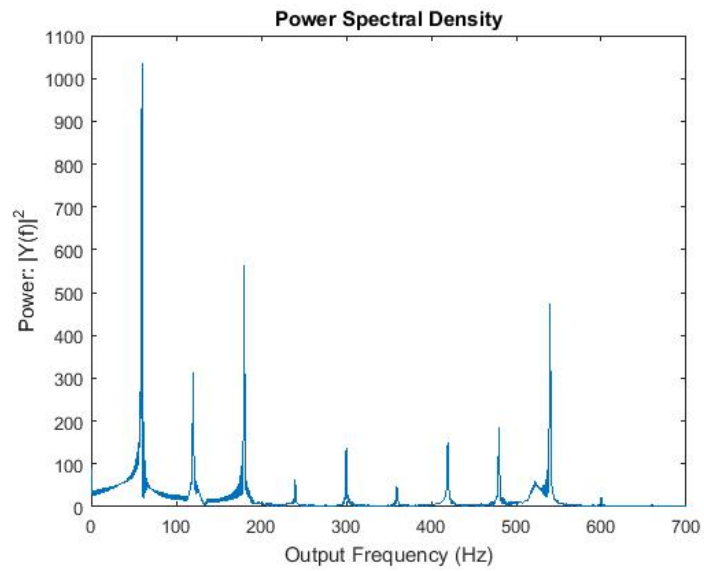
Figure 20: Power of frequency components throughout first 50 cycles (including transient and apparent steady state regions) with a deformation frequency of 60 Hz and 25% deformation for a single specimen.

Harmonic Wavelets

At a deformation frequency of 60 Hz and 10% displacement, the significant harmonics are the first and third harmonics. According to Table 14, the first harmonic corresponds to $j = 5$ level and the third harmonic corresponds to the $j = 7$ level. Additionally, at 25% displacement, there is also a significant ninth harmonic, which corresponds to the $j = 8$ level.

Table 14: Frequency ranges for j levels at a deformation frequency of 60 Hz under 0 % compression ($T = 0.8190$).

j level	Lower Frequency Bound (Hz)	Upper Frequency Bound (Hz)
0	1.2	2.4
1	2.4	4.9
2	4.9	9.8
3	9.8	19.5
4	19.5	39.1
5	39.1	78.1
6	78.1	156.3
7	156.3	312.6
8	312.6	625.2
9	625.2	1250.3
10	1250.3	2500.6

Tables 15 and 16 show the j and k levels at 10% displacement for a deformation frequency of 60 Hz. The Fourier analysis proved there to be significant first and third harmonics. The harmonics present within the signal are similar to that seen in 25 Hz and 50 Hz deformation frequencies. The first harmonic ($j = 5$) is present in small and large amplitude wavelets and throughout the transient and steady state regions. For the first set of 50 cycles, the third harmonic is present in the beginning of the signal and only contains small amplitude wavelets. However, just because the wavelet decomposition shows the third harmonic to be only in the transient region, this does not include the really small amplitude wavelets that are in bin 19 and 20, which could include third harmonic wavelets in the apparent steady state region. The third harmonic in the second set of 50 cycles at 10% displacement is in both the transient

and apparent steady state regions and composed of small amplitude wavelets.

Table 15: First 50 cycles at a deformation frequency of 60 Hz and 10% displacement for a single specimen (zshearsine71216a).

Bin Number	j level	k level
1	5	1
8	5	0
11	5	3
12	5, 5, 5	2, 4, 5
13	5	6
14	5, 5, 5, 5	7, 8, 9, 10
15	5, 5, 5, 5, 5, 5, 5, 5, 5	11, 12, 13, 14, 15, 16, 17, 19, 30
16	5, 5, 5, 5, 5, 5, 5, 5, 5, 5	18, 20, 21, 22, 23, 24, 25, 26, 27, 28
17	5	29
18	5, 7, 7, 7, 7	31, 2, 3, 4, 5

Table 16: Last 50 cycles at a deformation frequency of 60 Hz and 10% displacement for a single specimen (zshearsine71216a).

Bin Number	j level	k level
1	5	1
5	5	3
6	5, 5	2, 4
7	5, 5	5, 6
8	5, 5	7, 8
9	5, 5, 5	9, 10, 12
10	5, 5, 5, 5, 5, 5	11, 13, 14, 15, 16, 17
11	5, 5, 5, 5, 5, 5, 5, 5, 5	18, 19, 20, 21, 22, 23, 24, 26, 28
12	5, 5, 5	25, 27, 29
14	5	0
16	5, 7	30, 3
17	7, 7, 7, 7	2, 7, 11, 16

Similarly to the harmonic wavelet decomposition at a deformation frequency of 60 Hz and 10% displacement, at 25% displacement there are also significant first and third harmonics. However, there is also the addition of a significant ninth harmonic, which is represented by the $j = 8$ level. Tables 17 and 18 provide the j and k levels for

a deformation frequency of 60 Hz and 25% displacement. The first and ninth harmonic are both present in low numbered bins (composed of high amplitude wavelets). In the first 50 cycles, the first, third, and ninth harmonics are all only present in the transient region in the bins provided. The first, third, and ninth harmonics could still be in the apparent steady state region but composed in small amplitude wavelets in bins that were oversized (i.e. in bins 19 and 20). However in the second set of 50 cycles, the first harmonic is present only in the transient region and a high amplitude wavelet, the third harmonic is present only in the apparent steady state region, and the ninth harmonic is present in both the transient and apparent steady state regions.

Table 17: First 50 cycles at a deformation frequency of 60 Hz and 25% displacement for a single specimen (zshearsine61616d).

Bin Number	j level	k level
1	5	1
7	8	17
8	5, 8	0, 14
9	8	16
10	8	19
12	8, 8, 8	11, 13, 22
13	5	3
14	8, 8, 8	15, 18, 20
15	5, 5, 7, 8, 8	2, 5, 5, 35, 53

Table 18: Last 50 cycles at a deformation frequency of 60 Hz and 25% displacement for a single specimen (zshearsine61616d).

Bin Number	j level	k level
1	5	1
3	8	88
10	7, 7, 7, 7, 7, 8, 8, 8, 8, 8, 8, 8, 8, 8	17, 34, 41, 47, 50, 4, 39, 77, 103, 116, 125, 138, 142, 202
11	7, 7, 7, 7, 8, 8, 8, 8, 8, 8, 8, 8, 8	28, 30, 37, 60, 17, 30, 43, 69, 73, 99, 112, 129, 168
13	7, 7, 7, 8, 8, 8, 8, 8, 8, 8	11, 56, 84, 60, 82, 121, 146, 147, 159, 181

Analysis of Apparent Steady State

After the initial deformation occurs, the response reaches an apparent steady state that is marked by small change in amplitude of adjacent cycles. The magnitudes of significant harmonics are analyzed at cycle 20 for a deformation frequency of 60 Hz.

Significant Harmonics of Steady State Cycle and Fourier Decomposition

The magnitudes of significant harmonics in cycle 20 at a deformation frequency of 60 Hz are provided in Appendix B in Tables 99 through 102. Significant harmonics present within the apparent steady state are the first and third harmonics at 10% displacement; and the first, third, and ninth harmonics at 25% displacement.

Figure 21 shows the Fourier fit curve and the original stress response at 10% displacement. The higher harmonics are now appearing in the shoulder region at a displacement of 10%. Figure 22 shows the Fourier fit curve and original stress response at 25 % displacement. The Fourier fit curve contains a first, third, and ninth harmonic in order to accurately capture the morphology of the stress response curve. As shown in Figure 23, the Fourier decomposition demonstrates how the presence of a ninth harmonic disrupts the shoulder region. The transition from 60 Hz and 10% displacement to 60 Hz and 25% displacement marks a break in the patterns seen previously and a clear change in the morphology of the stress response curve. Figure 22 also exhibits a break in symmetry upon loading and unloading of the specimen.
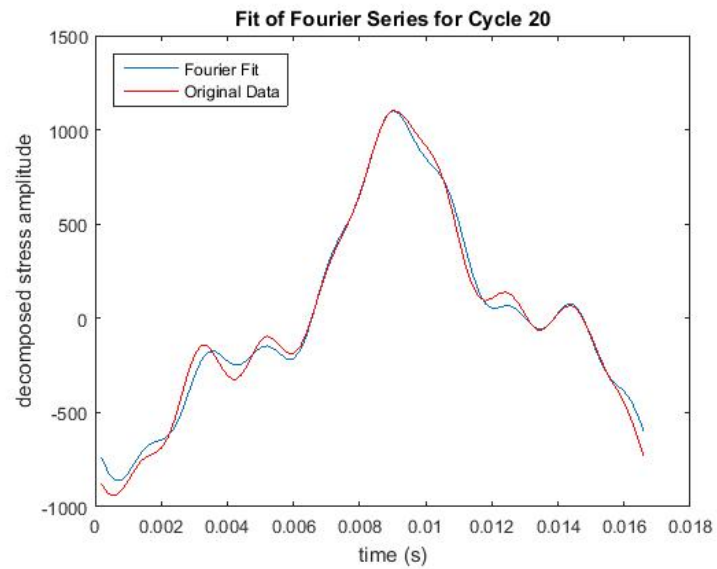
Figure 21: Example of Fourier fit function containing the first and third harmonics to the original data set with a deformation frequency of 60 Hz and 10% displacement.
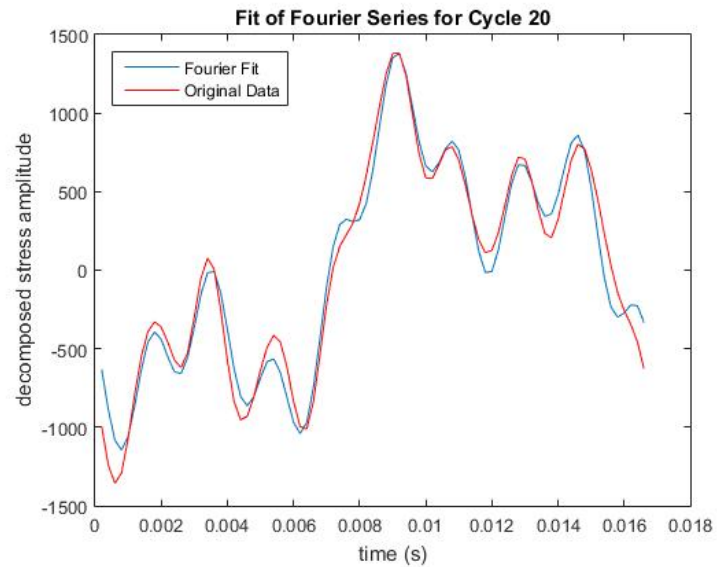
Figure 22: Example of Fourier fit function containing the first, third, and ninth harmonics to the original data set with a deformation frequency of 60 Hz and 25% displacement.
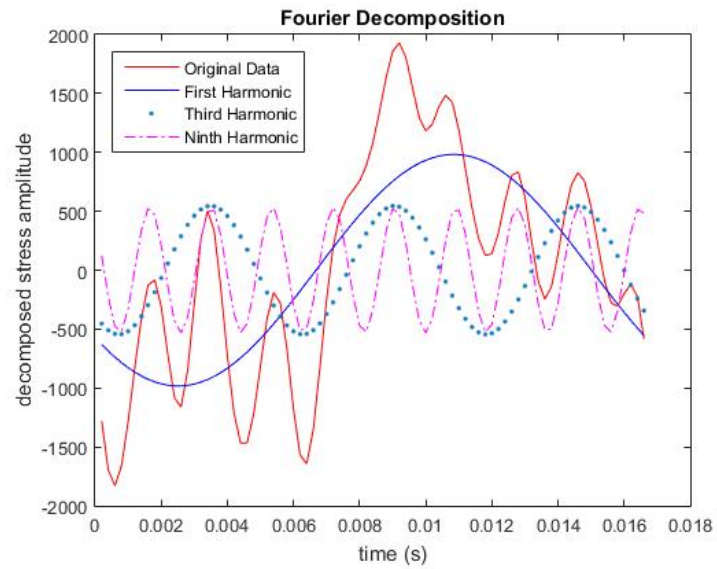
Figure 23: Fourier fit decomposition of the first, third, and ninth harmonics to the original data set with a deformation frequency of 60 Hz and 25% displacement.

4.1.4   Frequency Analysis of 75 Hz

Analysis of Transient and Steady State regions within set of 50 Cycles

Power Spectrum Analysis

At a deformation frequency of 75 Hz, the significant frequency components are the first, third, and seventh harmonics. Figure 24 shows the power through the first 50 cycles at 10% displacement, noting that the power of the seventh harmonic is significantly larger than the other harmonics. Along with the addition of higher harmonics, this is a significant change in the trends seen previously, because the power of the higher harmonics is now larger than the power of the lower harmonics. In deformation frequencies of 25 Hz through 60 Hz, the power of the lower harmonics were larger than those of the higher harmonics. Similarly to the lower deformation frequencies, the same trend continues in that the power of the frequency components at 25% displacement is larger than at 10 % displacement. Although the standard deviation of the first and last 50 cycles at a deformation amplitude of 25 % is very large, indicating a high variation in the response of individual specimens. A high variation is typical in testing of biological tissues. Tables 81 through 84 in Appendix A provide the power of the significant harmonic components at a deformation frequency of 75 Hz for individual specimen.
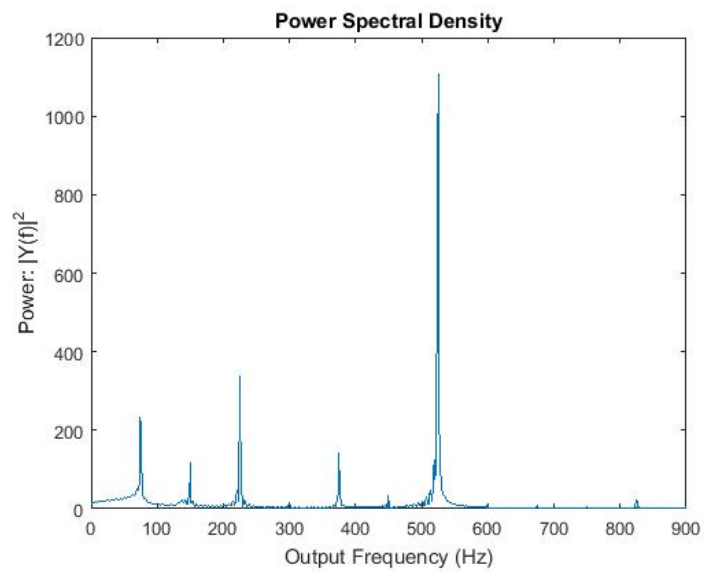
Figure 24: Power of frequency components throughout first 50 cycles (including transient and apparent steady state regions) with a deformation frequency of 75 Hz and 10% deformation for a single specimen(zshearsine61316g).

Harmonic Wavelet Analysis

Table 19 provides the j levels and its corresponding frequency range for a 75 Hz deformation frequency. The $j = 4$ level corresponds to the first harmonic, the $j = 5$ level corresponds to the second harmonic, the $j = 6$ level corresponds to the third harmonic, and the $j = 7$ level corresponds to both the fifth and seventh harmonics. This poses a problem as both the fifth and seventh harmonics are significant according to the Fourier analysis. However, the seventh harmonic is dominant compared to the fifth, so the $j = 7$ level is interpreted as the seventh harmonic.

Table 19: Frequency ranges for j levels at a deformation frequency of 75 Hz ($T = 0.4094$).

j level	Lower Frequency Bound (Hz)	Upper Frequency Bound (Hz)
0	2.4	4.9
1	4.9	9.8
2	9.8	19.5
3	19.5	39.1
4	39.1	78.2
5	78.2	156.3
6	156.3	312.7
7	312.7	625.3
8	625.3	1250.6
9	1250.6	2501.2

Table 20 and 21 provide the j and k levels at a deformation frequency of 75 Hz and 10% displacement. The harmonic wavelet decomposition shows that the seventh harmonic ($j=7$) is present throughout the entire signal (transient and steady state) and is composed of large amplitude wavelets. The first, second, and third harmonics are only present with low amplitude wavelets and in the transient region (small k levels); however they could be present in the apparent steady state in low amplitude wavelet bins. As seen previously, the higher harmonics were usually only present in the transient response and composed of low amplitude wavelets. This trend is similar to 60 Hz at 25% displacement.

Table 20: First 50 cycles at a deformation frequency of 75 Hz and 10% displacement for a single specimen (zshearsine61316g).

Bin Number	j level	k level
1	7, 7, 7, 7	59, 63, 80, 84
2	7, 7, 7, 7, 7, 7, 7, 7, 7, 7	38, 42, 55, 57, 61, 65, 67, 82, 88, 126
3	7, 7, 7, 7, 7, 7, 7	40, 44, 46, 76, 78, 86, 92
4	7, 7, 7, 7, 7, 7, 7, 7, 7	34, 36, 51, 53, 69, 71, 90, 113, 117
5	7, 7, 7, 7, 7, 7, 7, 7, 7, 7, 7, 7	32, 48, 50, 72, 74, 105, 107, 109, 111, 115, 121, 124
6	7, 7, 7, 7, 7, 7, 7, 7, 7, 7, 7, 7, 7, 7, 7	30, 47, 49, 52, 54, 70, 73, 75, 94, 96, 101, 103, 119, 123, 127
7	7, 7, 7, 7, 7, 7, 7	25, 68, 97, 99, 120, 122, 125
8	7, 7, 7, 7, 7, 7, 7, 7, 7, 7, 7, 7, 7, 7, 7, 7, 7, 7, 7, 7	21, 23, 27, 28, 29, 33, 43, 45, 56, 58, 60, 62, 64, 66, 77, 79, 95, 98, 100
9	7, 7, 7, 7, 7, 7, 7, 7, 7, 7, 7, 7, 7	26, 31, 35, 37, 39, 41, 81, 83, 85, 89, 91, 93, 118
10	7, 7, 7, 7, 7, 7, 7, 7	17, 19, 87, 102, 104, 108, 114, 116
11	7, 7	24, 112
12	7, 7, 7, 7	15, 22, 106, 110
13	7, 7	13, 20
14	7, 7	16, 18
15	7	14
16	7, 7, 7	0, 11, 12
17	4, 6, 7, 7	0, 2, 9, 10
18	4, 5, 6, 7	1, 0, 63, 8

Similarly to 10% displacement, at 25% displacement, the seventh harmonic is also present throughout the entire signal (transient and steady state) and it is composed of large and small amplitude wavelets. The third harmonic ($j = 6$) is present mostly in lower bins and in the transient region. The first harmonic ($j = 4$) and second harmonic ($j = 5$) are present at the very beginning of the signal (k= 0, 1) in the first

Table 21: Last 50 cycles at a deformation frequency of 75 Hz and 10% displacement for a single specimen (zshearsine61316g).

Bin Number	j level	k level
1	7, 7, 7, 7, 7, 7, 7, 7, 7, 7	28, 32, 53, 57, 78, 82, 99, 103, 107, 124
2	7, 7, 7, 7, 7, 7, 7, 7, 7, 7, 7, 7, 7, 7, 7, 7	7, 11, 30, 36, 49, 51, 55, 61, 74, 80, 86, 101, 105, 111, 120, 126
4	7, 7, 7, 7, 7, 7, 7, 7, 7, 7, 7, 7, 7, 7	5, 17, 19, 20, 22, 44, 47, 63, 72, 88, 90, 113, 116, 118
5	7, 7, 7, 7, 7, 7, 7, 7, 7, 7, 7, 7, 7, 7	16, 41, 42,43, 66, 67, 68, 69, 91, 92, 93, 94, 117, 127
6	7, 7, 7, 7, 7, 7, 7, 7, 7, 7, 7, 7, 7, 7, 7	18, 21, 23, 39, 46, 48, 62, 64, 73, 87, 89, 112, 114, 119, 121
8	7, 7, 7, 7, 7, 7, 7, 7, 7, 7, 7, 7, 7, 7	2, 6, 8, 54, 56, 75, 77, 79, 81, 100, 102, 104, 106 125
19	5, 6, 6	0, 0, 1

set of 50 cycles. In the last set of 50 cycles, the harmonic wavelet decomposition picks up on only the third and seventh harmonics. Similarly to the first set of 50 cycles, the seventh harmonic is present in large and small amplitude bins and throughout the signal, whereas the third harmonic is present only in small amplitude bins and in the transient region.

Table 22: First 50 cycles at a deformation frequency of 75 Hz and 25% displacement for a single specimen (zshearsine72516g).

Bin Number	j level	k level
1	7, 7	47, 51
2	7	49
3	4, 7, 7, 7, 7, 7	0, 34, 38, 43, 45, 55
4	7, 7, 7	30, 36, 53
5	7, 7	13, 32
6	6, 7, 7, 7, 7, 7, 7	2, 17, 40, 41, 42, 57, 59
7	7, 7, 7, 7, 7	15, 26, 39, 72, 76
8	7, 7, 7, 7, 7	44, 68, 70, 74, 80
9	7, 7, 7, 7, 7, 7, 7, 7	22, 61, 64, 66, 78, 97, 101, 126
10	7, 7, 7, 7, 7, 7, 7, 7, 7, 7, 7, 7	24, 28, 46, 63, 82, 84, 93, 95, 99, 103, 105, 122
11	5, 7, 7, 7, 7, 7, 7, 7, 7, 7, 7, 7, 7, 7	1, 11, 19, 20, 21, 37, 48, 60, 62, 91, 107, 118, 120, 124
12	7, 7, 7, 7, 7, 7, 7, 7, 7, 7, 7	35, 50, 52, 56, 58, 65, 86, 88, 89, 109, 116
13	5, 7, 7, 7, 7, 7, 7, 7, 7	0, 18, 54, 67, 85, 87, 111, 113, 114
14	7, 7, 7, 7, 7, 7, 7, 7	9, 14, 16, 69, 90, 92, 110, 112
15	6, 7, 7, 7, 7, 7, 7, 7, 7, 7, 7, 7	4, 6, 10, 23, 25, 31, 33, 71, 81, 83, 115, 117
16	6, 7, 7, 7, 7, 7, 7, 7, 7, 7, 7, 7, 7	1, 8, 29, 73, 75, 77, 79, 94, 96, 98, 104, 106, 108
17	4, 6, 6, 6, 7, 7, 7, 7, 7, 7, 7, 7, 7	1, 5, 6, 7, 5, 12, 27, 100, 102, 119, 121, 123, 127
18	3, 6, 6, 6, 6, 6, 6, 6, 7, 7, 7	0, 8, 9, 11, 23, 25, 27, 63, 0, 4, 125

Table 23: Last 50 cycles at a deformation frequency of 75 Hz and 25% displacement for a single specimen (zshearsine72516g).

Bin Number	j level	k level
1	7, 7, 7, 7, 7, 7, 7, 7, 7, 7	42, 46, 67, 71, 90, 92, 96, 115, 117, 121
2	7, 7, 7, 7, 7, 7, 7, 7, 7, 7, 7, 7, 7, 7	4, 17, 19, 21, 40, 44, 48, 65, 69, 88, 94, 113, 119, 127
3	7, 7, 7, 7, 7, 7, 7, 7, 7, 7, 7, 7, 7, 7	2, 15, 23, 25, 38, 50, 61, 63, 73, 75, 86, 98, 100, 111
4	7, 7, 7, 7, 7, 7	13, 36, 84, 109, 123, 125
5	7, 7, 7, 7, 7, 7, 7, 7	11, 27, 29, 52, 54, 59, 77, 102
6	7, 7, 7, 7, 7, 7, 7	8, 34, 57, 79, 82, 104, 107
7	7, 7, 7, 7, 7	6, 7, 9, 32, 105
8	7, 7, 7, 7, 7, 7, 7, 7	1, 31, 33, 55, 56, 58, 80, 81
9	7, 7, 7, 7, 7, 7	10, 78, 83, 103, 106, 108
10	7, 7, 7, 7	5, 30, 53, 124
11	7, 7, 7, 7, 7, 7, 7, 7, 7, 7, 7, 7, 7	3, 12, 28, 35, 37, 51, 60, 76, 85, 99, 101, 110, 126
12	7, 7, 7, 7, 7, 7, 7, 7	0, 14, 26, 49, 62, 74, 87, 112
14	7, 7, 7, 7, 7	18, 22, 43, 68, 93
17	6, 6, 6, 6, 6	2, 4, 6, 8, 63
19	6, 6, 6, 6, 6, 6, 6, 6	28, 30, 32, 53, 55, 57, 59, 62

Analysis of Apparent Steady State

After the initial deformation occurs, the response reaches an apparent steady state that is marked by small change in amplitude of adjacent cycles. The magnitudes of significant harmonics are analyzed at cycle 20 for a deformation frequency of 75 Hz.

Significant Harmonics of Steady State Cycle and Fourier Decomposition

The magnitudes of a significant harmonics within the apparent steady state at 75 Hz are provided in Appendix B in Tables 103 through 106. The significant harmonics present in the steady state at 10% and 25% displacement are the first, third, and seventh harmonics, noting that the seventh is much larger than both the first and third. There is also a significant fifth harmonic present at 25% displacement.

Figure 26 shows the addition of the first, third, and seventh harmonics in recreating the original data curve for a 75 Hz a deformation frequency. From Figure 25 , it is clear that the peaks and the troughs of the individual frequency components add together to produce the morphology seen in the original data curve. Similarly to at 60 Hz, the addition of the higher harmonics disrupts the presence of a shoulder in the stress response curve and is asymmetric about the vertical axis.
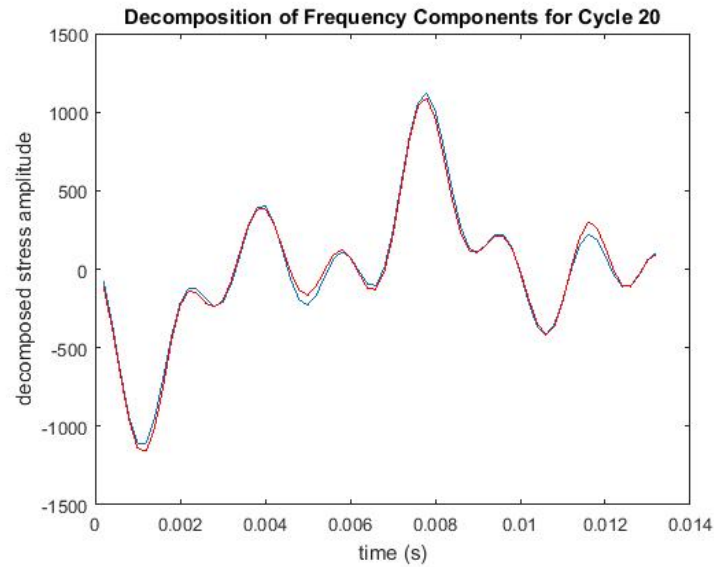
Figure 25: Example of Fourier fit function containing the first, third, fifth, and seventh harmonics to the original data set with a deformation frequency of 75Hz.
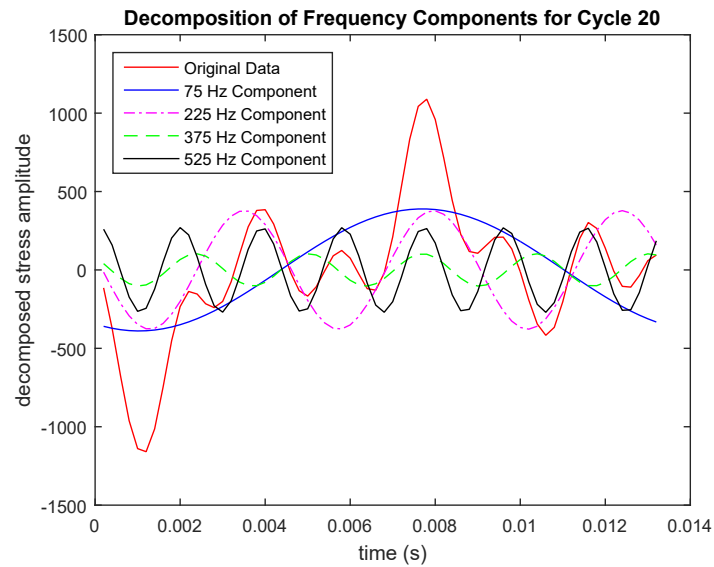
Figure 26: Frequency Decomposition containing the first, third, and seventh harmonics and the original data set with a deformation frequency of 75 Hz (for a single specimen).

4.1.5 Frequency Analysis of 100 Hz

Analysis of Transient and Steady State regions within set of 50 Cycles

Power Tables and Power Spectrum

At a deformation frequency of 100 Hz and 10% displacement, the significant frequency components are the first, third, and fifth harmonics. Similarly to at 75 Hz, the higher significant harmonics are larger in power than the lower harmonics. Figure 27 shows the power spectral density graph of a 100 Hz a deformation frequency signal which displays the increase in power at higher harmonics. However, at 25% displacement, the significant harmonics are the first, third, fifth, and sixth. Significant even harmonics suggest breaking in symmetry during the unloading and loading of the specimen. Significant even harmonics were not seen in the previous input frequencies at either displacements. Tables 85 through 88 in Appendix A provide the power of the significant harmonic components at a deformation frequency of 100 Hz for individual specimen.
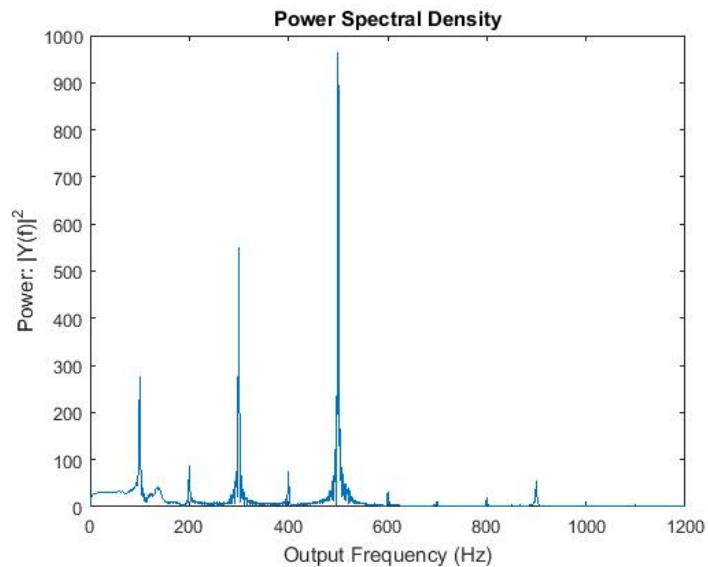
Figure 27: Power of frequency components throughout first 50 cycles (including transient and apparent steady state regions) with a deformation frequency of 100 Hz and 10% deformation for a single specimen.
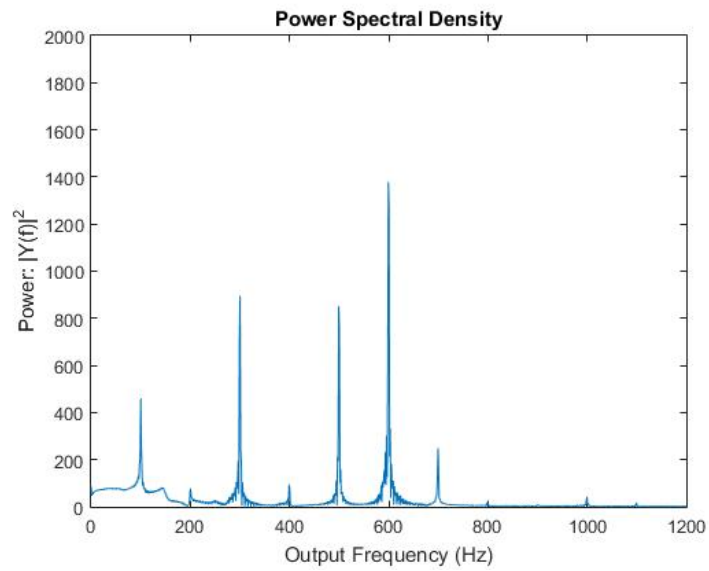
Figure 28: Power of frequency components throughout first 50 cycles (including transient and apparent steady state regions) with a deformation frequency of 100 Hz and 25% deformation for a single specimen.

Harmonic Wavelets

Table 24 provides the j levels and corresponding frequency ranges for a deformation frequency of 100 Hz. From the Fourier analysis, the 100 Hz signal at 10% displacement has significant first, third, and fifth harmonics. At 25% displacement, there is the addition of a significant sixth harmonic. The $j = 5$ level corresponds to the first harmonic, the $j = 6$ level corresponds to the third harmonic, and the $j = 7$ level corresponds to both the fifth and sixth harmonic. This is not a problem at 10% displacement because there is no significant sixth harmonic. However, this is a problem at 25% displacement where this is a significant fifth and sixth harmonic.

Table 24: Frequency ranges for j levels at a deformation frequency of 100 Hz ($T = 0.4094$).

j level	Lower Frequency Bound (Hz)	Upper Frequency Bound (Hz)
0	2.4	4.9
1	4.9	9.8
2	9.8	19.5
3	19.5	39.1
4	39.1	78.2
5	78.2	156.3
6	156.3	312.7
7	312.7	625.3
8	625.3	1250.6
9	1250.6	2501.2

Tables 25 and 26 provide the j and k levels at specific bins for a deformation frequency of 100 Hz and 10% displacement. The fifth harmonic ($j =7$) is composed of large amplitude wavelets that span throughout the signal. In contrast, the first ($j=5$) and third ($j=6$) harmonic have only smaller amplitude wavelets, and are present in the transient region, which is similar to the 75 Hz response.

As previously mentioned, the $j = 7$ level corresponds to the fifth and sixth harmonic. This was not an issue in the 10% displacement, as there was no significant sixth harmonic. However, at a displacement of 25% there is a significant fifth and

Table 25: First 50 cycles at a deformation frequency of 100 Hz and 10% displacement for a single specimen.

Bin Number	j level	k level
1	7, 7	100, 122
2	7, 7, 7, 7, 7, 7, 7, 7, 7, 7, 7, 7, 7, 7	56, 72, 75, 78, 81, 84, 97, 103, 106, 109, 112, 119, 125, 127
3	7, 7, 7, 7, 7, 7, 7, 7	47, 50, 53, 59, 69, 87, 94, 115
4	7, 7, 7, 7, 7, 7, 7, 7, 7, 7, 7	34, 37, 44, 62, 65, 66, 88, 90, 91, 116, 124
5	7, 7, 7, 7, 7, 7, 7, 7, 7, 7, 7, 7, 7, 7, 7, 7, 7, 7, 7, 7	22, 25, 28, 31, 38, 40, 41, 63, 68, 71, 85, 93, 96, 99, 107, 110, 113, 118, 121
6	7, 7, 7, 7, 7, 7, 7, 7, 7, 7, 7	35, 43, 46, 49, 57, 60, 74, 79, 82, 102, 104
7	7, 7, 7, 7, 7, 7, 7, 7, 7, 7	9, 19, 52, 54, 76, 77, 80, 101, 105, 126,
9	5, 7, 7, 7, 7, 7, 7, 7, 7, 7, 7, 7, 7	1, 13, 16, 23, 26, 27, 33, 36, 39, 42, 45, 61, 64
10	7, 7, 7, 7	11, 15, 18, 30
11	7, 7, 7	7, 8, 20
12	7	14
13	6, 7, 7	5, 6, 17
14	6	8
15	5, 5, 6, 6, 6, 6, 6, 6, 6, 6, 6, 6, 6, 6, 6, 6	0, 2, 11, 13, 14, 16, 19, 22, 27, 30, 33, 36, 41, 44, 47, 55, 58
16	6, 6, 6, 6, 6, 6, 6, 6, 6, 6, 6, 6, 6, 6, 6, 6	6, 7, 10, 21, 24, 25, 28, 35, 38, 39, 49, 50, 52, 53, 60, 61, 61
18	5, 5, 6, 6, 6, 6, 6, 7	3, 5, 0, 1, 9, 12, 62, 4
19	3, 5, 5, 5, 5, 5, 5, 6, 8	0, 4, 6, 7, 8, 9, 12, 4, 0

sixth harmonic. The harmonic wavelet decomposition cannot distinguish between these two harmonics, as they are in the same level. The trend seen Tables 27 and 28 are the same as in 10% displacement and 100 Hz a deformation frequency. The $j = 7$ level is present in large and small amplitude wavelet bins and in both the transient and apparent steady state region, whereas the first and third harmonics are present

Table 26: Last 50 cycles at a deformation frequency of 100 Hz and 10 % displacement for a single specimen.

Bin Number	j level	k level
1	7, 7, 7	116, 119, 126
2	7, 7, 7, 7, 7, 7, 7, 7, 7, 7, 7, 7, 7, 7	60, 63, 66, 79, 82, 85, 88, 91, 94, 101, 104, 107, 110, 113
3	7, 7, 7, 7, 7, 7, 7, 7, 7, 7, 7, 7, 7, 7	32, 35, 38, 41, 51, 54, 57, 69, 72, 73, 76, 97, 98, 122
4	7, 7, 7, 7, 7, 7, 7, 7, 7, 7, 7	44, 47, 48, 50, 70, 75, 78, 95, 100, 103, 123
5	7, 7, 7, 7, 7, 7, 7, 7, 7, 7, 7, 7, 7, 7, 7, 7, 7	6, 7, 23, 26, 29, 45, 53, 56, 67, 81, 92, 106, 109, 114, 117, 120, 125
6	7, 7, 7, 7, 7, 7, 7, 7, 7, 7, 7, 7, 7	8, 19, 20, 22, 28, 31, 42, 64, 84, 86, 89, 111, 124
8	7, 7, 7, 7, 7, 7, 7, 7, 7, 7, 7, 7, 7, 7, 7, 7, 7	5, 10, 37, 40, 43, 46, 49, 52, 55, 65, 68, 71, 74, 77, 80, 93, 102, 127
9	7, 7, 7, 7, 7, 7	9, 13, 17, 18, 21, 30
10	7, 7, 7, 7	4, 11, 24, 27
12	7, 7	14, 15
13	6, 6, 6, 7, 7	4, 5, 7, 3, 12
14	5, 6, 6, 6, 6, 6	2, 2, 10, 13, 21, 60
15	6, 6, 6, 6, 6, 6, 6, 6, 6, 6, 6, 6, 6, 6, 6, 6	15, 16, 18, 19, 24, 27, 29, 30, 32, 35, 38, 41, 43, 46, 49, 52, 57
16	5, 6, 6, 6, 6, 6, 6, 6, 6, 6, 6, , 6, 6, 6, 6, 6, 7	0, 8, 12, 22, 26, 33, 37, 40, 44, 47, 51, 54, 55, 58, 59, 61, 0
18	6	3
19	5, 5, 5, 5, 5, 5, 5, 5, 5, 6, 7, 7	3, 5, 6, 7, 8, 9, 10, 11, 12, 0, 1, 2

in the beginning of the signal and composed of small amplitude wavelets.

Table 27: First 50 cycles at a deformation frequency of 100 Hz and 25% displacement for a single specimen (J100H41416b).

Bin Number	j level	k level
1	7, 7, 7, 7, 7, 7, 7, 7, 7, 7	62, 65, 68, 87, 90, 93, 109, 112, 115, 118
2	7, 7, 7, 7, 7	59, 71, 84, 96, 121
3	7, 7, 7, 7	40, 43, 46, 106
4	7, 7, 7, 7, 7, 7	49, 56, 74, 81, 99, 124
5	5, 7, 7, 7	1, 37, 52, 102
6	7, 7, 7, 7	53, 77, 78, 103
7	7, 7	55, 105
8	7, 7, 7, 7	34, 75, 80, 100
9	7, 7, 7, 7, 7, 7	50, 58, 83, 108, 125, 127
11	7, 7, 7, 7, 7	61, 72, 86, 97, 122
12	7, 7, 7, 7, 7, 7	30, 31, 33, 36, 47, 111
13	5, 7, 7, 7, 7, 7, 7, 7, 7	0, 9, 10, 27, 39, 64, 89, 114, 119
14	6, 7, 7, 7, 7, 7	5, 6, 7, 42, 69, 94
15	7, 7, 7, 7, 7, 7, 7, 7, 7	0, 13, 24, 28, 44, 67, 92, 116, 117
16	4, 5, 7, 7, 7, 7, 7, 7, 7, 8	0, 2, 12, 45, 66, 70, 91, 95, 120, 0
17	6, 6, 6, 6, 7, 7, 7, 7, 7, 7, 7, 7, 7, 7	1, 8, 11, 13, 16, 21, 25, 41, 48, 63, 73, 88, 98, 113, 123

Table 28: Last 50 cycles at a deformation frequency of 100 Hz and 25% displacement for a single specimen (J100H41416b).

Bin Number	j level	k level
1	7, 7, 7, 7, 7, 7, 7, 7, 7, 7, 7	43, 65, 68, 87, 90, 93, 96, 112, 115, 118, 121
2	7, 7, 7, 7, 7, 7, 7, 7, 7	18, 37, 40, 46, 62, 71, 84, 109, 124
3	7, 7, 7, 7, 7, 7	15, 21, 34, 59, 74, 99
4	7, 7, 7, 7	24, 49, 81, 106
5	7, 7, 7, 7, 7, 7, 7	12, 27, 31, 52, 56, 77, 102
6	7, 7, 7, 7	30, 55, 80, 105
7	7, 7, 7, 7, 7, 7	5, 9, 28, 53, 78, 103
8	7, 7, 7, 7, 7, 7	6, 8, 33, 58, 83, 108
9	7, 7	100, 111
10	7, 7, 7, 7, 7, 7, 7, 7, 7, 7	2, 11, 25, 36, 50, 61, 75, 86, 122, 125
11	7, 7, 7, 7, 7, 7, 7	3, 14, 39, 64, 89, 97, 114
12	7, 7, 7, 7	17, 42, 47, 72
13	7, 7, 7, 7, 7, 7	20, 22, 67, 92, 117, 119
14	7, 7, 7, 7, 7, 7, 7, 7, 8	44, 45, 69, 70, 94, 95, 120, 123, 0
15	7, 7, 7, 7, 7, 7, 7	19, 23, 48, 73, 91, 98, 116
16	7, 7, 7, 7, 7, 7, 7, 7, 7	16, 26, 29, 41, 51, 66, 76, 101, 127
17	7, 7, 7, 7, 7, 7, 7, 7, 7, 7, 7, 7, 7, 7, 7, 7, 7	4, 7, 32, 35, 38, 54, 57, 60, 63, 79, 82, 85, 88, 104, 107, 110, 113, 126
18	6, 6, 6, 6, 6, 6, 6, 6, 6, 6, 7, 7	2, 5, 8, 11, 16, 19, 22, 30, 33, 63, 10, 13

Analysis of Apparent Steady State

After the initial deformation occurs, the response reaches an apparent steady state that is marked by small change in amplitude of adjacent cycles. The magnitudes of significant harmonics are analyzed at cycle 20 for a deformation frequency of 100 Hz.

Significant Harmonics of Steady State Cycle and Fourier Decomposition

The magnitudes of significant harmonics for a deformation frequency of 100 Hz at cycle 20 are found in Appendix B in Tables 107 through 110. At 10% displacement, the significant harmonics are the first, third, and fifth harmonics. At 25% displacement, the significant harmonics are the first, third, fifth, and sixth harmonics.

Figure 29 shows the Fourier fit curve containing the first, third, fifth, and sixth harmonic and the original stress response curve at 100 Hz and 25% displacement. With the addition of higher harmonics, any shoulder region representing the third harmonic is indistinguishable and there is no symmetry about the vertical axis. However, this does not mean there is no third harmonic, just that the higher harmonics dominate the third harmonic.
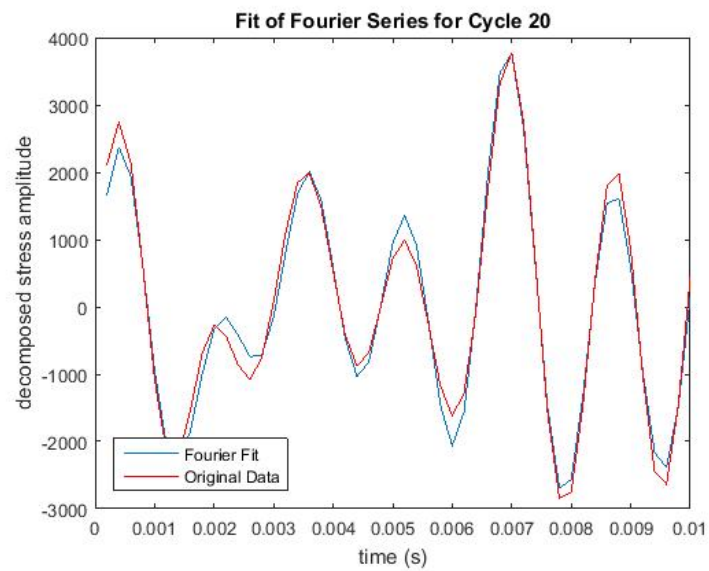
Figure 29: Example of Fourier fit function containing the first, third, fifth, and sixth harmonics to the original data set with a deformation frequency of 100 Hz and 25% displacement.

4.1.6   Frequency Analysis of 125 Hz

Analysis of Transient and Steady State regions within set of 50 Cycles

Power Spectrum Analysis

At a deformation frequency of 125 Hz, only 10% displacement is analyzed because of the limitations of the Bose machine. The significant harmonics in both the first and last set of 50 cycles are the first, third, fourth, fifth, sixth, and seventh. Figure 30 shows the power spectral density graph over the first 50 cycles. There is a very large fourth harmonic, which once again demonstrates symmetry breaking at the higher deformation frequencies. Tables 89 and 90 in Appendix A provide the power of significant harmonics for each specimen at a deformation frequency of 100 Hz and 10% displacement.
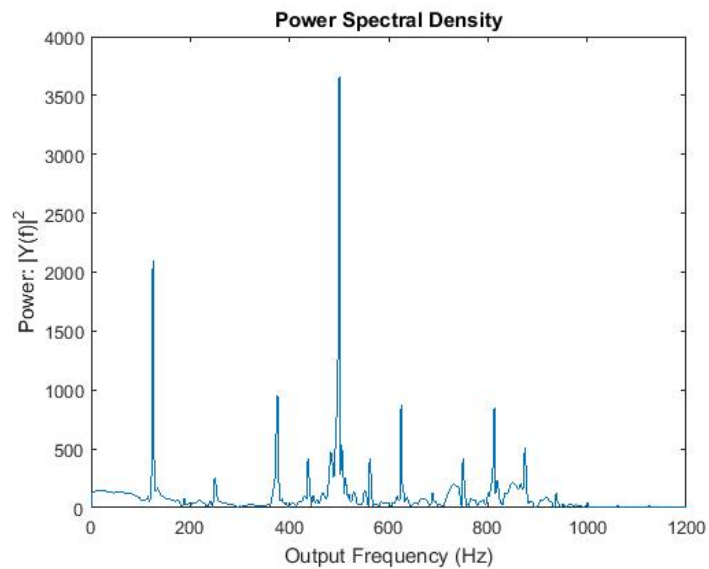
Figure 30: Power of frequency components throughout first 50 cycles (including transient and apparent steady state regions) with a deformation frequency of 125 Hz and 10 % deformation for a single specimen (zshearsine82216f).

Harmonic Wavelets

The significant harmonics in the 125 Hz deformation frequency are the first, third, fourth, and fifth harmonics. The $j = 4$ level corresponds to the first harmonic; the $j = 6$ level corresponds to the third, fourth, and fifth harmonics; and the $j = 7$ level corresponds to the sixth and seventh harmonics. The overlap in frequency ranges limits the ability to distinguish between specific harmonics.

Table 29: Frequency ranges for j levels at a deformation frequency of 125 Hz ($T = 0.2046$).

j level	Lower Frequency Bound (Hz)	Upper Frequency Bound (Hz)
0	4.9	9.8
1	9.8	19.6
2	19.6	39.1
3	39.1	78.2
4	78.2	156.4
5	156.4	312.8
6	312.8	625.6
7	625.6	1251.2
8	1251.2	2502.4

As shown in the Fourier analysis, a deformation frequency of 125 Hz has significant the first, third, fourth, fifth, sixth, and seventh harmonics. Because of the j level range, there is a problem in distinguishing many of the significant harmonics. These are all considered significant harmonics and cannot be distinguished from one another in harmonic wavelet decomposition. Although the harmonics cannot be individually distinguished, it is still apparent that the higher harmonics are present in the large amplitude bins and throughout the entirety of the signal. Whereas the first harmonic is only present in small amplitude wavelets and at the beginning of the signal. This trend is consistent with that seen at a deformation frequency of 100 Hz.

Table 30: First 50 cycles at a deformation frequency of 125 Hz and 10% displacement for a single specimen (zshearsine82316c).

Bin Number	j level	k level
1	6	28
5	6	33
6	6, 6	32, 37
7	6	42
8	6	63
9	6, 6, 6, 6, 6, 6, 6	31, 47, 51, 53, 56, 58, 61
10	6, 6, 6, 6, 6, 6, 6	14, 29, 36, 38, 43, 46, 48
11	6, 6, 6	27, 34, 41
12	6, 6, 6, 6, 7, 7, 7	11, 19, 30, 52, 45, 57, 67
13	6, 6, 6, 6, 7, 7, 7, 7	16, 44, 49, 57, 47, 50, 56, 68
14	6, 6, 6, 7	39, 54, 62, 46
15	6, 6, 6, 6, 7, 7, 7, 7, 7, 7, 7, 7, 7, 7, 7, 7, 7, 7, 7	9, 17, 26, 59, 51, 58, 59, 78, 87, 88, 94, 97, 100, 104, 107, 110, 117, 120, 127
16	6, 7, 7, 7, 7, 7, 7, 7	25, 66, 69, 77, 84, 90, 114, 124
17	4, 4, 6, 6, 6, 6, 6, 7, 7, 7, 7, 7, 7, 7	9, 15, 12, 13, 18, 22, 35, 44, 48, 80, 98, 103, 113, 123

Table 31: Last 50 cycles at a deformation frequency of 125 Hz and 10% displacement for a single specimen (zshearsine82316c).

Bin Number	j level	k level
1	6	25
4	6, 6	30, 34
5	6, 6	29, 39
7	6	44
8	6, 6, 7	28, 33, 45
9	6, 6	46, 49
10	6, 6, 6, 6	11, 35, 41, 51
11	6, 6, 6, 6, 7	31, 36, 40, 54, 40
12	6, 6, 6, 6, 6, 6, 6, 6, 7	16, 24, 38, 45, 56, 59, 61, 63, 46
13	6, 6, 6, 6, 6, 6, 6, 6, 6, 6	6, 9, 14, 23, 43, 48, 50, 53, 55, 58
14	6, 6, 7	26, 60, 41
15	6, 7, 7, 7, 7	27, 42, 51, 82, 92
16	6, 6, 6, 7, 7, 7, 7, 7, 7, 7, 7, 7, 7, 7	8, 13, 22, 39, 62, 72, 85, 91, 98, 101, 102, 108, 111, 122

Analysis of Apparent Steady State

After the initial deformation occurs, the response reaches an apparent steady state that is marked by small change in amplitude of adjacent cycles. The magnitudes of significant harmonics are analyzed at cycle 20 for a deformation frequency of 125 Hz.

Significant Harmonics of Steady State Cycle and Fourier Decomposition

The magnitudes of significant harmonics in cycle 20 at a deformation frequency of 125 Hz are provided in Appendix B in Tables 111 and 112.

Figure 31 shows the Fourier fit curve containing the first, third, fourth, fifth, sixth, and seventh harmonics and the original stress response curve for a single cycle and single specimen. The stress response curve is similar to that of 100 Hz, in that there is no visible shoulder and no symmetry due to the other dominant harmonics.
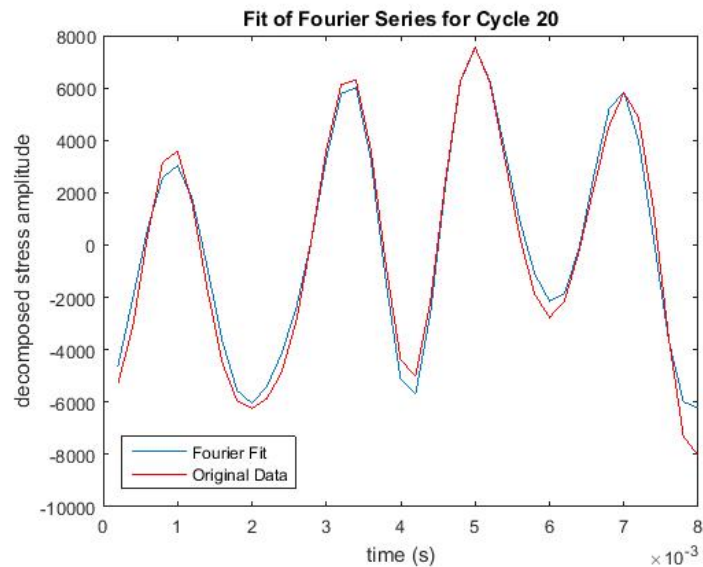
Figure 31: Example of Fourier fit function containing the first, third, fourth, fifth, sixth and seventh harmonics to the original data set with a deformation frequency of 125 Hz.

4.2 Damage

Section 4.1 characterizes the stress response of brain tissue with increasing deformation frequency. This section examines indicators of damage in the shear stress response in the transient and apparent steady state regions. Within the transient and apparent steady state regions, the power ratio of significant frequency components of the first and second set of 50 cycles are compared at each deformation frequency and displacement amplitude. The purpose of examining the power ratios are to determine any differences in the power of significant harmonics within the first set of 50 cycles compared to the second set of 50 cycles at a certain frequency and displacement. In the transient region, the initial peak stress value and the length of the transient region is recorded for each deformation frequency and displacement amplitude. The morphology of stress versus strain curves at each deformation frequency are compared to visualize the change in stress response from 25 Hz through 125 Hz. The stress versus strain graphs are completed over the entire set of 50 cycles. To characterize damage that occurs in the apparent steady state, a comparison of the ratio of magnitudes of significant harmonics in cycle 20, after the initial damage has already occurred is completed at each deformation frequency and displacement amplitude. A ratio of the magnitudes at significant harmonics between the set of first 50 cycles and last 50 cycles are compared to determine if there are any significant differences after a relaxation period of 60 seconds. Lastly, the shear stress magnitude of cycle 20 is compared at all deformation frequencies and displacement amplitudes.

4.2.1 Transient and Steady state Analysis

Power Ratios

The power ratio is calculated to determine if there is a significant difference in the power of significant harmonics between the first and second set of 50 cycles. The ratio is calculated by taking the power of significant harmonics in the first set of

50 cycles over the second set of 50 cycles. The ratio indicates the change in power between the first and second set of 50 cycles. A change in power between the sets of cycles offers information on possible damage or fluid redistribution during the 60 second period of relaxation between the sets of cycles. The tests were performed in deformation control, so if the specimen takes less stress to deform, it is not as strong. This indicates that a power ratio above 1 means damage occurs, because the power of significant harmonics is less in the second set of 50 cycles. A ratio that is greater than one means that the power in the first set of 50 cycles is larger than the power over the second set of 50 cycles. A ratio that is less than one means the power throughout the second set of 50 cycles is larger than the power throughout the first set of 50 cycles. Tables 32 through 37 provide the power ratios for 10% and 25% displacement at deformation frequencies of 25 Hz through 125 Hz.

The ratio of powers between the first and second set of 50 cycles at 25 Hz is given in Table 32. Ratios at all significant harmonics are greater than one (power in the first set of cycles is larger than that in the second set), except for the fifth harmonic. Table 33 provides the power ratios at a deformation frequency of 50 Hz. All significant harmonics have ratios greater than one, indicating that the power in the first set is larger than the set of 50 cycles at a deformation frequency of 50 Hz. At a deformation frequency of 60 Hz, the power ratio is greater than one in all significant harmonics except for the seventh harmonic at 10% displacement, as shown in Table 34. At a deformation frequency of 75 Hz, Table 35 shows all power ratios are greater than one except for the seventh and ninth harmonics at 10% displacement. Table reftab:PowerRatio100Hz shows all power ratios are greater than one except for the second and seventh harmonics at 10% displacement and deformation frequency of 100 Hz. Lastly, at a deformation frequency of 125 Hz, all power ratios are greater than one, as shown in Table 37.

Table 32: Ratio of power of significant harmonics between the set of first 50 cycles and last 50 cycles at a deformation frequency of 25 Hz.

Significant Harmonic	Ratio of first 50 cycles to last 50 cycles	
	10 % Displacement	25 % Displacement
1	1.08	1.04
2	1.26	1.04
3	1.07	1.01
5	0.98	0.91

Table 33: Ratio of power of significant harmonics between the set of first 50 cycles and last 50 cycles at a deformation frequency of 50 Hz.

Significant Harmonic	Ratio of first 50 cycles to last 50 cycles	
	10 % Displacement	25 % Displacement
1	1.17	1.14
2	1.38	1.10
3	1.09	1.13
5	1.85	1.12

Table 34: Ratio of power of significant harmonics between the set of first 50 cycles and last 50 cycles at a deformation frequency of 60 Hz.

Significant Harmonic	Ratio of first 50 cycles to last 50 cycles	
	10 % Displacement	25 % Displacement
1	1.13	1.22
2	1.24	1.47
3	1.12	1.15
5	1. 03	1.26
7	0.92	1.07
9	1.03	1.05

Table 35: Ratio of power of significant harmonics between the set of first 50 cycles and last 50 cycles at a deformation frequency of 75Hz.

Significant Harmonic	Ratio of first 50 cycles to last 50 cycles	
	10 % Displacement	25 % Displacement
1	1.32	1.34
2	1.21	1.16
3	1.27	1.28
5	1.22	1.13
7	0.98	1.11
9	0.91	1.50

Table 36: Ratio of power of significant harmonics between the set of first 50 cycles and last 50 cycles at a deformation frequency of 100 Hz.

Significant Harmonic	Ratio of first 50 cycles to last 50 cycles	
	10 % Displacement	25 % Displacement
1	1.43	1.15
2	0.85	1.19
3	1.19	1.21
5	1.16	1.41
6	1.39	0.96
7	0.85	1.32
9	1.10	0.93

Table 37: Ratio of power of significant harmonics between the set of first 50 cycles and last 50 cycles at a deformation frequency of 125 Hz.

Significant Harmonic	Ratio of first 50 cycles to last 50 cycles	
	10 % Displacement	25 % Displacement
1	1.22	NA
2	1.11	NA
3	1.18	NA
4	1.09	NA
5	1.13	NA
6	1.09	NA
7	1.29	NA
9	1.56	NA

4.2.2 Transient Region

Initial Peak Stress values

Comparing the initial peak stress values at varying deformation frequencies and between the first and second set of 50 cycles offers insight on damage occurring with increasing deformation frequencies and how stress relaxation effects the stress response. Tables 38 through 43 provide the peak stress values of the first cycle in the first and second set of 50 cycles for all deformation frequencies and displacements. At all deformation frequencies and at both 10% and 25% displacement, the initial peak stress is higher in the first set of 50 cycles than in the second set of 50 cycles. At 10% displacement, the initial peak stress average in the first set of 50 cycles increases with increasing deformation frequency. For example, the initial peak stress average at 25 Hz and 10% displacement is 1447.9 Pa, and the initial peak stress average at 125 Hz is 7033.6 Pa. This trend is not seen in the initial peak stress average in the second set of 50 cycles at 10% displacement. However, this increase of initial peak stress with increasing deformation frequency is not seen at 25% displacement, but only at 10% displacement. This may partially be due to the standard deviation at 25% displacement, which tends to be higher than that at 10% displacement, indicating high specimen variation which is typical of biological tissues.

Table 38: Peak stress of the first cycle in the first and second set of 50 cycles at 10% and 25% displacement a deformation frequency of 25 Hz.

Test Number	Initial Peak Stress Value (Pa)			
	10% displacement		25% displacement	
	First 50 Cycles	Last 50 Cycles	First 50 Cycles	Last 50 Cycles
1	2085	1084	5176	1656
2	1426	905.8	5682	2843
3	1194	933.6	3479	2130
4	1264	920.5	4135	3262
5	2366	1532	4712	1586
6	1079	789.7	3062	1687
7	1135	799.5	2446	1449
8	961.4	721	2632	2680
9	2551	1529	4351	1781
10	1856	1091	3005	1627
11	1086	727.6	3417	1602
12	1277	1025	4699	711.2
13	542.8	454.5	3124	1465
14	NA	NA	2917	1601
AVG	1447.9	962.6	3774.1	1862.9
SD	590.3	304.7	1013.1	660.0

Table 39: Peak stress of the first cycle in the first and second set of 50 cycles at 10% and 25% displacement a deformation frequency of 50 Hz.

Test Number	Initial Peak Stress Value (Pa)			
	10% displacement		25% displacement	
	First 50 Cycles	Last 50 Cycles	First 50 Cycles	Last 50 Cycles
1	1158	773.4	5530	1411
2	2044	1248	5422	2153
3	2590	1373	5150	4603
4	1333	963	4189	1879
5	1292	1184	4359	1424
6	1985	1197	5302	1828
7	1784	1133	4109	1951
8	1341	882.9	4858	1228
9	1509	1058	4920	1913
10	3358	1730	6424	2493
11	NA	NA	5464	2441
12	NA	NA	6162	1064
AVG	1839.4	1154.2	5157.4	2032.3
SD	692.3	269.9	723.5	925.8

Table 40: Peak stress of the first cycle in the first and second set of 50 cycles at 10% and 25% displacement a deformation frequency of 60 Hz.

Test Number	Initial Peak Stress Value (Pa)			
	10% displacement		25% displacement	
	First 50 Cycles	Last 50 Cycles	First 50 Cycles	Last 50 Cycles
1	2992	1717	5147	1700
2	1095	763.5	7109	2050
3	1422	873.1	4589	1751
4	2161	1143	5019	1476
5	1856	1063	4002	2796
6	1444	1122	5186	2039
7	3231	1785	3057	1517
8	1931	1439	4866	2057
9	1319	842	1.13E+04	2430
10	1625	1267	8442	1774
11	2881	1633	4313	1658
12	1620	1010	4567	1110
13	1130	763.5	2215	1370
14	1802	1382	2672	1372
15	2580	1145	1913	1058
AVG	1939.3	1196.5	4959.8	1743.9
SD	687.4	335.4	2454.4	473.6

Table 41: Peak stress of the first cycle in the first and second set of 50 cycles at 10% and 25% displacement a deformation frequency of 75 Hz.

Test Number	Initial Peak Stress Value (Pa)			
	10% displacement		25% displacement	
	First 50 Cycles	Last 50 Cycles	First 50 Cycles	Last 50 Cycles
1	2273	1597	6386	3492
2	1937	2222	1.04E+04	5103
3	1592	1400	6914	1969
4	2776	2022	4161	2441
5	2132	2439	5304	2647
6	1130	896	4604	2137
7	1906	1141	6099	2238
8	2328	979.4	6220	1218
9	2802	1436	5804	3556
10	2184	1099	8253	6417
11	2386	1323	NA	NA
12	2662	1419	NA	NA
12	2006	1210	NA	NA
14	2369	1310	NA	NA
AVG	2177.4	1463.8	6414.5	3121.8
SD	455.6	461.1	1814.0	1581.2

Table 42: Peak stress of the first cycle in the first and second set of 50 cycles at 10% and 25% displacement a deformation frequency of 100 Hz.

Test Number	Initial Peak Stress Value (Pa)			
	10% displacement		25% displacement	
	First 50 Cycles	Last 50 Cycles	First 50 Cycles	Last 50 Cycles
1	4416	1911	6502	6860
2	1987	1391	6563	2261
3	2472	1138	3630	1339
4	1543	1375	2381	1288
5	2884	1880	4485	1305
6	3296	2518	3501	681.8
7	2605	954.8	3224	1424
8	2268	1557	4128	1135
9	2242	1184	5261	1745
10	NA	NA	3937	1333
11	NA	NA	2524	961.4
AVG	2634.8	1545.4	4194.2	1848.5
SD	836.6	486.1	1415.9	1710.8

Table 43: Peak stress of the first cycle in the first and second set of 50 cycles at 10% and 25% displacement a deformation frequency of 125 Hz.

Test Number	Initial Peak Stress Value (Pa)	
	10% displacement	
	First 50 Cycles	Last 50 Cycles
1	9445	4918
2	7089	3548
3	5018	6388
4	5212	3510
5	8875	3422
6	7735	6775
7	5929	5584
8	5976	2067
9	8023	6574
AVG	7033.6	4754
AD	1596.8	1687.4

Table 44: Average inital peak stress value for all deformation frequencies and displacement amplitudes in the first and second sets of 50 cycles.

Deformation Frequency	Average Initial Peak Stress (Pa)			
	10% displacement		25% displacement	
	First 50 Cycles	Last 50 Cycles	First 50 Cycles	Last 50 Cycles
25	1447.9	962.6	3774.1	1862.9
50	1839.4	1154.2	5157.4	2032.3
60	1939.3	1196.5	4959.8	1743.9
75	2177.4	1463.8	6414.5	3121.8
100	2634.8	1545.4	4194.2	1848.5
125	7033.6	4754.0	NA	NA

Length of Transient Region in first and second set of 50 Cycles

The length of the transient region is calculated for both the first and second set of 50 cycles at all deformation frequencies and displacements. To find the length of the transient region, the magnitude of five adjacent cycles is taken. When the magnitudes of all five adjacent cycles are within 10% of each other, they are considered to be in the apparent steady state. The transient region contains cycles with magnitudes that differ greater than 10%. The k range of the transient region is then found using $t = 2^{n-j}k\Delta$ where t is the time it takes to complete the amount of cycles in the transient region, as discussed in Section 3.4.4. The length of the transient regions and associated k ranges for all deformation frequencies and displacement amplitudes is found in Appendix C. Appendix C includes both 10% and 25% displacement amplitudes, however, since the length of the transient region is used to quantify differences occurring between the first and second set of 50 cycles, only graphs for 10% displacement amplitude are provided in this section.

On average, at 25 Hz and 10% displacement, it takes between 3 and 4 cycles to reach steady state within the first set of 50 cycles (Figure 38a). Whereas at the same deformation frequency and displacement, it only takes 1 cycle to reach an apparent steady state in the second set of 50 cycles (Figure 38b). In contrast, at a deformation frequency of 25 Hz and 25% displacement, it takes on average 7 cycles to reach an apparent steady state in the first set of 50 cycles, and about 4 cycles to reach an apparent steady state in the second set of 50 cycles.

At a deformation frequency of 50 Hz and 10% displacement, it takes on average 4 to 5 cycles to reach an apparent steady state within the first 50 cycles (Figure 39a). However, in the second set of 50 cycles (Figure 39b), an apparent steady state is reached after only one cycle, similarly to the 25 Hz deformation frequency. At a deformation frequency of 50 Hz and 25% displacement, an apparent steady state is reached after an average of 14 cycles within the first set of cycles and after only 5

cycles in the second set of cycles. Similar trends exist at deformation frequencies of 60 Hz through 125 Hz.

Briefly, at 60 Hz and 10% displacement, it takes on average 5 to 6 cycles to reach an apparent steady state in the first set of 50 cycles (Figure 40a), whereas it only takes 2 cycles on average to reach an apparent steady state in the second set of 50 cycles (Figure 40b). At 60 Hz and 25% displacement, an apparent steady state is reached after an average of 12 cycles in the first set of 50 cycles, and an average of 2 to 3 cycles in the second set of 50 cycles. Similarly, at 75 Hz and 10% displacement, an apparent steady state is reached after an average of 6 to 7 cycles in the first set of 50 cycles (Figure 41a), and only 1 cycle in the second set of 50 cycles (Figure 41b). At 75 Hz and 25% displacement, an apparent steady state is reached after an average of 16 cycles in the first set of 50 cycles and only 4 cycles in the second set of 50 cycles. At a deformation frequency of 100 Hz and 10% displacement, an apparent steady state is reached after 7 cycles in the first set of 50 cycles (Figure 42a) and 1 to 2 cycles in the second set of 50 cycles (Figure 42b). At 100 Hz and 25% displacement, an apparent steady state was reached after 13 cycles in the first set of 50 cycles, and only 3 to 4 cycles in the second set of 50 cycles. At 125 Hz and 10% displacement, it takes on average 18 cycles to reach an apparent steady state in the first set of 50 cycles (Figure 43a), and 8 cycles on average to reach an apparent steady state in the second set of 50 cycles (Figure 43b).

Overall, at all deformation frequencies and displacement amplitudes, there is a longer transient region in the first set of 50 cycles compared to the second set of 50 cycles. Also, the transient region at 25% displacement is longer than at 10% displacement for all deformation frequencies. At 10% displacement, in the first set of 50 cycle, the length of the transient region increases with increasing deformation frequency. The length of the transient region in the last set of 50 cycles at 10% displacement stays around 1 to 2 cycles for all deformation frequencies, except at

(a) Set of first 50 cycles

(b) Set of last 50 cycles
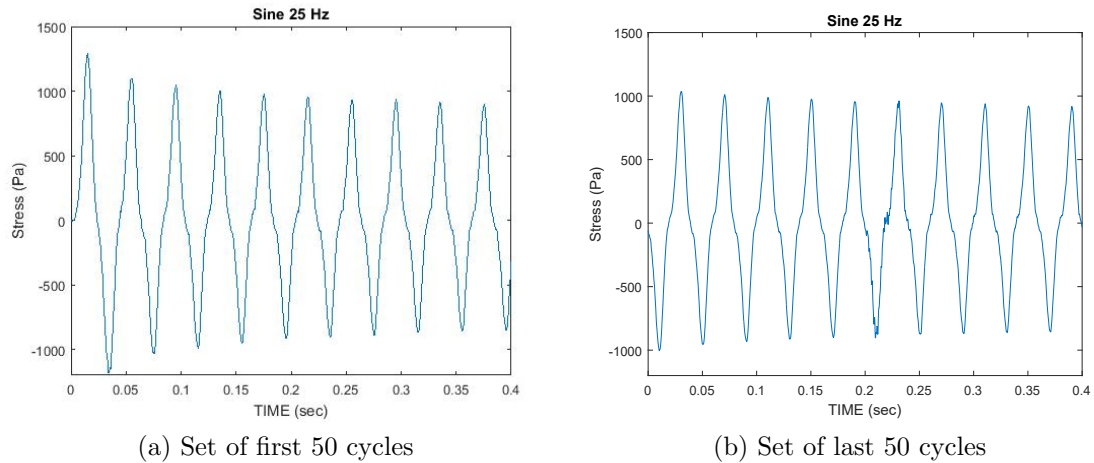
Figure 32: First 10 cycles of stress response of a single specimen with a deformation frequency of 25 Hz and 10% displacement.

125 Hz deformation frequency, which has a transient region length of 8 cycles. At 25% displacement amplitude in the first set of 50 cycles, there is not a clear trend in the length of the transient region with respect to deformation frequency. The average length of the transient regions at all deformation frequencies and displacement amplitudes are summarized in Table 45.

Figures 32 through 37 show examples from a single specimen of the first 10 cycles at each deformation frequency and at 10% displacement. At all deformation frequencies at 10% displacement, there is a much more noticeable transient region in the first set of 50 cycles. Although there still is a transient region in the second set of 50 cycles, it is less prominent and reaches an apparent steady state quicker than that in the first 50 cycles. All figures are for a single specimen, however, they represent a typical response. The stress response graphs at 25% displacement are omitted because they have the same morphology as the 10% displacement; they only differ in amplitude.

(a) Set of first 50 cycles

(b) Set of last 50 cycles
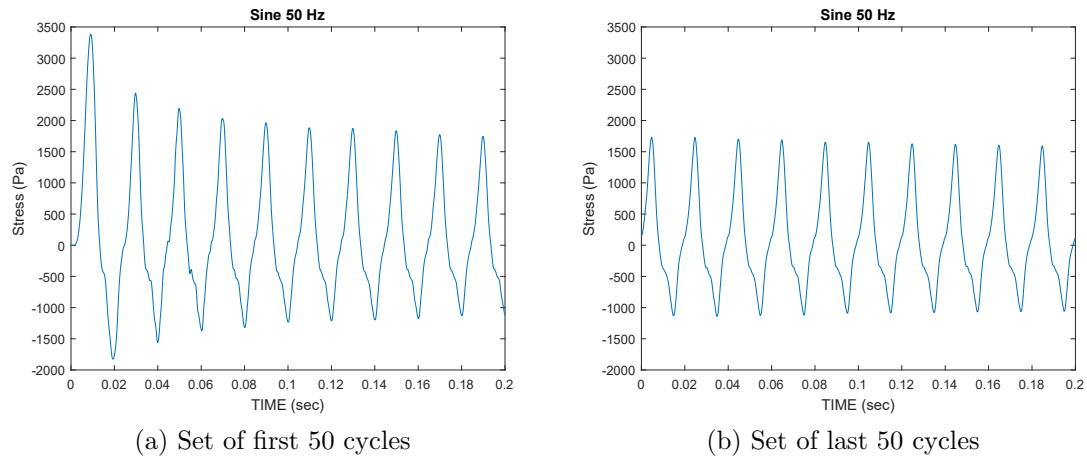
Figure 33: First 10 cycles of stress response of a single specimen with a deformation frequency of 50 Hz and 10% displacement.

(a) Set of first 50 cycles

(b) Set of last 50 cycles
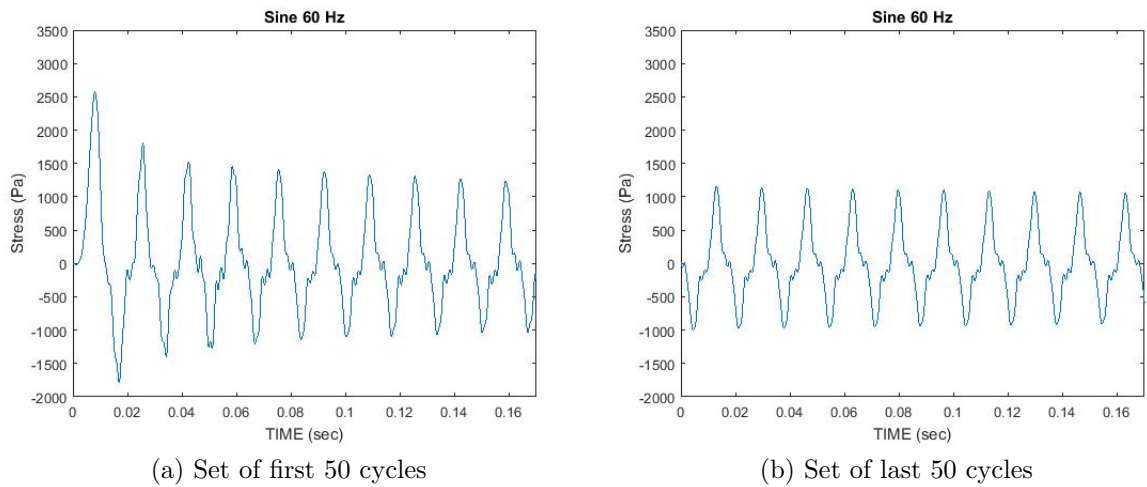
Figure 34: First 10 cycles of stress response of a single specimen with a deformation frequency of 60 Hz and 10% displacement.
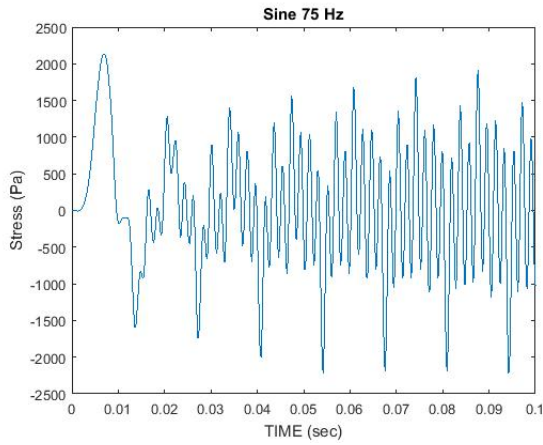
(a) Set of first 50 cycles
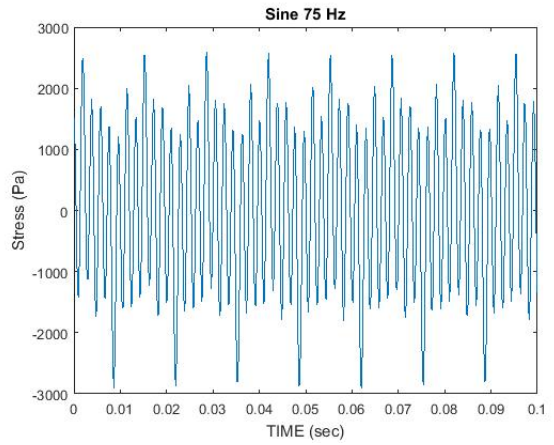
(b) Set of last 50 cycles

Figure 35: First 10 cycles of stress response of a single specimen with a deformation frequency of 75 Hz and 10% displacement.
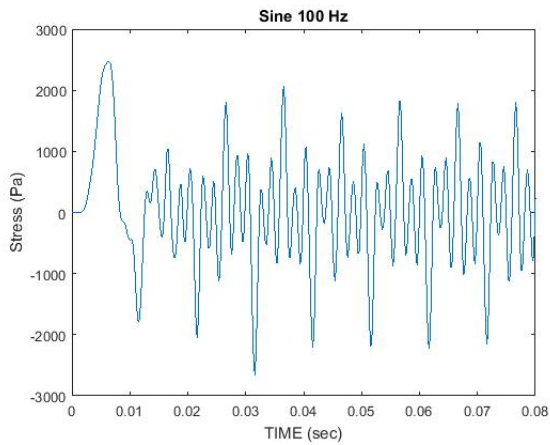
(a) Set of first 50 cycles
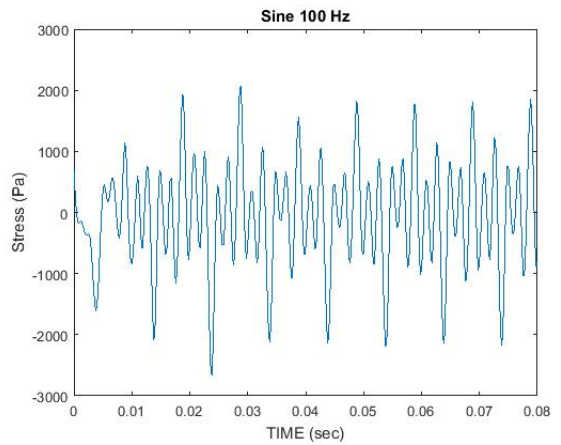
(b) Set of last 50 cycles

Figure 36: First 10 cycles of stress response of a single specimen with a deformation frequency of 100 Hz and 10% displacement.

(a) Set of first 50 cycles

(b) Set of last 50 cycles
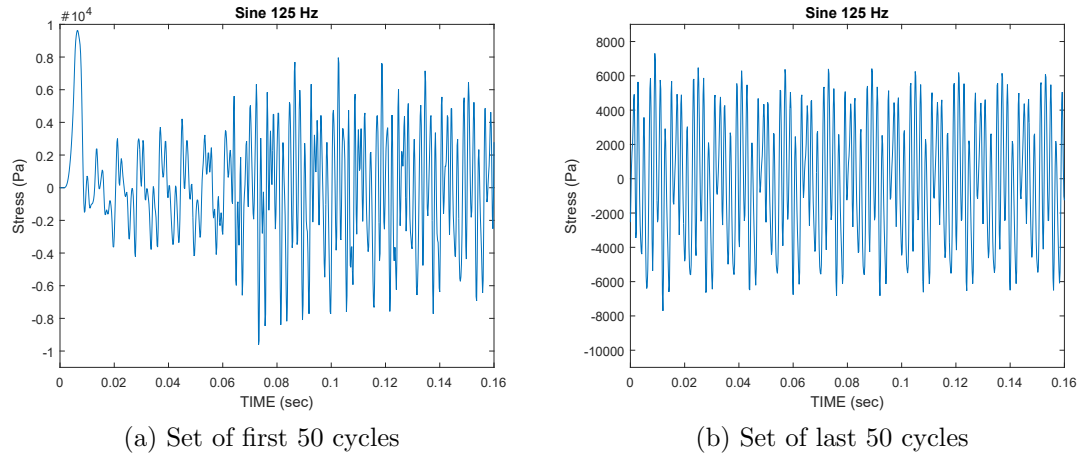
Figure 37: First 10 cycles of stress response of a single specimen with a deformation frequency of 125 Hz and 10% displacement.

Table 45: Average Length of Transient Region for all deformation frequencies and displacement amplitudes in the first and second sets of 50 cycles.

Deformation Frequency	Length of Transient Region			
	10% displacement		25% displacement	
	First 50 Cycles	Last 50 Cycles	First 50 Cycles	Last 50 Cycles
25	3.5	1.2	7.4	3.8
50	4.5	1.2	14.3	5.1
60	5.6	2.1	11.6	2.6
75	6.7	1.1	16.1	3.9
100	7	1.8	13.4	3.7
125	18.3	8	-	-

4.2.3   Damage Indicators in Apparent Steady State Reigon

Stress Versus Strain Curves

Stress versus strain graphs over the first and last set of 50 cycles are plotted to visualize changes in stress response with increasing deformation frequency. There is a clear change in the morphology of the stress versus strain graph with increasing deformation frequency. The stress versus strain graph for a deformation frequency of 25 Hz (Figure 38) has an s-shaped curve with a flat region in between two loops in the regions of higher strain. As the deformation frequency is increased to 75 Hz and above, the s-shape that was previously seen is now indistinguishable. However, there is still a clear pattern in the response at higher deformation frequencies, as shown by Figures 41 through 43. The differences in the stress versus strain graphs are quantified in the following section by examining the cycle 20 that is representative of the apparent steady state region. There is a clear difference between the first set of 50 cycles and the second set of 50 cycles at a given deformation frequency. This indicates the tissue structure changed due to the first set of cycles and relaxation, and therefore has a different restress response upon the second set of deformation cycles.
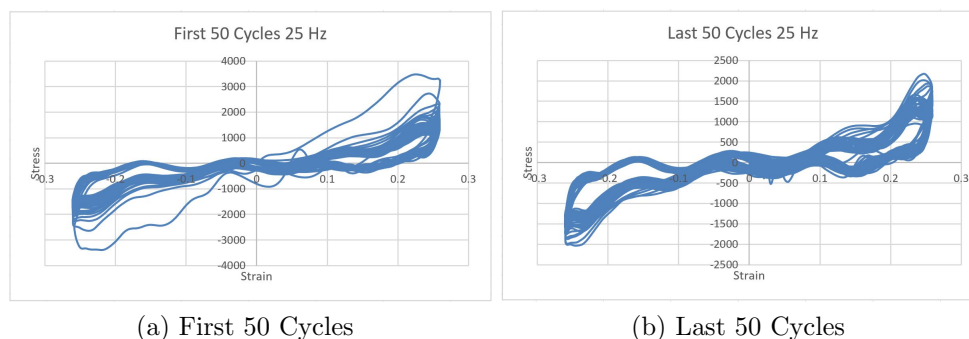
(a) First 50 Cycles

(b) Last 50 Cycles

Figure 38: Stress versus strain curve at 25 Hz and 10% displacement for a single specimen.
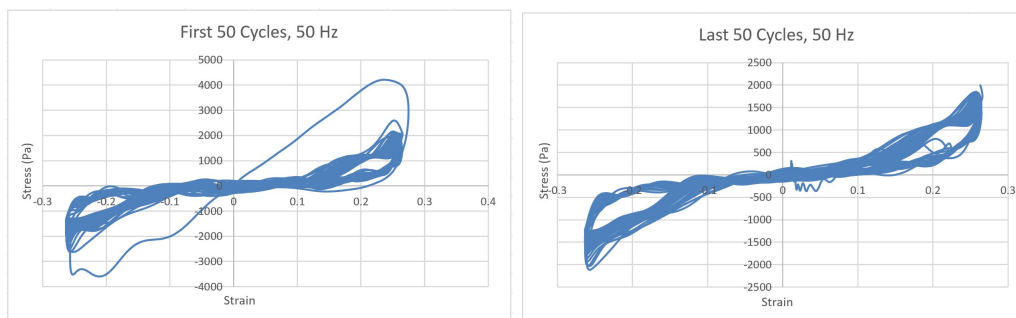
(a) First 50 Cycles

(b) Last 50 Cycles

Figure 39: Stress versus strain curve at 50 Hz and 10% displacement for a single specimen.
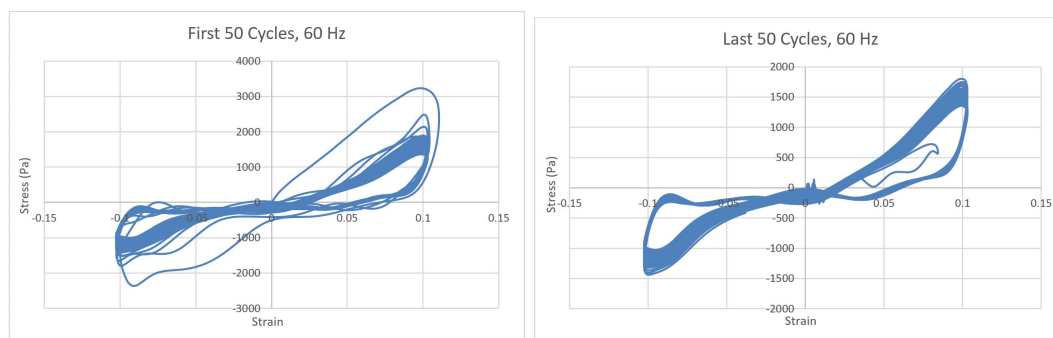
(a) First 50 Cycles

(b) Last 50 Cycles

Figure 40: Stress versus strain curve at 60 Hz and 10% displacement for a single specimen.

(a) First 50 Cycles
(b) Last 50 Cycles
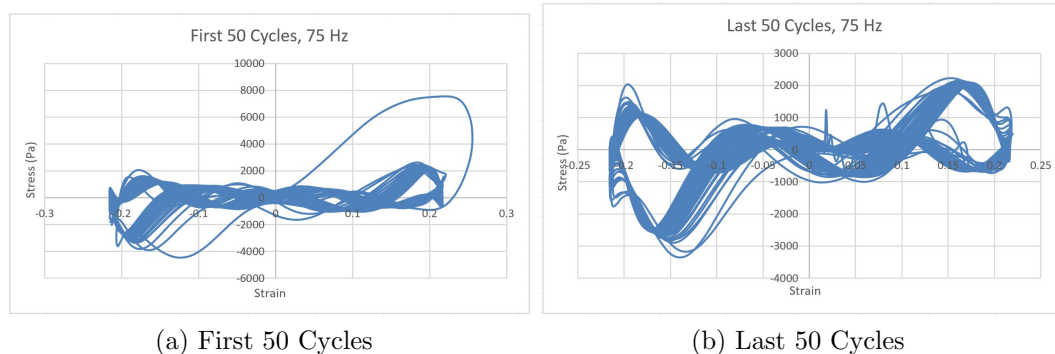
Figure 41: Stress versus strain curve at 75 Hz and 10% displacement for a single specimen.

(a) First 50 Cycles
(b) Last 50 Cycles
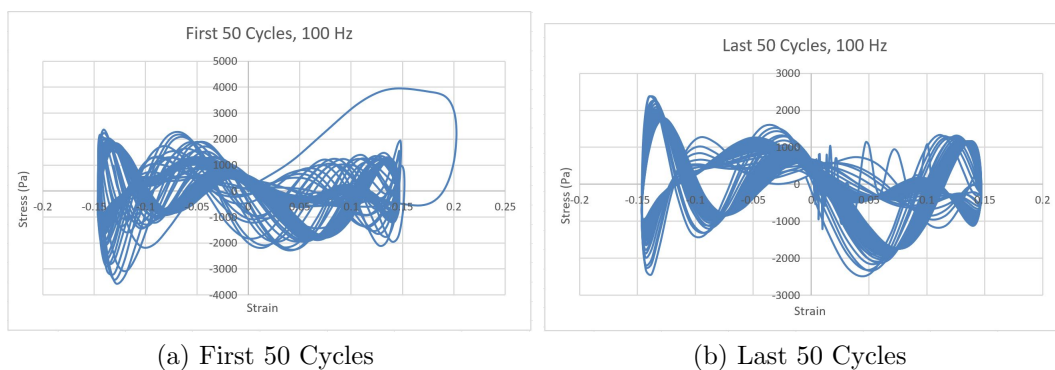
Figure 42: Stress versus strain curve at 100 Hz and 10% displacement for a single specimen.

(a) First 50 Cycles
(b) Last 50 Cycles
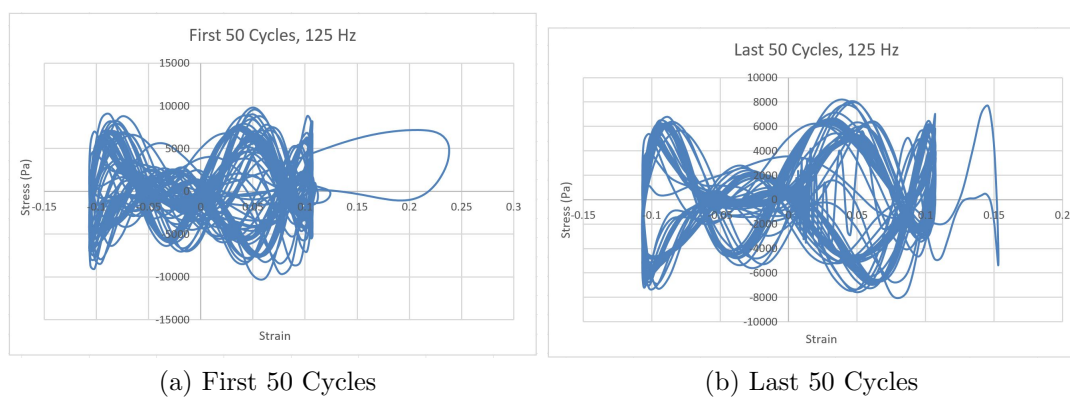
Figure 43: Stress versus strain curve at 125 Hz and 10% displacement for a single specimen.

Ratio of Magnitudes of Significant Frequency Components in Cycle 20 of the First and Second set of 50 Cycles

The magnitudes of significant frequency components within cycle 20 in the apparent steady state region at all deformation frequencies are given in Tables 91 through 112 in Appendix B. This section provides the ratios of magnitudes of significant frequency components in cycle 20, as the ratios of significant frequency components within the apparent steady state is indicative of damage that occurs after the initial deformation.

A ratio of the magnitudes of significant harmonics in cycle 20 at a deformation frequency of 25 Hz is given in Table 46. The significant harmonics, as indicated by the largest magnitudes, within the apparent steady state are the first and third harmonics. At a deformation frequency of 25 Hz and 10% displacement, the magnitude in the first 50 cycles is larger (although not by a high margin) than that in the second set of 50 cycles. However, at 25% displacement, the magnitude is larger in the second set of 50 cycles, except for the third harmonic, which has a larger magnitude in the first set of 50 cycles. In contrast to the ratio of powers of significant harmonics, where the ratio was only less than 1 in higher harmonics, there is no obvious pattern in the ratio of magnitudes of significant harmonics.

Table 46: Ratio of magnitude of significant harmonics in cycle 20 between the set of first 50 cycles and last 50 cycles at a deformation frequency of 25 Hz.

Significant Harmonic	Ratio of cycle 20 components in first 50 cycles to last 50 cycles	
	10 % Displacement	25 % Displacement
1	1.02	0.93
2	1.05	0.92
3	1.03	1.04
5	1.05	0.95

Similar to the 25 Hz deformation frequency, at a deformation frequency of 50 Hz, there are also significant first and third harmonics within the apparent steady state cycles. There is a similar trend in that the 25% displacement has larger magnitudes of

significant harmonics than the 10% displacement amplitude. At 10% displacement, the magnitudes of the third and fifth harmonics are larger in the second set of 50 cycles, while the magnitude of the second harmonic is larger in the first set of 50 cycles. The magnitude of the first harmonic is about the same in both the first and second set of 50 cycles. At 25% displacement, the magnitude of the second harmonic is larger in the first set of 50 cycles, and the magnitudes of the third and fifth harmonics are only slightly larger in the second set of 50 cycles. In contrast to the 25 Hz data, where the ratios of magnitudes in the significant harmonics are relatively close to each other, the 50 Hz data has a higher variation in the magnitude ratios of significant harmonics.

Table 47: Ratio of magnitudes of significant harmonics in cycle 20 between the set of first 50 cycles and last 50 cycles at a deformation frequency of 50 Hz.

Significant Harmonic	Ratio of cycle 20 components in first 50 cycles to last 50 cycles	
	10 % Displacement	25 % Displacement
1	1.00	0.99
2	1.31	1.91
3	0.89	0.97
5	0.57	0.99

At deformation frequency of 60 Hz and 10% displacement, the significant harmonics within cycle 20 are the first and third harmonics. At 25% displacement, there are significant first, third, and ninth harmonics. At both 10% displacement and 25% displacement, the first harmonic is slightly larger in the second set of 50 cycles. However, due to the large variation, it is not a significant difference. The second harmonic is larger in the first set of 50 cycles at both displacements. In contrast, the third harmonic is larger in the second set of cycles for both displacements. At 25% displacement, the ninth harmonic is slightly larger in the second set of 50 cycles.

The significant harmonics within cycle 20 at 75 Hz are the first, third, and seventh harmonics. The ratio of the magnitude of the significant harmonics are provided

Table 48: Ratio of magnitude of significant harmonics in cycle 20 between the set of first 50 cycles and last 50 cycles at a deformation frequency of 60 Hz.

Significant Harmonic	Ratio of cycle 20 components in first 50 cycles to last 50 cycles	
	10 % Displacement	25 % Displacement
1	0.98	0.98
2	1.40	1.32
3	0.92	0.92
5	0.91	1.01
7	1.01	0.88
9	1.02	0.95

in Table 49. The ratios at 10% displacement are all slightly above one, with the exception of the second and seventh harmonics, which are slightly below one. At 25% displacement, the ratios are all larger than one, except for the second harmonic. There is a smaller difference between magnitudes in the first and second set of 50 cycles at 10% displacement than there is at 25% displacement.

Table 49: Ratio of magnitudes of significant harmonics in cycle 20 between the set of first 50 cycles and last 50 cycles at a deformation frequency of 75 Hz.

Significant Harmonic	Ratio of cycle 20 components in first 50 cycles to last 50 cycles	
	10 % Displacement	25 % Displacement
1	1.07	1.03
2	0.96	0.94
3	1.00	1.22
5	1.01	1.27
7	0.90	1.17
9	1.02	1.46

At deformation frequency of 100 Hz and 10% displacement, the magnitudes of the first and second harmonics in the first 50 cycles is larger than that of the second 50 cycles, whereas at 25% displacement, the magnitudes of the first and second harmonics of the second set of 50 cycles is larger than the first set of 50 cycles. The magnitudes of the third and fifth harmonics are larger in the first set of 50 cycles than in the last set of 50 cycles for both 10% and 25% displacement. The magnitude of the sixth

harmonic is larger in the second set of 50 cycles for both 10% and 25% displacements.
The magnitudes of the seventh and ninth harmonics are larger in the second set of 50
cycles at 10% displacement and larger in the first set of 50 cycles at 25% displacement.

Table 50: Ratio of magnitudes of significant harmonics in cycle 20 between the set of first
50 cycles and last 50 cycles at a deformation frequency of 100 Hz.

Significant Harmonic	Ratio of cycle 20 components in first 50 cycles to last 50 cycles	
	10 % Displacement	25 % Displacement
1	1.07	0.94
2	1.01	0.92
3	1.05	1.08
5	1.00	1.25
6	0.64	0.95
7	0.80	1.03
9	0.69	1.08

The significant harmonic components at deformation frequency of 125 Hz are the
first, third, fourth, fifth, sixth, and seventh. As shown in Table 51, the magnitudes
at the first, third, sixth, and seventh harmonics are larger in the first set of 50 cycles
than the second set of 50 cycles. The magnitudes of the second, fourth, fifth, and
ninth are greater in the second set of 50 cycles.

Table 51: Ratio of magnitudes of significant harmonics in cycle 20 between the set of first
50 cycles and last 50 cycles at a deformation frequency of 125 Hz.

Significant Harmonic	Ratio of cycle 20 components in first 50 cycles to last 50 cycles
	10 % Displacement
1	1.01
2	0.95
3	1.25
4	0.93
5	0.81
6	1.47
7	1.65
9	0.91

Shear Stress Magnitude of Cycle 20

The shear stress magnitude of cycle 20, which lies in the apparent steady state region, is taken from the stress response curve (Figure 11). The tests are completed in deformation control, so the stress magnitude is a measure of the force required to deform the tissue to a programmed displacement. Higher values of shear stress mean that larger forces are required to deform the tissue, so this offers insight on the tissues response to deformation. Table 52 provides the average values for the shear stress magnitude, at each deformation frequency and displacement amplitude, of cycle 20 from each set of 50 cycles. At 10% displacement, the average shear stress magnitude of cycle 20 increases with increasing deformation frequency. The average shear stress magnitude is nearly the same between the first and second set of cycles at 10% displacement for each deformation frequency. At 25% displacement amplitude, the average shear stress magnitude generally increases with increasing deformation frequency, however, at a deformation frequency of 75 Hz, the average shear stress is larger than that of 100 Hz. This may be in part due to the higher standard deviations seen in the 25% displacement amplitude tests. Similarly to at 10% displacement, the average shear stress between the first and second set of 50 cycles is very similar. The main difference between the 10% and 25% displacement amplitudes is that the 25% displacement amplitude has larger magnitudes at each deformation frequency.

Table 52: Average shear stress magnitude for all deformation frequencies and displacement amplitudes in the first and second sets of 50 cycles.

Deformation Frequency (Hz)	Average Shear Stress Magnitude of Cycle 20 (Pa)			
	10% displacement		25% displacement	
	First 50 Cycles	Last 50 Cycles	First 50 Cycles	Last 50 Cycles
25	776.3	772.8	1100.2	1188.8
50	939.9	962	1498.1	1547.7
60	1015	991.9	1505.1	1501.7
75	1463.1	1531.4	2852.7	2488
100	1707.6	1689.4	2542.5	2591.5
125	6829.1	6743.1	NA	NA

4.3 Results Summary

The shear stress response to higher frequency deformations contains higher harmonics and often breaks in symmetry between loading and unloading, which is shown by the presence of even harmonics (i.e. the fourth or sixth harmonic). Deformation frequencies of 25 Hz and 50 Hz both have significant first and third harmonics, and a clear shoulder due to their third harmonic in the stress response curve. In both 25 and 50 Hz, the first harmonic is seen in the transient and apparent steady state regions and contains large amplitude wavelets. In contrast, the third harmonic is in the transient and apparent steady state at 10% displacement, and appears in the transient at 25% displacement. Although wavelet analysis only picks up the third harmonic in the transient region at 25% displacement, the third harmonic is still present in the apparent steady state region within small wavelet amplitude bins (i.e. bins 19 and 20) that were oversized and not considered for analysis. At both displacements, the third contains low amplitude wavelets. At a deformation frequency of 60 Hz and 10% displacement, there is a shoulder created on the stress response curve but it is not smooth as seen in 25 Hz and 50 Hz stress response curves. At 60 Hz and 25% displacement, no shoulder appears in the stress response curve due to the disruption of the curve from the higher harmonics. At all higher frequencies and deformations, there is no shoulder effect seen in the stress response curves. At 60 Hz, the third harmonic is seen in the transient region at 10% deformation, whereas at 25% deformation, it is only in the apparent steady state region. What majorly breaks the previous trends is that at 60 Hz and 25% displacement is the addition of a ninth harmonic. The ninth harmonic only appears in the apparent steady state region. At 75 Hz, there is also the addition of a higher odd harmonic, which is the seventh harmonic. In contrast to what was seen at lower deformation frequencies, the seventh harmonic contains large amplitude wavelets in both transient and apparent steady state regions whereas the lower harmonics (first and third) are seen in the transient region and contains low

amplitude wavelets. At a deformation frequency of 100 Hz and 10% displacement, the first and third harmonics are in the transient region; whereas the fifth harmonic is larger in magnitude and in both the transient and steady state regions. At 100 Hz and 25% displacement, there is the addition of a significant sixth harmonic. A significant even harmonic indicates symmetry breaking in the loading and un-loading cycle and is not previously seen at lower deformation frequencies. There is a similar trend at a deformation frequency of 125 Hz, with significant first, third, fourth, fifth, sixth, and seventh harmonics. The higher harmonics contain large amplitude wavelets in both transient and steady state regions, whereas the first harmonic is seen in the transient region.

Tables 53 and 54 provide the average power tables for significant odd harmonics at each deformation frequency in the first and last set of 50 cycles, respectively. Tables 53 and 54 do not include the even harmonics or the ninth harmonic, which does not mean they are less significant. The even harmonics do not show up until high frequencies and therefore were not included in the average table but are still significant in determining damage. Of particular interest is the third and fifth harmonics. As stated previously, the third harmonic represents the fluid drag force. The fifth harmonic is also of interest because the in vivo operating frequency of 1 Hz has significant first, third, and fifth harmonics.

Tables 55 and 56 provide the average magnitude tables for significant odd harmonics at each deformation frequency in the first and last set of 50 cycles, respectively.

Table 53: Average power values in the first set of 50 cycles for the first, third, fifth, and seventh harmonics for deformation frequencies of 25 Hz through 125 Hz.

| Frequency | Average Power | | | | | | | |
| | 10% Displacement | | | | 25% Displacement | | | |
	First	Third	Fifth	Seventh	First	Third	Fifth	Seventh
25	585.3	172.0	26.4	NA	844.3	302.0	82.0	NA
50	709.9	188.1	37.1	NA	1077.5	407.7	89.0	NA
60	646	234.3	33.7	42.5	842.4	480.6	150.2	137.3
75	311.6	336.6	108.9	635.0	680.4	743.6	418.0	2448.8
100	227.0	529.1	888.1	3.7	382.8	643.1	667.4	185.6
125	2041.0	880.5	982.8	363.5	NA	NA	NA	NA

Table 54: Average power values in the last set of 50 cycles for the first, third, fifth, and seventh harmonics for deformation frequencies of 25 Hz through 125 Hz.

| Frequency | Average Power | | | | | | | |
| | 10% Displacement | | | | 25% Displacement | | | |
	First	Third	Fifth	Seventh	First	Third	Fifth	Seventh
25	538.5	160.4	26.8	NA	812.9	298.0	90.3	NA
50	603.0	171.9	20.0	NA	943.4	359.4	79.2	NA
60	572.3	209.4	32.8	46.5	687.3	417.0	119.2	128.2
75	236.8	261.6	89.3	648.6	506.8	577.6	369.1	2213.7
100	158.6	443.3	766.2	4.3	332.8	530.1	473.4	141.1
125	1666.8	744.2	871.8	281.6	NA	NA	NA	NA

Table 55: Average magnitude values in the first set of 50 cycles for the first, third, fifth, and seventh harmonics for deformation frequencies of 25 Hz through 125 Hz.

| Frequency | Average Magnitude | | | | | | | |
| | 10% Displacement | | | | 25% Displacement | | | |
	First	Third	Fifth	Seventh	First	Third	Fifth	Seventh
25	573.1	180.4	33.5	NA	781.8	308.9	97	NA
50	683.2	180.2	18.7	NA	1025.5	400.1	87.6	NA
60	630.7	224.5	37.1	54.5	786.4	457.7	156.2	145.0
75	379.5	391.9	124.3	722.6	700.4	830.9	539.5	2888.7
100	195.6	589.8	1035.7	23.7	365.7	711.7	775.9	196.6
125	2155.6	1357.0	1100.1	1100.4	NA	NA	NA	NA

Table 56: Average magnitude values in the last set of 50 cycles for the first, third, fifth, and seventh harmonics for deformation frequencies of 25 Hz through 125 Hz.

Frequency	Average Magnitude							
	10% Displacement				25% Displacement			
	First	Third	Fifth	Seventh	First	Third	Fifth	Seventh
25	561.9	175.8	31.9	NA	837.3	296.3	102.2	NA
50	682.9	202.4	32.9	NA	1029.9	411.9	88.5	NA
60	641.8	242.8	40.7	54.1	799.8	495.0	155.2	164.3
75	355.2	390.6	122.6	801.0	681.0	680.7	424.7	2462.7
100	182.3	559.3	1035.5	29.5	391.0	659.1	623.0	190.2
125	2141.0	1086.0	1352.7	667.9	NA	NA	NA	NA

Table 57: Overview of j-levels present, where the j- levels occur and the wavelet amplitude in the first set of 50 cycles at each deformation frequency.

Freq.	Wavelet Overview					
	10% Displacement			25% Displacement		
	j-level (harmonic)	Region of Signal	Amp.	j-level (harmonic)	Region of Signal	Amp.
25	first (5)	T, SS	large, small	first (5)	T, SS	large, small
	third (6)	T, SS	small	third (6)	T, SS	small
50	first (5)	T, SS	large, small	first (5)	T, SS	large, small
	third (6)	T, SS	small	third (6)	T	mid, small
60	first (5)	T, SS	large, small	first (5)	T	large, small
	third (7)	T	small	third (7)	T	mid, small
				8 (ninth)	T	mid
75	first (4)	T	small	first (4)	T	large, small
	second (5)	T	small	second (5)	T	mid, small
	third (6)	T, SS	small	third (6)	T, SS	mid, small
	fifth, seventh (7)	T, SS	large, small	fifth, seventh (7)	T, SS	large, small
100	first (5)	T, SS	mid, small	first (5)	T	mid
	third (6)	T, SS	mid, small	third (6)	T	small
	fifth, sixth (7)	T, SS	large, mid	fifth, sixth (7)	T,SS	large, small
	seventh, ninth (8)	T	small	seventh, ninth (8)	T	small
125	first (4)	T, SS	small			
	third, fourth, fifth (6)	T, SS	large, small			
	sixth, seventh (7)	T, SS	mid, small			

Table 58: Overview of j-levels present, where the j- levels occur and the wavelet amplitude in the second set of 50 cycles at each deformation frequency.

Freq.	Wavelet Overview					
	10% Displacement			25% Displacement		
	j-level (harmonic)	Region of Signal	Amp.	j-level (harmonic)	Region of Signal	Amp.
25	first (5)	T, SS	large, small	first (5)	T, SS	large, small
	third (6)	T, SS	small	third (6)	T, SS	small
50	first (5)	T, SS	large, small	first (5)	T, SS	large, small
	third (6)	T, SS	small	third (6)	T, SS	small
60	first (5)	T, SS	large, small	first (5)	T	large
	third (7)	T, SS	small	third (7)	SS	mid
				ninth (8)	T, SS	mid
75	second (5)	T	small			
	third (6)	T	small	third (6)	T, SS	small
	fifth, seventh (7)	T, SS	large, small	fifth, seventh (7)	T, SS	large, mid
100	first (5)	T, SS	mid, small	-	-	-
	third (6)	T, SS	mid, small	third (6)	T, SS	small
	fifth, sixth (7)	T, SS	large, small	fifth, sixth (7)	T,SS	large, small
	-	-	-	seventh, ninth (8)	T	mid
125	third, fourth, fifth (6)	T, SS	large, small			
	sixth, seventh (7)	SS	mid, small			

5   Discussion

Brain tissue contains about 20% by volume extracellular fluid (ECF) [28], which is an important part of the glymphatic system. The glymphatic system is a system of channels formed by astroglial cells that functions in nutrient transport, waste removal, and fluid redistribution in the central nervous system [29]. Within the glymphatic pathway, cerebral spinal fluid (CSF) acting as ECF is driven by a combination of pulsing arteries and pressure gradients [30]. The pulsing arteries cause a pressure change between the para-arterial and paravenous pathways. Pulsation generated by smooth muscle cells creates pulse waves along the whole length of the pial artery and arteries that penetrate into the brain from the cortical surface [31]. The flow in the glymphatic system is known to be forced by pulsations of the cranial arteries at about 1 Hz [31]. ECF interaction with solid matter including axons, glial processes, or blood vessels may significantly influence the mechanical response of brain tissue.

Fourier analysis and harmonic wavelet decomposition show a significant 1 Hz and 3 Hz component and small 5 Hz component in rat brain tissue subjected to a deformation frequency of 1 Hz [32]. The 3 Hz component creates a shoulder effect seen on the stress response curve (Figure 44) and is likely induced by an internal fluid-solid interaction that the shear stress must overcome in response to an applied sinusoidal translational shear deformation [32]. When the brain tissue is not subjected to external forces, the hydrostatic pressure in the ECF is balanced by tension in the solid matter (glial processes, axons, dendrites) to maintain the tissue structure. An external mechanical insult might accelerate the ECF flow or increase the ECF hydrostatic pressure and disrupt axonal and glial connections which in turn disrupts the flow of the ECF. Since the in vivo frequency of 1 Hz has first, third, and fifth harmonics, these harmonics are followed closely through increasing deformation frequencies. The results demonstrate the presence of higher harmonics, such as the fifth, becoming more significant with increasing deformation frequency. Also, the significant harmon-

ics remain in both the first and second sets of cycles and displacement amplitudes for a given deformation frequency. The same significant harmonics in each set of deformation cycles suggests that there is a possible physical tissue source that generates the harmonics at a given deformation frequency.
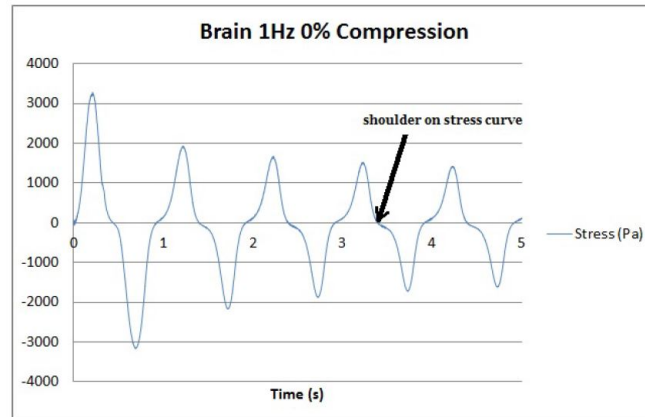
Figure 44: Stress response curve of 1 Hz deformation frequency showing shoulder effect due to 3 Hz component [32].

The tests are performed in deformation control, so the shear stress is calculated from the necessary force required to deform the tissue. Therefore, a higher force required to deform the tissue results in a higher shear stress. The shear stress is interpreted as bond and synapse mechanical strength, so a higher shear stress is indicative of more force being required to break bonds or synapses within the tissue. The amount of stress required to deform the tissue is used as a damage indicator. Indicators of damage are examined for all deformation frequencies between the first and second set of 50 cycles and 10% and 25% displacement. Damage is interpreted as bond breaking due to shearing or axonal stretching. Damage with respect to the deformation frequency appears in the length of the transient in the first set and in the symmetry breaking in a deformation cycle compared to that induced by the normal 1 Hz deformation [32]. Other damage indicators include the relative magnitude of initial peak stress in the first set and second set of 50 cycles, and changes in frequency components with respect to deformation frequency. With increasing deformation fre-

quencies, many changes in morphology of the stress response curve likely indicate damage. Higher deformation frequencies, induce not only higher significant frequencies but also the presence of even harmonics, which are not seen at lower deformation frequencies.

Patients with persistent post-concussion symptoms exhibit functional connectivity loss within the cerebrum [33]. The reduced connectivity is attributed to diffuse axonal injury due to axonal stretching and shearing. Stretching and shearing of neuronal synapses may also cause synaptic injury, leading to loss of neuronal communication that could be responsible of some symptoms of mTBI [3]. Damage indicators are interpreted as bond breaking between glial processes and axons that cause reduced functional connectivity. Conventional imaging techniques such as CT or MRI are unable to accurately detect mTBI injuries [2], [34], [35]. However, analysis of shear stress response induced by sinusoidal deformation does capture bond breaking that may in part cause loss of functional connectivity. Stress as a measure of damage can capture more subtle changes, such as broken synapses and bonds, compared to current imaging techniques or histology. Also, histopathology does not detect mild damage due to mTBI [36].

5.1 Frequency Component Analysis

The frequency content of the shear stress response for 50 cycles at each frequency verifies the dependence of shear stress on deformation frequency. Since it is frequency dependent, the shear stress response to constant rate shear deformation [4] does not fully characterize the shear stress-stretch behavior of the tissue. The first, third, and fifth harmonics are analyzed closely at each deformation frequency because of their presence in the in vivo 1 Hz deformation frequency. In addition, the seventh and ninth harmonics are also analyzed because they become significant at higher deformation frequencies.

5.1.1 Significant Frequency Components

Power of Frequency Components within 50 Cycles

The power of significant frequency components, which is taken over the entire 50 cycles, includes both the transient and apparent steady state regions. The significant frequency components within the set of 50 cycles change with the deformation frequency. The power of the signal components measures which harmonics are dominant throughout the signal.

The same significant harmonics exist in both the first and second set of 50 cycles at all deformation frequencies. These significant harmonics remain the same at both 10% and 25% displacement amplitude. Although the same significant harmonics exist in each displacement amplitude, the power of the significant harmonics is larger at 25% displacement. Since the significant frequency components are the same between sets of cycles and displacement amplitudes, the harmonics might be generated from a specific unknown region.

The power of both the third and fifth harmonics increases with increasing deformation frequency at both 10% and 25% displacement amplitude. The increase in power of the third harmonic shows there is a larger fluid drag force at higher deformation frequencies. The increase of deformation frequency could cause a larger acceleration of the ECF, and thus create a larger drag force exerted on the solid phase.

Magnitude of Frequency Components in Apparent Steady State Region

The magnitude calculation characterizes the frequency components that are present after the initial damage has already occurred in the transient region. Similarly to the power of significant frequency components, the magnitude of the third and fifth harmonics increases with increasing deformation frequency. The increase of the magnitude of the third harmonic demonstrates the significance of the fluid drag force in the apparent steady state. Interestingly, at higher deformation frequencies, higher harmonics often become more dominant than the first and third harmonics. The

presence of significant higher harmonics in both 10% and 25% displacement, and first and second sets of cycles, further suggests the harmonics might originate from a specific region. Since the higher harmonics are present in the apparent steady state, they are not just a result of the initial deformation but persist throughout the entirety of the deformation. A higher applied deformation frequency could generate resonance with an internal structure that creates more dominant higher harmonics. It is also possible that the increased deformation frequency causes shearing between boundaries of varying stiffness regions in the heterogenous tissue which could create higher harmonics.

Wavelet analysis

The power and magnitude analysis identifies the significant frequency components that are present in the transient and apparent steady states. Harmonic wavelet analysis allows one to distinguish which frequency components are in the transient versus apparent steady state region, or both regions. Distinguishing which frequency components are in specific regions offers insight on whether the frequency component is a result of initial damage and confined to the transient region or extends throughout the signal. The transient response includes the initial acceleration of the fluid within the tissue, and the initial breaking of bonds and synapses due to the mechanical insult. Since the transient and apparent steady state regions are characterized by differences in acceleration of fluid, pressure gradients, and bond breaking; the frequency components within each region can aid in relating the significant harmonics to sub-structural responses of the tissue under deformation. As the deformation frequency increases, the higher harmonics become more significant as shown by the fact that they contain large amplitude wavelets.

Characterization of Stress Response Curve upon Loading and Unloading of Specimen

One cycle in the stress response curve corresponds to the specimen being loaded and unloaded. The symmetry of the stress response curve offers insight on the influence of the higher harmonics effects on the stress response. A symmetric curve means that the tissue is responding in the same way when it is loaded versus unloaded. However, at higher deformation frequencies, the stress response curve is asymmetric upon loading and unloading.

The stress response curve at 25 Hz and 50 Hz is symmetric upon loading and unloading of the specimen in each deformation cycle, and shows a defined shoulder that is attributed to the third harmonic due to fluid drag forces. However, increasing deformation frequency produces a considerable transition in the stress response curve. This transition begins at 60 Hz and 10% displacement, where the shoulder region is markedly less smooth than at lower deformation frequencies, which demonstrates the asymmetry in loading and unloading of the specimen. The asymmetry in the stress response curve means that the specimen is responding differently to the applied load based on the direction of the mover. The difference in stress response could be attributed to changes in tissue structure within the specimen. As the displacement amplitude is increased to 25% at 60 Hz deformation frequency, the shoulder region becomes visually indistinguishable. From the harmonic wavelet analysis, it is clear that at 60 Hz and 25% displacement, the wavelets containing the higher harmonics are not only confined to small amplitude bins, as they were previously at lower deformation frequencies. The higher harmonics become more significant, as shown by their presence in large amplitude bins. The shoulder continues to be visually indistinguishable throughout the higher deformation frequencies. At these higher deformation frequencies (60 Hz through 125 Hz), the third harmonic is still significant. As shown previously, the magnitude and power of the third harmonic is larger at

these higher deformation frequencies as compared to lower deformation frequencies. However, the power of the other higher harmonics (fifth, seventh and ninth) is larger than the third harmonic, which disrupts the symmetry in the curve and makes the shoulder indistinguishable. There are no higher harmonics present at 25 Hz and 50 Hz, so there is no disruption in the shoulder.

The asymmetry and disruption in the shoulder is due to the addition of higher harmonics, and is interpreted as damage due to bond or synapse breaking. Breaking of bonds could cause the tissue to respond differently when it is unloaded versus loaded, creating asymmetry in the stress response curve.

5.1.2   Relation of Frequency Components to Tissue Structure

The prevalence of the higher harmonics, in particular the fifth harmonic, at all deformation frequencies suggests there is an internal source in the tissue responsible for the higher harmonics. Not only is the fifth harmonic present at all deformation frequencies, but it increases in power and magnitude with increasing deformation frequency. Since the frequency response is confined to specific harmonics and becomes more significant at higher deformation frequencies, this suggests that the tissue responds as a unit, rather than randomly. Moving multiple layers of tissue as a unit could result in a higher force required, creating peaks in the power spectrum at specified harmonics. For this reason, it is proposed that an internal substructure generates these higher harmonics when deformed.

There are various possible internal sources that could generate these higher harmonics. One possibility is that the applied deformation frequency could be in resonance with the substructure that produces naturally occurring brain waves. Resonance with the structure that produces brain waves could cause a significant frequency response, due to moving the substructure as a unit, which could generate the higher harmonics. Another possibility is the shearing between the hippocampal layers due

to damage occurring between bonds of the layers. Lastly, the rat cerebrum is heterogenous, containing regions of soft grey matter and stiff white matter. It is possible that when the deformation frequency is applied, shearing between the boundaries of varying stiffness regions could cause higher harmonics due to the difference in material properties.

Shearing between Hippocampal Layers

The Hippocampus is an internal structure of the brain located in the medial temporal lobe of the rat brain (Figure 45). Following mTBI, considerable neurophysiological changes occur in the hippocampus [37]. Hippocampal lamellar organization is critical for understanding hippocampal connectivity [38]. The hippocampus is defined by the dentate gyrus and the Cornu Ammonis (CA), which is differentiated into four distinct subregions CA1, CA2, CA3, and CA4 (Figure 45). The CA3 pyramidal cells have an axon collateral system that send information to the CA1 pyramidal cells. The CA1 cells provide the major output of the hippocampus to the entorhinal cortex. The CA3 pyramidal neurons have many different firing patterns that depend on how the cells are excited. The majority of the cells (90%) in the hippocampus are excitatory.
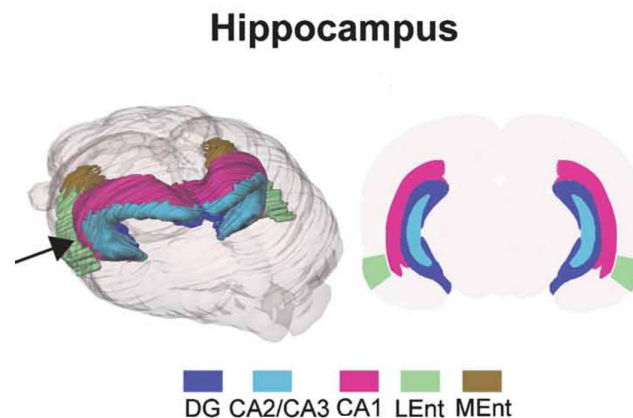
Figure 45: 3D image of hippocampus in rat brain [39].

Neuronal signals through the hippocampus combine to form a loop (Figure 46). External inputs come from the entorhinal cortex and into the dentate gyrus and CA3 region. Granule cells in the dentate gyrus send their axons, called mossy fibers, to CA3. Pyramidal cells of CA3 send their axons to CA1. Pyramidal cells of CA1 send their axons to deep layers of the entorhinal cortex, thus closing the loop. The lamellar hypothesis proposes that the hippocampus can be thought of as a series of parallel strips that are functionally independent from each other. However, there has been recent data showing longitudinal connections within the hippocampal system [40]. Shearing between these layers, or movement of the layers as a unit, serves as a possible source of higher harmonics as bonds break between the layers causing damage within the tissue.
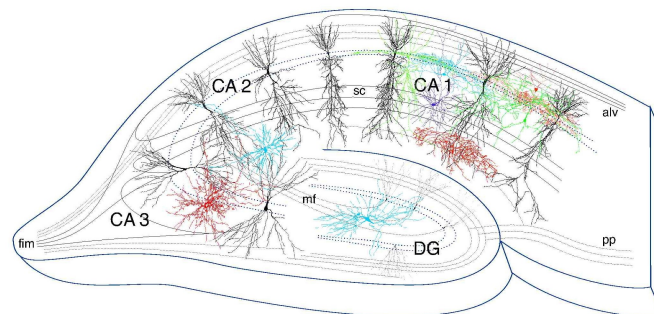
Figure 46: Regions of Hippocampus in rat brain [41].

Previous studies have found that rats subjected to shock tube tests mimicking mTBI conditions found lesions that produced a discontinuity in the tissue causing separation of hippocampal layers and the dentate gyrus [36]. These lesions were found to likely be a result of shear injury that is unique to blast trauma. The separation spanned through the hippocampal CA1 and dentate gyrus, resulting in a misalignment of the hippocampal layers. The shearing of these layers within the hip-

pocampus could possibly be a source of the fifth harmonic.

Deformation Frequency in Resonance with Structure that Creates Brain Waves

One possible source of the presence of higher harmonics are regions that generate brain waves. Brainwaves are produced by synchronized electrical pulses from masses of neurons communicating with each other, which can be detected on an electroencephalography (EEG) [38]. It is possible that brain waves can be generated by deformation induced excitation of large populations of neurons. Brainwaves are divided into bandwidths that are correlated with specific functions. Infra-low brainwaves are characterized by a frequency of less than 0.5 Hz and are thought to be the basic cortical rhythms that underlie higher brain functions. Delta waves have a bandwidth of 0.5 to 3 Hz and are characterized by their deeply penetrating and low frequency. Theta waves span from 3 to 8 Hz, and are known to be prevalent in the hippocampus. Higher frequency brain waves include alpha waves (from 8 to 12 Hz), beta waves (from 12 to 38 Hz), and lastly, gamma waves (from 38 to 42 Hz). Gamma waves are above the frequency of neuronal firing (0 to approximately 38 Hz), so it is unknown how they are generated [42]. These brain waves communicate information from one section of the brain to another and can couple with other frequencies to communicate between multiple regions.

Theta waves are of particular interest because they contain the 5 Hz frequency, which is seen as a harmonic under a 1 Hz deformation frequency, so it is possible that resonance with the sub-structures creating theta waves could be responsible for the fifth harmonic. Theta oscillations represent the on-line state of the hippocampus, which is believed to be a primary site of mTBI damage [43], and are strongly correlated with memory efficiency [44]. The extracellular currents underlying theta waves are generated mainly by CA3 collaterals (branches that extend to other cells)

within the hippocampus. Neuron channels controlling electrical activity in the brain can be activated with mechanical pressure [44]. Applied mechanical pressure waves were shown to stimulate gamma oscillations in the hippocampus of a mouse [45], so it could be possible that an applied sinusoidal deformation could evoke a response from the sub-region of the brain responsible for generating theta waves in the rat cerebrum.

Material Properties of Heterogeneous Cerebrum

Another possible underlying cause of the fifth harmonic is the difference in material properties of various regions in the heterogeneous cerebrum. The cerebrum is composed of white matter and grey matter, each with different material properties. White matter is much stiffer (>25%) than grey matter [46]. The stiffness of a material represents the material's ability to resist deformation. Differences in material stiffness between different regions result in larger deformations at sites of variation [47]. The larger the stiffness, the greater the force required to cause a given deformation.

The corpus callosum, which lies above the hippocampus, is a tract of white matter and a primary site of damage in mTBI. The corpus callosum exhibits greater stiffness and less viscous damping compared to other white matter in the brain [48]. During impact, stretching can damage axons, especially at the boundary of the white and grey matter. Shearing at the boundary of the corpus callosum is often visible following large deformation shear testing of the specimens (Figure 47). Impact also causes a nonuniform stress and strain distribution inside anisotropic white matter which can cause significant local damage [49]. As deformation frequency is applied, bonds breaking between stiffer white matter and softer grey matter is a possible source of higher harmonics. As the deformation frequency is applied to regions with varying stiffness, the response to the deformation depends on the material properties of the tissue. It has been found that blast-associated shear strain is highest at the interface between brain and ECF, and at grey-white matter interfaces [50]. The difference in

shear strain between varying regions under an applied deformation could cause the different higher harmonics seen in the stress response due to the higher shear force required.
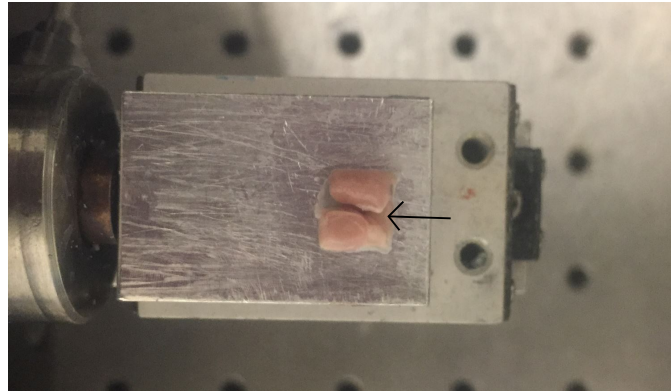
Figure 47: Large deformation results in split due to shearing in cerebrum specimen along corpus callosum boundary (shown with an arrow).

5.2   Damage indicators

Damage is correlated to bond breaking between axons, dendrites and glial processes, which is assumed to underlie some symptoms of mTBI. Specifically, bond and synapse breaking in the hippocampal region could be partly responsible for memory loss often associated with mTBI. The shear stress is interpreted as a measure of bond strength and is calculated from the necessary force required to deform the tissue. A decrease in stress magnitude indicates that bonds have been broken or damaged, resulting in easier deformation of the tissue. Most of the characteristics of the shear stress response appear to reflect bond breaking of cell adhesion molecules and of synapses in the tissue. Other characteristics of the shear stress response are influenced by the behavior of the ECF.

5.2.1 Length of Transient Region in First 50 Cycles

The length of the transient region depends on the deformation frequency and can be used as a mild damage indicator. The transient region is distinguished by a substantial (>10%) decrease in shear stress amplitude from deformation cycle to subsequent deformation cycle over time. It is proposed that the rapid rate of decrease in shear stress amplitude is due to breaking of bonds that aid in holding the tissue together. As the bonds break, less bonds are in place and therefore there is lower resistance to deformation.

The transient response exhibited in the rat cerebrum is similar to the Mullins effect in rubbers. The Mullins effect is the phenomena that rubber-like materials change in mechanical properties resulting from the first extension [51]. The material typically exhibits a stiffer response in the initial loading cycle, then upon unloading and reloading, the material exhibits stress softening. Some proposed physical interpretations of stress-softening underlying the Mullins effect are chain breakage at the interface of rubber and the fillers, slipping of molecules, and chain disentanglements. The Mullins effect has also been attributed to bond and crosslinking rupture [52]. Stress softening is characterized by a lower resulting stress for the same applied strain after the first load. After a few number of cycles, the material responses coincide during successive cycles. The Mullins effect was first observed in rubbers undergoing tensile deformation; however, rat brain cerebrum exhibits similar patterns in sinusoidal translational shear deformation. The length of the transient region offers insight on the amount of damage that occurs within the cerebrum upon sinusoidal deformation. Within the first set of 50 cycles, the length of the transient region increases with increasing deformation frequency at 10% displacement amplitude. A longer transient region at higher deformation frequencies could indicate that the deformations must create greater acceleration of fluid. The greater acceleration of fluid could cause more bond breaking, resulting in a longer transient region. The higher deformation frequencies

could also cause a higher buildup of pressure within the tissue, which would require more time to reach an apparent steady state resulting in a longer transient region. At each deformation frequency, the 25% displacement amplitude has a longer transient region as compared to 10% displacement amplitude. Once again, this is likely due to the increased pressure and more difficult bond breaking at a larger deformation.

Over the first set of 50 cycles, the stress response drops within the first few cycles and levels off to an apparent steady state. Damage of the solid matter or breaking of bonds could create additional pathways for the fluid to flow, causing less resistance to deformation within the tissue. The lower stress seen in the apparent steady state could be caused from fluid redistribution causing a decrease in resisting pressure within the tissue or from the breaking of bonds resulting in reduced stress carrying ability.

5.2.2   Comparison of First and Second Sets of Cycles

The first set of deformation cycles damages the tissue, while the second set of deformation cycles serves to assess the effect of rest on damaged tissue. Upon initial deformation, bonds of cell adhesion molecules break, which leads to a more open path for ECF to flow within the tissue. The open pathways and easier flow of ECF decreases the stress required to deform the tissue, resulting in an apparent steady state, during which few additional bonds are broken. The second set of cycles that follows the period of rest is analogous to a second injury similar to repeated concussions and mTBI. This rest period that is 60 seconds is not equivalent to several days rest, that is required in vivo in humans, but demonstrates the possible reformation of some bonds. Although there is reformation of some bonds during rest, the bonds are not fully reformed and therefore the tissue does not fully recover.

The presence of a transient region in the second set of 50 cycles demonstares that

some of the bonds have reformed within the period of stress relaxation. The transient region is significantly shorter in the second set of 50 cycles than in the first set of 50 cycles (Table 45). This shorter transient region is likely due to the previous damage that has occurred within the solid matter upon the first set of 50 cycles and that only some bonds reform. With previously damaged axons and bonds between axons and glial processes, pathways are already partially open, which makes ECF flow easier.

Ratio of Power of Significant Frequency Components

The ratio of power of significant frequency components between the first and second set of cycles demonstrates the difference in required force to displace the tissue (Tables 32 through 37). If the power of significant frequency components is smaller in the second set of 50 cycles (i.e. a ratio larger than one), less force is required to displace the tissue. The majority of ratios of power at significant harmonics are greater than one, with a few exceptions. This suggests that bonds are broken in the first set of 50 cycles, which requires a larger force. After the stress relaxation period, the majority of the bonds are already broken so the second set of 50 cycles exhibits a smaller power because less force is required to deform the tissue.

Comparison of Initial Peak Stress

The initial peak stress value in the first set of 50 cycles compared to the second set of 50 cycles is indicative of damage because the stress is a measure of bond strength. Bond strength is highest in the initial deformation cycle due to bonds being completely intact. The shear stress magnitude of the first cycle within the first set of 50 cycles is always larger compared to the first cycle within the second set of 50 cycles. The higher initial peak stress in the first set of 50 cycles shows that a higher stress is required to displace the tissue by a controlled amount in the first set of 50 cycles as compared to the second set of 50 cycles. The lower stress value in second set

of 50 cycles is indicative of damage because it demonstrates its decreased ability to carry a load. For the initial peak stress in the second set of 50 cycles, the damage that occurs in the first 50 cycles is not fully recovered in the stress relaxation during zero deformation. The second set of 50 cycles still has a small transient region and supports a smaller load, indicating that stress relaxation may aid in some recovery of the tissue via fluid redistribution, but the tissue does not fully recover in the time allowed in the test. The initial peak stress value increases with increasing deformation frequency at 10% displacement, however this is not true at 25% displacement (Tables 38 through 43). Although, the initial peak stress at a specific deformation frequency is higher at 25% displacement as compared to 10% displacement. Since the initial peak stress value increases as the deformation frequency is increased, the stress required to break bonds within the tissue is increased.

Shear Stress Magnitude of Apparent Steady State Deformation Cycle

The shear stress magnitude of cycle 20 increases with increasing deformation frequency (Table 52). As the applied deformation frequency increases, a higher force is required to deform the tissue by the desired amount within the apparent steady state region. The increase in shear stress magnitude of cycle 20 could possibly be due to the increased drag force and fluid inertia at higher deformation frequencies. However, at each deformation frequency, the shear stress amplitude of cycle 20 is the same in the first set of 50 cycles as it is in the second set of 50 cycles. This could possibly be due to breaking the same bonds that were broken in the first set of cycles, resulting in a similar steady state.

Relation of Shear Response in the Two Sets of 50 Cycles

Brain tissue is heterogeneous and biphasic, meaning it is composed of both water and solid phases. The water content of white matter and grey matter in humans has

been measured to be 0.71 g/ml and 0.83 g/ml, respectively [2]. Brain tissue's mechanical response to deformation is influenced by the high fluid content in the tissue. Brain tissue structure is maintained by the interaction between solid matter (neurons and glial cells) and the ECF. Bonds between neurons and glial cells (specifically astrocytes) form a structurally weak network that maintains the integrity of the brain tissue by a combination of tension in the axons, dendrites and glial processes that is balanced by hydrostatic pressure in the ECF [53]. Under mechanical deformation, such as applied sinusoidal translational shear loading, a disruption of the balance of tension in the axons, dendrites and glial processes with the ECF hydrostatic pressure, may lead to damage of the tissue. A sudden increase in pressure could lead to tissue damage at the interface of high and low pressure areas [36].

The combination of the bonds between the solid phases and the water content of the brain tissue offers a possible explanation of the comparative mechanical response in the two sets of 50 deformation cycles of brain tissue to shear deformation. Following the initial set of 50 deformation cycles, the tissue is relaxed for 60 seconds until another set of 50 deformation cycles is applied. Stress relaxation is largely due to fluid redistribution to reduce the pressure gradient in hydrated viscoelastic materials such as brain tissue [6]. During the stress relaxation period, the tissue relaxes to nearly zero stress, and then on the second set of deformation cycles, it supports a load again. As previously mentioned, during a non-deformed state, the tissue is held together by tension in the solid matter that is balanced by hydrostatic pressure in the ECF. During deformation, these internal forces are no longer balanced which may create a pressure gradient in the fluid. During stress relaxation, redistribution of ECF occurs which allows the tissue to support stress in the second set of cycles. Following stress relaxation some bonds between solid matter reform, even in vitro. Because the second set of deformation cycles has an initial peak stress and transient region, it does not continue the steady state of the first set of deformation cycles.

5.3 Limitations and Future work

Within the harmonic wavelet analysis, at higher frequencies of 100 Hz and 125 Hz, the j-level range is too broad to pick up specific harmonics. The broad j-level range is a result of the sampling frequency, which is an artifact of the Bose machine, with a minimum sampling interval of 5,000 points per second. Sampling more data points per second would narrow the j-level range, however, this is not possible with the Bose machine. With the limitations of the j-level range in the harmonic wavelet analysis, future work could include using Empirical Mode Decomposition to distinguish the frequency in the j-level that can be used for non-linear and non-stationary signals. Another limitation of the study is that the Bose machine can only get up to 10% deformation at 125 Hz.

The results have demonstrated that damage occurs due to increasing deformation frequencies. These results are purely experimental. No model currently exists for sinusoidal deformation of heterogeneous rat brain tissue. A mathematical model to fit the results would be beneficial in further studying the frequency analysis of stress to locate damage due to shear waves. A model may also be able to further aid the identification of subregions within the heterogenous brain tissue that generates the harmonics. For example, the third order Burgers equation predicts only odd harmonics [54] and so is not valid for the rat cerebrum. A future study should also include an analysis of subharmonics that are occasionally present in the transient region of some tests.

6   Conclusion

Sinusoidal shear deformation waves permeate brain tissue when subjected to an external insult such as an impact or blast wave. Brain tissue, which is composed of multiple sub-regions and layered structures, is heterogenous with a high fluid content. The complexity of the solid matter and the high fluid content effects its shear stress response to deformation that disrupts the structural balance of ECF pressure and axonal tension. A shear deformation likely causes an increase in pressure gradients due to fluid being unevenly distributed by shear forces during deformation. Increases in pressure gradients and shearing forces cause bonds between neurons, cell adhesion molecules, and glial cells to break. The breaking of bonds ultimately results in a lowered stress carrying ability of the tissue due to a lowered resistance to deformation.

Signal characteristics analyzed by Fourier and harmonic wavelet analysis possibly correlate with the behavior of structural components of the tissue and the ECF. The third harmonic, which is associated with the fluid drag force, increases with increasing deformation frequency showing the importance of fluid and its pressure distribution in response to a high frequency mechanical insult. A higher deformation frequency requires greater acceleration of the ECF and creates a larger fluid drag force between the ECF and solid matter, producing a higher third harmonic. The presence of a fifth harmonic, that also increases with increasing deformation frequency, may indicate a physical tissue source responsible for generating the fifth harmonic when exposed to a sinusoidal deformation. Higher deformation frequencies also induce higher significant harmonics and symmetry breaking in the loading and unloading of a deformation cycle. The change in significant frequency components with increasing deformation frequency, as shown by Fourier and harmonic wavelet analysis verifies that rat brain cerebrum is deformation frequency rate dependent.

The shear deformation applied in two sets of 50 cycles separated by a 60 second

period of relaxation models the response of brain tissue to repeated mild injury by shear. The repeated insult to the tissue produces damage indicators that reflect possible sources for injury related to mTBI such as bond and synapse breaking. This bond and synapse breaking is believed to underlie some symptoms of mTBI, and may occur in conjunction with other mechanisms. Bond breaking occurs as a result of the applied sinusoidal shear deformation as exhibited in the transient shear stress response. Higher deformation frequencies show longer transient regions and larger shear stress magnitudes, which is indicative of the difficulty of moving the ECF at high deformation frequencies. The extent of the bond breaking depends on both the applied deformation frequency and displacement amplitude. The transient region that is characterized by bond breaking is followed by an apparent steady state in which little additional bond breaking occurs, as shown by a small change in shear stress amplitude. The second set of deformation cycles provides evidence that even in vitro rest allows partial reformation of broken bonds that occurred due to the first insult, but not total recovery. The period of relaxation allows for ECF redistribution and some reformation of bonds, which is verified by the tissue's ability to maintain a load upon a second insult. However, the significant decrease in length of transient region and magnitude of initial peak stress shows that the bonds are not completely reformed and are able to support less force on the second insult. Such recovery models that which occurs during treatment of mTBI in humans.

The shear stress response of rat cerebrum characterizes mild tissue damage due to an applied deformation frequency. The comparison of shear stress magnitudes in the transient and apparent steady state regions, and the length of transient regions of the first and second set of 50 cycles at all deformation frequencies confirm the presence of bond breaking that occurs in the tissue due to shear. This experiment provides direct evidence that the mechanism by which sinusoidal shear deformation causes mTBI involves bond breaking at displacement amplitudes of at least 10%. Bond and

synapse breaking due to an applied mechanical insult is believed to cause reduced functional connectivity, often seen in mTBI patients. It is possible that broken bonds due to shear deformation in an impact wave are partially responsible for reduced connectivity and brain communication. Analysis of shear stress response induced by translational sinusoidal deformation may offer an alternative method of capturing mild damage underlying mTBI that cannot be seen through imaging or histology.

Appendix A   Power Tables

Tables 59 through 89 contain the power of significant frequency components for every individual specimen at each deformation frequency, displacement amplitude, and set of 50 cycles. The power is calculated over the entire 50 cycles and therefore contains the significant frequency components within the transient and apparent steady state regions.

Table 59: Power of frequency components of the first 50 cycles at input frequency of 25 Hz and 10% displacement.

Test Name	Power at Significant Harmonics			
	1	2	3	5
zshearsine60116a	844.3	81.7	305.7	67.5
zshearsine60116b	484.7	37.4	130.5	18.4
zshearsine60116c	511.7	6.4	153.9	20.7
zshearsine60116d	569.9	18.9	149.6	14.7
zshearsine60116e	822.1	44.9	257.4	45.2
zshearsine60116f	434.7	30.1	123.5	13.7
zshearsine60116g	524.6	6.4	159.3	19.5
zshearsine60716a	509.7	33.8	132.9	17.8
zshearsine60716b	784.9	80.9	246.9	43
zshearsine60716c	704.6	10.5	215.9	37.9
zshearsine60716d	480.7	28.1	119.2	14.6
zshearsine60716e	615.8	13.1	172.3	21.7
zshearsine60716f	320.7	8.6	69.3	8.3
AVG	**585.3**	**30.8**	**172.0**	**26.4**
SD	**159.9**	**25.7**	**66.2**	**16.9**

Table 60: Power of frequency components of the first 50 cycles at input frequency of 25 Hz and 25% displacement.

Test Name	Power at Significant Harmonics			
	1	2	3	5
zshearsine20816a	1193	28.4	509.7	135.6
zshearsine20816b	1141	177.7	381.9	91.2
zshearsine20816e	1110	47.8	441.2	99.9
zshearsine20816g	1192	75.1	436.3	109.1
zshearsine20816h	667.1	45.3	223.6	56.7
zshearsine21016a	857.6	61.2	348.6	108.7
zshearsine21016b	411.7	12.4	86.1	36.5
zshearsine21016c	445.7	12.5	124.5	43.5
zshearsine21016d	1007	11.5	381.4	101.1
zshearsine21016e	847.6	16.9	308.1	64.7
zshearsine60716g	913.7	19.8	345.3	75.2
zshearsine60716h	590.2	27.9	99.6	80.8
zshearsine60716i	660.5	9.8	221.6	64.3
zshearsine60716j	783.5	15.7	319.7	80.5
AVG	**844.3**	**40.1**	**301.9**	**81.9**
SD	**264.8**	**44.5**	**132.8**	**27.6**

Table 61: Power of frequency components of the last 50 cycles at input frequency of 25 Hz and 10% displacement.

Test Name	Power at Significant Harmonics			
	1	2	3	5
zshearsine60116a	692.3	55.7	246.9	57.9
zshearsine60116b	452.2	31.4	122.5	18.3
zshearsine60116c	518.9	3.5	157.1	26.4
zshearsine60116d	529.4	19.8	138.1	21.5
zshearsine60116e	774.1	22.2	251.6	49.4
zshearsine60116f	406.7	30.3	122.7	17.9
zshearsine60116g	464.6	14.3	142.8	12.6
zshearsine60716a	474.3	30.6	130.6	19.4
zshearsine60716b	709.6	56.5	219.5	42.2
zshearsine60716c	629.1	7.9	194.2	34.2
zshearsine60716d	423.9	22.8	106.7	13.4
zshearsine60716e	601.1	12.4	177.9	26.4
zshearsine60716f	323.9	10.4	74.2	8.5
AVG	**538.5**	**24.4**	**160.3**	**26.7**
SD	**133.7**	**16.6**	**54.5**	**15.1**

Table 62: Power of frequency components of the last 50 cycles at input frequency of 25 Hz and 25% displacement.

Test Name	Power at Significant Harmonics			
	1	2	3	5
zshearsine20816a	839.3	13.2	363.1	110.5
zshearsine20816b	911.5	151.7	319.6	78.9
zshearsine20816e	937.2	8.7	394.1	107.1
zshearsine20816g	1320.5	74.4	541.1	158.3
zshearsine20816h	707.8	64.6	231.8	68.5
zshearsine21016a	814.9	30.3	318.1	92.9
zshearsine21016b	593.3	15	160.9	54.8
zshearsine21016c	1026.9	48.6	414.5	120.7
zshearsine21016d	879.6	19.9	328.8	107.5
zshearsine21016e	798.1	51.9	243.7	69.6
zshearsine60716g	735.9	5.9	275.2	66.2
zshearsine60716h	456.4	30.1	49.3	59.4
zshearsine60716i	682.2	3.3	257.5	88.3
zshearsine60716j	677.6	22.1	273.9	81.7
AVG	**812.9**	**38.5**	**297.9**	**90.3**
SD	**207.8**	**39.4**	**117.2**	**28.4**

Table 63: Power of frequency components of the first 50 cycles at input frequency of 50 Hz and 10% displacement.

Test Name	Power at Significant Harmonics			
	1	2	3	5
zshearsine60916a	573.9	29.5	117.5	192.7
zshearsine60916b	743.7	48.4	208.7	20.1
zshearsine60916c	832.8	91.2	267.9	43.9
zshearsine60916d	576.1	30.3	141.6	14.5
zshearsine60916e	615.6	1.7	153.3	6.5
zshearsine60916f	723	80.1	198.7	13.9
zshearsine60916g	763.9	24.3	232.6	12.4
zshearsine60916h	593.8	21.3	148.2	9.7
zshearsine61316a	663.9	31.7	164.7	8.9
zshearsine61316b	1012.6	194.4	247.3	48.1
AVG	**709.9**	**55.2**	**188.1**	**37.1**
SD	**138.2**	**55.9**	**50.4**	**56.6**

Table 64: Power of frequency components of the first 50 cycles at input frequency of 50 Hz and 25% displacement.

Test Name	Power at Significant Harmonics			
	1	2	3	5
zshearsine31016a	1008	53.2	349.7	64.1
zshearsine31016b	1205.2	6	446.9	96.9
zshearsine31016c	1113.6	118.6	511.4	196.6
zshearsine31016d	1103.1	4.4	412.1	54.8
zshearsine31016e	1008.5	32.4	292.8	83.8
zshearsine31016f	973.3	20.2	424.9	69.2
zshearsine31016g	1018.1	10.9	361.8	153.2
zshearsine31016h	857.7	9.3	321.4	56.5
zshearsine32116a	1182.3	6.6	423.9	78.5
zshearsine32116b	1393.4	54	586.1	91.4
zshearsine32116c	1182.6	100.4	460.2	34.6
zshearsine32116d	884.5	12.4	301.5	88.6
AVG	**1077.5**	**35.7**	**407.7**	**89.0**
SD	**150.6**	**38.7**	**87.8**	**44.8**

Table 65: Power of frequency components of the last 50 cycles at input frequency of 50 Hz and 10% displacement.

Test Name	Power at Significant Harmonics			
	1	2	3	5
zshearsine60916a	479.1	26.6	100.1	13.5
zshearsine60916b	628.7	42.9	197.3	33.1
zshearsine60916c	635.4	60.2	215.6	35.6
zshearsine60916d	560.3	7.7	145.3	17.9
zshearsine60916e	652.6	6.1	164.9	8.9
zshearsine60916f	584.9	58.2	175.1	21.1
zshearsine60916g	601.7	18.2	213.7	23.8
zshearsine60916h	510.3	9.1	132.1	2.2
zshearsine61316a	595.5	24.6	155.4	20.1
zshearsine61316b	781.3	145.5	219.2	23.6
AVG	**602.9**	**39.9**	**171.8**	**19.9**
SD	**83.1**	**42.1**	**39.9**	**10.2**

Table 66: Power of frequency components of the last 50 cycles at input frequency of 50 Hz and 25% displacement.

Test Name	Power at Significant Harmonics			
	1	2	3	5
zshearsine31016a	746.4	52.8	223.7	10.3
zshearsine31016b	1135	46.5	489.3	100.6
zshearsine31016c	1143	95.1	475.8	163.8
zshearsine31016d	1019.3	24.6	349	49.4
zshearsine31016e	782.2	14.1	186.8	99.5
zshearsine31016f	861.7	14.3	422.5	46.6
zshearsine31016g	880.1	15.9	366.6	153.6
zshearsine31016h	805.5	42.2	314.6	34
zshearsine32116a	1004	5.2	330.5	65.8
zshearsine32116b	1132.6	60.8	480.8	86.4
zshearsine32116c	1114	17.3	464.6	20.2
zshearsine32116d	697.4	2.6	209.1	119.7
AVG	**943.4**	**32.6**	**359.4**	**79.2**
SD	**166.7**	**27.4**	**110.3**	**50.1**

Table 67: Power of frequency components of the first 50 cycles at input frequency of 60 Hz and 10% displacement.

Test Name	Power at Significant Harmonics					
	1	2	3	5	7	9
zshearsine71216a	879.3	140.6	353.1	46.3	54.8	104.3
zshearsine71216b	514.1	10.7	184.8	54.7	66.9	85.4
zshearsine71216c	571.6	60.3	200.1	25.2	61.9	83.4
zshearsine71216d	575.7	124.8	232.4	33.8	9.6	11.4
zshearsine71216e	616.7	65.8	222.3	34.3	35.9	52.5
zshearsine71416a	618.1	82.2	212.3	31.7	60.8	168.9
zshearsine71416b	949.4	164.2	379.1	53.9	29.5	49.3
zshearsine71416c	629.7	20.1	245.3	44.2	41.7	89.5
zshearsine71416d	546.2	27.9	197.8	9.9	60.1	96.3
zshearsine71416e	688.4	94.2	217.1	71	79.4	77.7
zshearsine71416f	718.5	206.3	263.5	37.1	23.4	13.9
zshearsine71416g	548.6	51.3	211.7	24.1	39.3	56.8
zshearsine71416h	517.4	26.9	163.4	2.7	16.8	86.5
zshearsine71816a	670.3	41.5	197.7	2.7	15.3	86.5
zshearsine71816b	693.4	74.2	217.5	8.1	25.9	42.4
AVG	**646**	**79.7**	**234.3**	**33.7**	**42.5**	**75.8**
SD	**130.1**	**59.3**	**61.3**	**19.9**	**21.8**	**39.3**

Table 68: Power of frequency components of the first 50 cycles at input frequency of 60 Hz and 25% displacement.

Test Name	Power at Significant Harmonics						
	1	2	3	5	7	8	9
zshearsine61416a	1036	313.8	563.3	135.9	142.8	181.8	451.7
zshearsine61416b	858.7	99.1	511.5	129.5	82.7	28.9	251.2
zshearsine61416c	808.3	32.6	486.1	196.2	103.8	15.3	188.3
zshearsine61416d	964.1	56.7	594.8	138.8	138.3	42.6	457.2
zshearsine61416e	1039	30.4	639.5	285.9	296.1	96.8	805.4
zshearsine61416g	611.9	30.5	307.8	91.6	57.6	13.2	93.5
zshearsine61416h	840.3	19.9	555.7	320.6	232.8	110.1	509.7
zshearsine61616a	967.2	25.1	687.4	260.2	279.1	44.3	705.8
zshearsine61616b	1380	390.1	779.8	201.8	222.8	63.4	251.4
zshearsine61616c	572.3	90.8	364.1	69.7	88.1	31.3	155.2
zshearsine61616d	888.2	0.6	618.2	258.1	252.4	46.5	618.1
zshearsine61616e	616.5	50.9	249.1	50.1	54.8	64.9	104.9
zshearsine61616f	667.7	15.1	306.4	65.8	26.8	21.4	53.9
zshearsine61616g	736.8	182.4	303.1	45.7	44.4	31.1	83.4
zshearsine61616h	649.2	120.2	241.6	2.5	36.3	2.1	83.5
AVG	**842.4**	**97.2**	**480.5**	**150.2**	**137.3**	**52.9**	**320.8**
SD	**216.3**	**114.8**	**172.9**	**98.7**	**94.8**	**46.6**	**250.7**

Table 69: Power of frequency components of the last 50 cycles at input frequency of 60 Hz and 10% displacement.

Test Name	Power at Significant Harmonics					
	1	2	3	5	7	9
zshearsine71216a	781.9	122.1	326.4	46.1	44.9	93.1
zshearsine71216b	435.9	4.1	160.5	46.2	60.2	79.9
zshearsine71216c	516.3	59.4	180.5	23.8	62.4	77.5
zshearsine71216d	494.8	85.5	204.2	27.7	14.4	21.6
zshearsine71216e	534.9	47.3	203.3	30.1	31.6	46.5
zshearsine71416a	478.8	71.9	165.8	29.1	48.9	132.8
zshearsine71416b	796.2	126.5	334.7	53.5	41.6	46.1
zshearsine71416c	688.6	16.2	263.8	19.1	62.8	117.5
zshearsine71416d	442.3	11.2	161.5	2.6	45.7	78.4
zshearsine71416e	685.8	79.9	121.9	60.7	84.1	104
zshearsine71416f	698.1	170.9	260.2	42.3	24.7	31.8
zshearsine71416g	453.3	42.9	179.8	5.3	36.8	70.1
zshearsine71416h	403.7	14.3	142.2	48.4	52.5	78.2
zshearsine71816a	650.6	93.9	232.7	28.6	66.7	90.7
zshearsine71816b	523.9	24.5	203.6	28.8	19.5	33.9
AVG	**572.3**	**64.7**	**209.4**	**32.8**	**46.4**	**73.4**
SD	**131.5**	**49.1**	**63.2**	**16.7**	**19.2**	**32.3**

Table 70: Power of frequency components of the last 50 cycles at input frequency of 60 Hz and 25% displacement.

Test Name	Power at Significant Harmonics						
	1	2	3	5	7	8	9
zshearsine61416a	705.1	201.9	394.7	104.3	119.6	145.3	338.8
zshearsine61416b	770.2	58.2	513.1	93.7	135.2	1.4	385.6
zshearsine61416c	715.6	33.8	469.6	138.8	129.6	73.1	316.7
zshearsine61416d	650.8	55.1	389.9	83.4	89.8	11.1	282.1
zshearsine61416e	1017	37.9	588.2	221.3	250.8	151.1	698.1
zshearsine61416g	815.3	84.6	520.8	125.9	83.7	54.9	291.7
zshearsine61416h	643.6	14.1	414.1	241.2	175.4	87.3	327.4
zshearsine61616a	698.3	13.1	486.4	199.6	246.3	20.8	588.9
zshearsine61616b	861.8	197.2	558.3	138.3	152.9	9.5	236.5
zshearsine61616c	680.4	74.3	485.3	67.3	139.2	56.9	301.9
zshearsine61616d	627.1	13.6	429.5	181.7	211.1	51.5	448.5
zshearsine61616e	462.9	14.8	286.6	81.1	131.6	33.9	207.8
zshearsine61616f	603.6	8.9	290.4	65.1	21.3	17.4	41.1
zshearsine61616g	557.4	120.9	236.1	36.8	10.9	28.9	71.3
zshearsine61616h	499.8	63.8	191.	9.1	25.2	22.5	59.8
AVG	**687.3**	**66.1**	**416.9**	**119.2**	**128.2**	**51.0**	**306.4**
SD	**141.4**	**62.8**	**119.3**	**67.9**	**74.7**	**46.4**	**181.8**

Table 71: Power of frequency components of the first 50 cycles at input frequency of 75 Hz and 10% displacement.

Test Name	Power at Significant Harmonics					
	1	2	3	5	7	9
zshearsine61316c	265.1	83.9	330.4	167.2	1233	0.5
zshearsine61316d	241.3	230.7	331.2	120.1	1610.7	3.5
zshearsine61316e	149.8	154.1	272.6	126.4	995.5	14.3
zshearsine61316f	369.9	151.1	408.8	165.2	1451.4	3.8
zshearsine61316g	233.4	116.2	339.2	143.4	1109	2.9
zshearsine61316h	75.8	65.1	255.6	125.4	764.1	0.1
J75H32416a	349.2	124.1	361.7	125.2	372.1	4.9
J75H32416b	331.7	10.9	337.7	94.1	250.7	6.6
J75H32416c	341.1	12.8	383.1	96.1	117.2	1.2
J75H32416d	369.8	148.3	350.9	29.9	399.1	8.8
J75H32416e	451.8	157.2	391.5	101.2	416.7	24.9
J75H32416f	449.2	33.6	442.4	150.3	87.2	196.4
J75H32416g	311.1	3.6	227.4	36.3	26.8	93.9
J75H32416h	422.5	10.1	280.2	43.7	56.6	490.6
AVG	**311.5**	**92.9**	**336.6**	**108.8**	**635.0**	**60.8**
SD	**109.3**	**71.8**	**60.9**	**45.3**	**550.5**	**135.1**

Table 72: Power of frequency components of the first 50 cycles at input frequency of 75 Hz and 25% displacement.

Test Name	Power at Significant Harmonics					
	1	2	3	5	7	9
zshearsine72516a	1550.1	599.3	918.8	480.2	2427.3	543.7
zshearsine72516b	1751.9	503.5	955.1	400.1	5768.2	302.6
zshearsine72516c	409.3	234.6	908.4	497.2	2269.8	66.6
zshearsine72516d	266.9	251.6	702.5	379.8	858.3	69.1
zshearsine72516e	339.3	358.8	846.7	664.2	2809.2	53.1
zshearsine72516f	341.6	173.7	385.5	169.8	612.3	30.2
zshearsine72516g	198.7	248.8	512.9	312.9	1052	7.1
zshearsine72516h	261.5	277.6	731.2	443.1	1416.6	40.2
zshearsine72616a	488.1	410.7	952.8	462	2214.9	58.7
zshearsine72616b	1196.1	610.7	521.8	370.3	5059.1	374.6
AVG	**680.3**	**366.9**	**743.5**	**417.9**	**2448.7**	**154.5**
SD	**585.9**	**157.8**	**208.0**	**129.1**	**1731.0**	**184.5**

Table 73: Power of frequency components of the last 50 cycles at input frequency of 75 Hz and 10% displacement.

Test Name	Power at Significant Harmonics					
	1	2	3	5	7	9
zshearsine61316c	156.4	108.4	284.3	165.3	1273.2	7.2
zshearsine61316d	180.8	212.7	268.7	100.1	1714	0.7
zshearsine61316e	93.5	140.3	269.4	106.9	1006.1	10.7
zshearsine61316f	303.4	93.5	369.4	143.9	1778.5	5.5
zshearsine61316g	249.7	29.9	211.1	90.1	1299.4	3.7
zshearsine61316h	30.9	52.7	220.4	112.5	871.2	2.2
J75H32416a	195.4	93.5	38.9	39.1	127.3	3.9
J75H32416b	265.3	37.5	242.3	86.6	212.5	4.1
J75H32416c	223.3	32.2	365.6	75.4	56.2	3.8
J75H32416d	346.1	90.1	283.8	28.1	244.1	15.2
J75H32416e	389.1	99.8	287.5	62.9	353.1	5.3
J75H32416f	277.8	25.2	320.3	98.8	37.6	209.9
J75H32416g	241	29.5	319.1	71.4	43.2	256.8
J75H32416h	362	30.6	181.7	68.8	63.9	410.1
AVG	**236.76**	**76.8**	**261.6**	**89.2**	**648.5**	**67.0**
SD	**100.9**	**54.1**	**83.9**	**36.9**	**653.2**	**128.8**

Table 74: Power of frequency components of the last 50 cycles at input frequency of 75 Hz and 25% displacement.

Test Name	Power at Significant Harmonics					
	1	2	3	5	7	9
zshearsine72516a	1030.1	480.8	165.9	290.2	2122	398.9
zshearsine72516b	1507	504.4	858.4	628.4	5378	130.2
zshearsine72516c	370.3	222.8	791.3	394.5	1794	17.9
zshearsine72516d	130.2	177.3	570.3	327.8	620.2	28.6
zshearsine72516e	140.4	267.1	529.7	438.8	1546	5.1
zshearsine72516f	142.8	191.6	484.9	268.3	1236.3	15.3
zshearsine72516g	84.7	196.7	574.8	339.5	1388.9	14.2
zshearsine72516h	39.6	154.4	468.3	226.6	684.6	47.7
zshearsine72616a	300.8	319.3	740.8	367.9	2012.7	36.8
zshearsine72616b	1321.7	646.7	591.2	408.9	5354	334.6
AVG	**506.8**	**316.1**	**577.6**	**369.1**	**2213.7**	**102.9**
SD	**558.2**	**169.4**	**195.4**	**112.3**	**1733.9**	**144.3**

Table 75: Power of frequency components of the first 50 cycles at input frequency of 100 Hz and 10% displacement.

Test Name	Power at Significant Harmonics						
	1	2	3	5	6	7	9
zshearsine80216b	462.5	43.7	637.3	870.8	21.5	0.4	99.8
zshearsine80216c	82.3	28.7	412.5	680.7	19.3	3.8	5.1
zshearsine80216d	277.7	55.6	550.1	964.3	32.2	1	26.8
zshearsine80216e	70.7	38.6	461.7	745.2	18.5	0.3	16.8
zshearsine80216f	179.5	10.3	518.8	848.5	25.3	3.5	31.6
zshearsine80216g	414.1	4.3	666.6	1187.4	42.3	5.1	65.7
zshearsine80216h	251.5	80.2	492.9	738.6	22.41	0.5	2.6
zshearsine80316a	155	97.5	491.8	931.2	12.4	3.8	80.8
zshearsine80316b	149.8	8.8	530.5	1025.8	22.3	14.9	39.1
AVG	**227.0**	**40.9**	**529.1**	**888.1**	**24.0**	**3.7**	**40.9**
SD	**138.0**	**32.5**	**80.6**	**159.6**	**8.7**	**4.6**	**34.1**

Table 76: Power of frequency components of the last 50 cycles at input frequency of 50 Hz and 25% displacement.

Test Name	Power at Significant Harmonics			
	1	2	3	5
zshearsine31016a	746.4	52.8	223.7	10.3
zshearsine31016b	1135	46.5	489.3	100.6
zshearsine31016c	1143	95.1	475.8	163.8
zshearsine31016d	1019.3	24.6	349	49.4
zshearsine31016e	782.2	14.1	186.8	99.5
zshearsine31016f	861.7	14.3	422.5	46.6
zshearsine31016g	880.1	15.9	366.6	153.6
zshearsine31016h	805.5	42.2	314.6	34
zshearsine32116a	1004	5.2	330.5	65.8
zshearsine32116b	1132.6	60.8	480.8	86.4
zshearsine32116c	1114	17.3	464.6	20.2
zshearsine32116d	697.4	2.6	209.1	119.7
AVG	**943.4**	**32.6**	**359.4**	**79.2**
SD	**166.7**	**27.4**	**110.3**	**50.1**

Table 77: Power of frequency components of the first 50 cycles at input frequency of 60 Hz and 10% displacement.

Test Name	Power at Significant Harmonics					
	1	2	3	5	7	9
zshearsine71216a	879.3	140.6	353.1	46.3	54.8	104.3
zshearsine71216b	514.1	10.7	184.8	54.7	66.9	85.4
zshearsine71216c	571.6	60.3	200.1	25.2	61.9	83.4
zshearsine71216d	575.7	124.8	232.4	33.8	9.6	11.4
zshearsine71216e	616.7	65.8	222.3	34.3	35.9	52.5
zshearsine71416a	618.1	82.2	212.3	31.7	60.8	168.9
zshearsine71416b	949.4	164.2	379.1	53.9	29.5	49.3
zshearsine71416c	629.7	20.1	245.3	44.2	41.7	89.5
zshearsine71416d	546.2	27.9	197.8	9.9	60.1	96.3
zshearsine71416e	688.4	94.2	217.1	71	79.4	77.7
zshearsine71416f	718.5	206.3	263.5	37.1	23.4	13.9
zshearsine71416g	548.6	51.3	211.7	24.1	39.3	56.8
zshearsine71416h	517.4	26.9	163.4	2.7	16.8	86.5
zshearsine71816a	670.3	41.5	197.7	2.7	15.3	86.5
zshearsine71816b	693.4	74.2	217.5	8.1	25.9	42.4
AVG	**646**	**79.7**	**234.3**	**33.7**	**42.5**	**75.8**
SD	**130.1**	**59.3**	**61.3**	**19.9**	**21.8**	**39.3**

Table 78: Power of frequency components of the first 50 cycles at input frequency of 60 Hz and 25% displacement.

Test Name	Power at Significant Harmonics						
	1	2	3	5	7	8	9
zshearsine61416a	1036	313.8	563.3	135.9	142.8	181.8	451.7
zshearsine61416b	858.7	99.1	511.5	129.5	82.7	28.9	251.2
zshearsine61416c	808.3	32.6	486.1	196.2	103.8	15.3	188.3
zshearsine61416d	964.1	56.7	594.8	138.8	138.3	42.6	457.2
zshearsine61416e	1039	30.4	639.5	285.9	296.1	96.8	805.4
zshearsine61416g	611.9	30.5	307.8	91.6	57.6	13.2	93.5
zshearsine61416h	840.3	19.9	555.7	320.6	232.8	110.1	509.7
zshearsine61616a	967.2	25.1	687.4	260.2	279.1	44.3	705.8
zshearsine61616b	1380	390.1	779.8	201.8	222.8	63.4	251.4
zshearsine61616c	572.3	90.8	364.1	69.7	88.1	31.3	155.2
zshearsine61616d	888.2	0.6	618.2	258.1	252.4	46.5	618.1
zshearsine61616e	616.5	50.9	249.1	50.1	54.8	64.9	104.9
zshearsine61616f	667.7	15.1	306.4	65.8	26.8	21.4	53.9
zshearsine61616g	736.8	182.4	303.1	45.7	44.4	31.1	83.4
zshearsine61616h	649.2	120.2	241.6	2.5	36.3	2.1	83.5
AVG	**842.4**	**97.2**	**480.5**	**150.2**	**137.3**	**52.9**	**320.8**
SD	**216.3**	**114.8**	**172.9**	**98.7**	**94.8**	**46.6**	**250.7**

Table 79: Power of frequency components of the last 50 cycles at input frequency of 60 Hz and 10% displacement.

Test Name	Power at Significant Harmonics					
	1	2	3	5	7	9
zshearsine71216a	781.9	122.1	326.4	46.1	44.9	93.1
zshearsine71216b	435.9	4.1	160.5	46.2	60.2	79.9
zshearsine71216c	516.3	59.4	180.5	23.8	62.4	77.5
zshearsine71216d	494.8	85.5	204.2	27.7	14.4	21.6
zshearsine71216e	534.9	47.3	203.3	30.1	31.6	46.5
zshearsine71416a	478.8	71.9	165.8	29.1	48.9	132.8
zshearsine71416b	796.2	126.5	334.7	53.5	41.6	46.1
zshearsine71416c	688.6	16.2	263.8	19.1	62.8	117.5
zshearsine71416d	442.3	11.2	161.5	2.6	45.7	78.4
zshearsine71416e	685.8	79.9	121.9	60.7	84.1	104
zshearsine71416f	698.1	170.9	260.2	42.3	24.7	31.8
zshearsine71416g	453.3	42.9	179.8	5.3	36.8	70.1
zshearsine71416h	403.7	14.3	142.2	48.4	52.5	78.2
zshearsine71816a	650.6	93.9	232.7	28.6	66.7	90.7
zshearsine71816b	523.9	24.5	203.6	28.8	19.5	33.9
AVG	**572.3**	**64.7**	**209.4**	**32.8**	**46.4**	**73.4**
SD	**131.5**	**49.1**	**63.2**	**16.7**	**19.2**	**32.3**

Table 80: Power of frequency components of the last 50 cycles at input frequency of 60 Hz and 25% displacement.

Test Name	Power at Significant Harmonics						
	1	2	3	5	7	8	9
zshearsine61416a	705.1	201.9	394.7	104.3	119.6	145.3	338.8
zshearsine61416b	770.2	58.2	513.1	93.7	135.2	1.4	385.6
zshearsine61416c	715.6	33.8	469.6	138.8	129.6	73.1	316.7
zshearsine61416d	650.8	55.1	389.9	83.4	89.8	11.1	282.1
zshearsine61416e	1017	37.9	588.2	221.3	250.8	151.1	698.1
zshearsine61416g	815.3	84.6	520.8	125.9	83.7	54.9	291.7
zshearsine61416h	643.6	14.1	414.1	241.2	175.4	87.3	327.4
zshearsine61616a	698.3	13.1	486.4	199.6	246.3	20.8	588.9
zshearsine61616b	861.8	197.2	558.3	138.3	152.9	9.5	236.5
zshearsine61616c	680.4	74.3	485.3	67.3	139.2	56.9	301.9
zshearsine61616d	627.1	13.6	429.5	181.7	211.1	51.5	448.5
zshearsine61616e	462.9	14.8	286.6	81.1	131.6	33.9	207.8
zshearsine61616f	603.6	8.9	290.4	65.1	21.3	17.4	41.1
zshearsine61616g	557.4	120.9	236.1	36.8	10.9	28.9	71.3
zshearsine61616h	499.8	63.8	191.	9.1	25.2	22.5	59.8
AVG	**687.3**	**66.1**	**416.9**	**119.2**	**128.2**	**51.0**	**306.4**
SD	**141.4**	**62.8**	**119.3**	**67.9**	**74.7**	**46.4**	**181.8**

Table 81: Power of frequency components of the first 50 cycles at input frequency of 75 Hz and 10% displacement.

Test Name	Power at Significant Harmonics					
	1	2	3	5	7	9
zshearsine61316c	265.1	83.9	330.4	167.2	1233	0.5
zshearsine61316d	241.3	230.7	331.2	120.1	1610.7	3.5
zshearsine61316e	149.8	154.1	272.6	126.4	995.5	14.3
zshearsine61316f	369.9	151.1	408.8	165.2	1451.4	3.8
zshearsine61316g	233.4	116.2	339.2	143.4	1109	2.9
zshearsine61316h	75.8	65.1	255.6	125.4	764.1	0.1
J75H32416a	349.2	124.1	361.7	125.2	372.1	4.9
J75H32416b	331.7	10.9	337.7	94.1	250.7	6.6
J75H32416c	341.1	12.8	383.1	96.1	117.2	1.2
J75H32416d	369.8	148.3	350.9	29.9	399.1	8.8
J75H32416e	451.8	157.2	391.5	101.2	416.7	24.9
J75H32416f	449.2	33.6	442.4	150.3	87.2	196.4
J75H32416g	311.1	3.6	227.4	36.3	26.8	93.9
J75H32416h	422.5	10.1	280.2	43.7	56.6	490.6
AVG	**311.5**	**92.9**	**336.6**	**108.8**	**635.0**	**60.8**
SD	**109.3**	**71.8**	**60.9**	**45.3**	**550.5**	**135.1**

Table 82: Power of frequency components of the first 50 cycles at input frequency of 75 Hz and 25% displacement.

Test Name	Power at Significant Harmonics					
	1	2	3	5	7	9
zshearsine72516a	1550.1	599.3	918.8	480.2	2427.3	543.7
zshearsine72516b	1751.9	503.5	955.1	400.1	5768.2	302.6
zshearsine72516c	409.3	234.6	908.4	497.2	2269.8	66.6
zshearsine72516d	266.9	251.6	702.5	379.8	858.3	69.1
zshearsine72516e	339.3	358.8	846.7	664.2	2809.2	53.1
zshearsine72516f	341.6	173.7	385.5	169.8	612.3	30.2
zshearsine72516g	198.7	248.8	512.9	312.9	1052	7.1
zshearsine72516h	261.5	277.6	731.2	443.1	1416.6	40.2
zshearsine72616a	488.1	410.7	952.8	462	2214.9	58.7
zshearsine72616b	1196.1	610.7	521.8	370.3	5059.1	374.6
AVG	**680.3**	**366.9**	**743.5**	**417.9**	**2448.7**	**154.5**
SD	**585.9**	**157.8**	**208.0**	**129.1**	**1731.0**	**184.5**

Table 83: Power of frequency components of the last 50 cycles at input frequency of 75 Hz and 10% displacement.

Test Name	Power at Significant Harmonics					
	1	2	3	5	7	9
zshearsine61316c	156.4	108.4	284.3	165.3	1273.2	7.2
zshearsine61316d	180.8	212.7	268.7	100.1	1714	0.7
zshearsine61316e	93.5	140.3	269.4	106.9	1006.1	10.7
zshearsine61316f	303.4	93.5	369.4	143.9	1778.5	5.5
zshearsine61316g	249.7	29.9	211.1	90.1	1299.4	3.7
zshearsine61316h	30.9	52.7	220.4	112.5	871.2	2.2
J75H32416a	195.4	93.5	38.9	39.1	127.3	3.9
J75H32416b	265.3	37.5	242.3	86.6	212.5	4.1
J75H32416c	223.3	32.2	365.6	75.4	56.2	3.8
J75H32416d	346.1	90.1	283.8	28.1	244.1	15.2
J75H32416e	389.1	99.8	287.5	62.9	353.1	5.3
J75H32416f	277.8	25.2	320.3	98.8	37.6	209.9
J75H32416g	241	29.5	319.1	71.4	43.2	256.8
J75H32416h	362	30.6	181.7	68.8	63.9	410.1
AVG	**236.76**	**76.8**	**261.6**	**89.2**	**648.5**	**67.0**
SD	**100.9**	**54.1**	**83.9**	**36.9**	**653.2**	**128.8**

Table 84: Power of frequency components of the last 50 cycles at input frequency of 75 Hz and 25% displacement.

Test Name	Power at Significant Harmonics					
	1	2	3	5	7	9
zshearsine72516a	1030.1	480.8	165.9	290.2	2122	398.9
zshearsine72516b	1507	504.4	858.4	628.4	5378	130.2
zshearsine72516c	370.3	222.8	791.3	394.5	1794	17.9
zshearsine72516d	130.2	177.3	570.3	327.8	620.2	28.6
zshearsine72516e	140.4	267.1	529.7	438.8	1546	5.1
zshearsine72516f	142.8	191.6	484.9	268.3	1236.3	15.3
zshearsine72516g	84.7	196.7	574.8	339.5	1388.9	14.2
zshearsine72516h	39.6	154.4	468.3	226.6	684.6	47.7
zshearsine72616a	300.8	319.3	740.8	367.9	2012.7	36.8
zshearsine72616b	1321.7	646.7	591.2	408.9	5354	334.6
AVG	**506.8**	**316.1**	**577.6**	**369.1**	**2213.7**	**102.9**
SD	**558.2**	**169.4**	**195.4**	**112.3**	**1733.9**	**144.3**

Table 85: Power of frequency components of the first 50 cycles at input frequency of 100 Hz and 10% displacement.

Test Name	Power at Significant Harmonics						
	1	2	3	5	6	7	9
zshearsine80216b	462.5	43.7	637.3	870.8	21.5	0.4	99.8
zshearsine80216c	82.3	28.7	412.5	680.7	19.3	3.8	5.1
zshearsine80216d	277.7	55.6	550.1	964.3	32.2	1	26.8
zshearsine80216e	70.7	38.6	461.7	745.2	18.5	0.3	16.8
zshearsine80216f	179.5	10.3	518.8	848.5	25.3	3.5	31.6
zshearsine80216g	414.1	4.3	666.6	1187.4	42.3	5.1	65.7
zshearsine80216h	251.5	80.2	492.9	738.6	22.41	0.5	2.6
zshearsine80316a	155	97.5	491.8	931.2	12.4	3.8	80.8
zshearsine80316b	149.8	8.8	530.5	1025.8	22.3	14.9	39.1
AVG	**227.0**	**40.9**	**529.1**	**888.1**	**24.0**	**3.7**	**40.9**
SD	**138.0**	**32.5**	**80.6**	**159.6**	**8.7**	**4.6**	**34.1**

Table 86: Power of frequency components of the first 50 cycles at input frequency of 100 Hz and 25% displacement.

Test Name	Power at Significant Harmonics						
	1	2	3	5	6	7	9
J100H41416a	1885.1	522.7	573.5	851.6	2977.8	274.2	260.2
J100H41416b	459.8	77.9	894.8	852.1	1379.3	248.5	9.4
J100H41416c	243.4	104.8	692.2	776.3	796.5	231.8	0.9
J100H41416d	192.9	133.4	560.3	593.9	653.1	137.7	6.7
J100H41416e	165.9	133.1	666.8	663.9	681.7	177.4	2.4
J100H41416f	195.6	79.2	577.2	608.4	357.9	136.9	9.6
J100H41416g	178.1	113.8	638.1	646.7	537.7	158.2	2.7
zshearsine42116a	313.3	80.1	603.2	580.8	560.6	227.8	8.4
zshearsine42116b	216.2	55.9	648.3	565.4	1858.7	136.1	3.7
zshearsine42116c	163.7	73.9	669	673.4	448.3	197.5	3.2
zshearsine42116d	196.9	60.4	550.3	528.9	481.7	115.1	9.7
AVG	**382.8**	**130.5**	**643.1**	**667.4**	**975.8**	**185.6**	**28.8**
SD	**505.7**	**132.8**	**96.6**	**112.4**	**802.6**	**53.6**	**76.8**

Table 87: Power of frequency components of the last 50 cycles at input frequency of 100 Hz and 10% displacement.

Test Name	Power at Significant Harmonics						
	1	2	3	5	6	7	9
zshearsine80216b	281.1	74.1	531.4	763.5	12.6	0	53.9
zshearsine80216c	35.7	33.8 387.1	654.9	15.3	0.1	1.2	
zshearsine80216d	266.1	88.4	559.4	933.4	24.3	4.7	35.9
zshearsine80216e	43.4	34.3	344.2	578.6	16.7	7.1	16.4
zshearsine80216f	84.2	10.6	354.4	690.2	14.5	0.9	11.5
zshearsine80216g	387.7	32.7	654.5	1170.3	32.1	7.6	73.3
zshearsine80216h	140.1	95.2	370.8	553.1	25.5	1.8	25.9
zshearsine80316a	58.5	41.3	328.7	658.2	10.2	14.5	56.2
zshearsine80316b	130.2	20.6	459.4	893.5	3.9	2.4	61.8
AVG	**158.6**	**47.9**	**443.3**	**766.2**	**17.2**	**4.3**	**37.3**
SD	**124.6**	**30.3**	**114.8**	**199.3**	**8.7**	**4.7**	**25.2**

Table 88: Power of frequency components of the last 50 cycles at input frequency of 100 Hz and 25% displacement.

Test Name	Power at Significant Harmonics						
	1	2	3	5	6	7	9
J100H41416a	1589	554.5	370.8	327.8	3372.6	183.1	302.5
J100H41416b	277.4	69.9	746.4	649.6	1761.2	184.2	2.2
J100H41416c	221.3	54.4	496.6	543.8	770.5	143.8	8.5
J100H41416d	253.6	72.9	455.2	359.9	387.9	92.9	0.7
J100H41416e	122.7	110.8	725.2	682.3	971.3	195.8	2.1
J100H41416f	148.1	25.8	411.6	349.1	308.2	86.5	6.5
J100H41416g	232.3	79.1	535.8	490.8	583.8	120.5	6.7
zshearsine42116a	291.3	73.2	419.2	384.5	601.3	141.5	3.1
zshearsine42116b	151.2	40.5	636.9	513.6	1474.9	131.5	0.8
zshearsine42116c	189.5	64.8	576.7	544.8	501.9	177.5	1.7
zshearsine42116d	184.5	56.9	456.6	361.5	451.5	94.5	4.4
AVG	**332.8**	**109.3**	**530.1**	**473.4**	**1016.8**	**141.1**	**30.8**
SD	**420.2**	**149.2**	**127.4**	**125.1**	**906.6**	**39.9**	**90.1**

Table 89: Power of frequency components of the first 50 cycles at input frequency of 125 Hz and 10% displacement.

Test Name	Power at Significant Harmonics							
	1	2	3	4	5	6	7	9
zshearsine82216b	2168.5	214.5	993.8	2956.3	740.3	203.6	512.5	40.7
zshearsine82216c	2082	175.5	941.2	3314.7	1342	316.9	307.8	23.1
zshearsine82216d	1893.6	273.2	787.6	3424	954.8	79.8	305.9	7.8
zshearsine82216e	1954.3	199.1	697.8	2418	838.3	158.2	175.6	1.4
zshearsine82216f	2101	256.8	960.1	3668	871.3	414.6	509.3	19.7
zshearsine82216g	2175.3	144.3	929.9	3941	1219	240.2	644.9	36.9
zshearsine82216h	1994.7	278.5	857.4	3077	1042	320.9	155.9	2.7
zshearsine82316a	1902	241.9	802.4	3108	847	421.2	223.5	3.5
zshearsine82316b	2098	17.4	954	3434	990.9	232.2	436.3	22.3
AVG	**2041.0**	**200.1**	**880.5**	**3260.1**	**982.8**	**265.3**	**363.5**	**17.6**
SD	**108.1**	**82.0**	**99.6**	**439.9**	**193.6**	**113.9**	**170.4**	**14.8**

Table 90: Power of frequency components of the last 50 cycles at input frequency of 125 Hz and 10% displacement.

Test Name	Power at Significant Harmonics							
	1	2	3	4	5	6	7	9
zshearsine82216b	1552	19.2	751.2	2777.3	688.9	218.9	304	26.7
zshearsine82216c	1698	178.6	766.6	2876	1055.1	283.4	121.5	5.3
zshearsine82216d	1392	184.4	598.5	2804	809.7	68.3	276.5	19.7
zshearsine82216e	1942	188.7	684.8	2530	861.3	186.5	143.9	3.4
zshearsine82216f	1688	215.4	894.9	3369	738.5	276.8	482.5	2.7
zshearsine82216g	2122	293.4	899.6	4148	1263	286.1	612.4	32.5
zshearsine82216h	1089	151.2	541.8	1904	620.7	177.6	27.3	6.2
zshearsine82316a	1894	232.4	786.3	3319.1	919.7	455.6	232.6	1.1
zshearsine82316b	1624	160.8	774.5	3135	889.4	238.4	333.9	3.8
AVG	**1666.8**	**180.5**	**744.2**	**2984.7**	**871.8**	**243.5**	**281.6**	**11.3**
SD	**308.3**	**74.2**	**120.3**	**622.2**	**196.0**	**105.1**	**181.9**	**11.8**

Appendix B   Magnitude Tables

Tables 91 through 112 contain the magnitude of significant frequency components within cycle 20 for every individual specimen at each deformation frequency, displacement amplitude, and set of 50 cycles. The magnitude is calculated only within cycle 20 of the apparent steady state and therefore contains the significant frequency components within just the apparent steady state region.

Table 91: Magnitude of frequency components at a cycle in the steady state region (cycle 20) within the first 50 cycles at input frequency of 25 Hz under and 10% displacement.

Test Name	Magnitude at Significant Harmonics			
	1	2	3	5
zshearsine60116a	832.7	86.6	321.3	78.7
zshearsine60116b	473.8	34.5	137.5	24.2
zshearsine60116c	501.7	4.62	160.5	30.1
zshearsine60116d	557.6	17.9	156.5	21.7
zshearsine60116e	799.5	40.8	268.5	56.2
zshearsine60116f	427.5	29.3	130.7	18.9
zshearsine60116g	515.5	17.1	166.8	26.5
zshearsine60716a	499.3	32.6	139.3	22.6
zshearsine60716b	762.8	79.1	260.4	54.4
zshearsine60716c	684. 7	2.2	224.8	46.3
zshearsine60716d	472.3	29.7	125.3	18.5
zshearsine60716e	606.4	11.9	181.1	25.8
zshearsine60716f	317.1	12.5	73.1	12.1
AVG	**573.1**	**30.7**	**180.4**	**33.5**
SD	**155.2**	**26.0**	**69.3**	**19.4**

Table 92: Magnitude of frequency components at a cycle in the steady state region (cycle 20) within the first 50 cycles at input frequency of 25 Hz under and 25% displacement.

Test Name	Magnitude at Significant Harmonics			
	1	2	3	5
zshearsine20816a	1116	8.4	527.1	165.7
zshearsine20816b	1,069.1	185.5	412.5	120.2
zshearsine20816e	1,062.4	52.1	462.1	126.7
zshearsine20816g	1,127.4	74.1	458.7	135.3
zshearsine20816h	595.6	52.7	219.3	61.9
zshearsine21016a	815.2	61.2	348.6	108.7
zshearsine21016b	325.1	17.4	77.3	41.9
zshearsine21016c	375.7	21.7	124.3	44.1
zshearsine21016d	946.9	16.1	394. 8	117.7
zshearsine21016e	800.5	16.7	320.2	79.0
zshearsine60716g	868	18	356.1	94.6
zshearsine60716h	494.4	24.2	69.9	88.4
zshearsine60716i	606.5	15.9	226.4	76.1
zshearsine60716j	742.9	18.8	327.5	97.8
AVG	**781.8**	**41.6**	**308.9**	**97.0**
SD	**270.5**	**46.2**	**145.6**	**35.2**

Table 93: Magnitude of frequency components at a cycle in the steady state region (cycle 20) within the last 50 cycles at input frequency of 25 Hz under and 10% displacement.

Test Name	Magnitude at Significant Harmonics			
	1	2	3	5
zshearsine60116a	757.7	71.7	278.6	68.2
zshearsine60116b	461.8	31.6	133.6	21.3
zshearsine60116c	531.0	2.3	174.1	30.6
zshearsine60116d	539.2	25.1	151.1	19.4
zshearsine60116e	786.7	33.8	267.7	58.1
zshearsine60116f	424.8	31.8	134.6	23.3
zshearsine60116g	496.2	21.8	160.3	23.6
zshearsine60716a	499.5	33.8	142.7	22.7
zshearsine60716b	719.8	65.3	233.6	46.2
zshearsine60716c	667.4	6.7	216.9	42.8
zshearsine60716d	450.8	24.7	118.7	16.7
zshearsine60716e	613.7	14.5	188.8	30.8
zshearsine60716f	356.4	17.9	84.76	10.4
AVG	**561.9**	**29.3**	**175.8**	**31.9**
SD	**135.6**	**20.1**	**58.6**	**17.1**

Table 94: Magnitude of frequency components at a cycle in the steady state region (cycle 20) within the last 50 cycles at input frequency of 25 Hz under and 25% displacement.

Test Name	Magnitude at Significant Harmonics			
	1	2	3	5
zshearsine20816a	884.2	23.4	391.6	129.1
zshearsine20816b	989.3	173.9	382.0	115.2
zshearsine20816e	967.1	18.7	424.9	119.4
zshearsine20816g	1,308	73.4	548.2	174.2
zshearsine20816h	724.2	74.0	251.5	74.4
zshearsine21016a	833.7	37.3	349.4	108.1
zshearsine21016b	613.3	19.0	178.1	63.9
zshearsine21016c	1003.4	73.8	415.6	118.7
zshearsine21016d	937.0	10.9	35.4	111.2
zshearsine21016e	789.7	46.8	260.5	76.2
zshearsine60716g	774.1	7.0	300.0	78.5
zshearsine60716h	484.5	30.9	44.9	73.2
zshearsine60716i	739.5	21.6	278.5	95.5
zshearsine60716j	674.4	24.6	287.1	93.7
AVG	**837.3**	**45.4**	**296.3**	**102.2**
SD	**202.1**	**43.6**	**142.1**	**29.3**

Table 95: Magnitude of frequency components at a cycle in the steady state region (cycle 20) within the first 50 cycles at input frequency of 50 Hz under and 10% displacement.

Test Name	Magnitude at Significant Harmonics			
	1	2	3	5
zshearsine60916a	557.8	41.6	111.9	29.1
zshearsine60916b	711.2	66.5	199.8	19.9
zshearsine60916c	798.5	109.2	261.6	33.5
zshearsine60916d	556.9	46.6	134.1	10.9
zshearsine60916e	592.2	25.1	144.8	11.7
zshearsine60916f	695.5	95.7	193.2	6.6
zshearsine60916g	735.7	45.6	225.6	4.8
zshearsine60916h	574.4	42.6	139.5	16.1
zshearsine61316a	639.6	49.4	153.9	16.3
zshearsine61316b	969.9	217.1	237.8	37.7
AVG	**683.2**	**73.9**	**180.2**	**18.6**
SD	**130.3**	**56.6**	**50.5**	**11.3**

Table 96: Magnitude of frequency components at a cycle in the steady state region (cycle 20) within the first 50 cycles at input frequency of 50 Hz under and 25% displacement.

Test Name	Magnitude at Significant Harmonics			
	1	2	3	5
zshearsine31016a	952.2	83.5	339.2	46.9
zshearsine31016b	1145.4	20.2	447.0	65.4
zshearsine31016c	1080.0	149.5	489.0	203.7
zshearsine31016d	1082.1	38.4	418.6	34.2
zshearsine31016e	969.2	63.5	291.4	94.1
zshearsine31016f	923.8	59.7	411.2	69.9
zshearsine31016g	1008.4	55.1	369.1	162.2
zshearsine31016h	797.5	46.0	307.7	49.4
zshearsine32116a	1119.1	56.1	416.7	73.4
zshearsine32116b	1315.0	87.9	583.3	144.7
zshearsine32116c	1112.4	128.1	452.0	16.0
zshearsine32116d	800.3	45.4	275.4	91.5
AVG	**1025.5**	**69.5**	**400.1**	**87.6**
SD	**148.5**	**37.4**	**89.3**	**55.9**

Table 97: Magnitude of frequency components at a cycle in the steady state region (cycle 20) within the last 50 cycles at input frequency of 50 Hz under and 10% displacement.

Test Name	Magnitude at Significant Harmonics			
	1	2	3	5
zshearsine60916a	562.0	27.8	123.7	20.4
zshearsine60916b	705.6	44.9	237.6	53.9
zshearsine60916c	754.4	76.5	264.3	50.1
zshearsine60916d	595.2	35.8	154.8	27.6
zshearsine60916e	642.0	12.2	173.0	23.1
zshearsine60916f	687.1	74.7	221.2	31.8
zshearsine60916g	724.2	44.2	252.3	31.9
zshearsine60916h	564.9	28.8	156.1	5.7
zshearsine61316a	658.8	45.1	168.4	24.9
zshearsine61316b	935.1	175.7	272.6	59.4
AVG	**682.9**	**56.6**	**202.4**	**32.9**
SD	**110.3**	**46.4**	**53.2**	**16.8**

Table 98: Magnitude of frequency components at a cycle in the steady state region (cycle 20) within the last 50 cycles at input frequency of 50 Hz under and 25% displacement.

Test Name	Magnitude at Significant Harmonics			
	1	2	3	5
zshearsine31016a	793	64.3	252.6	8.7
zshearsine31016b	1301.1	45.9	598.2	125.4
zshearsine31016c	1162.6	100.6	488.4	171.7
zshearsine31016d	1016.5	9.5	340.8	14.2
zshearsine31016e	902.3	18.6	233.9	120.2
zshearsine31016f	998.9	18.4	515.8	47.4
zshearsine31016g	1067.3	12.7	481.5	207.3
zshearsine31016h	824.6	45.8	338.8	27.9
zshearsine32116a	1042.7	13.9	367.7	70.4
zshearsine32116b	1178.7	35.9	508.9	74.2
zshearsine32116c	1262.2	49.1	549.7	47.8
zshearsine32116d	808.6	20.9	265.9	147.0
AVG	**1029.9**	**36.3**	**411.9**	**88.5**
SD	**174.1**	**26.8**	**126.2**	**64.9**

Table 99: Magnitude of frequency components at a cycle in the steady state region (cycle 20) within the first 50 cycles at input frequency of 60 Hz under and 10% displacement.

Test Name	Magnitude at Significant Harmonics					
	1	2	3	5	7	9
zshearsine71216a	848.2	180.3	332.9	65.1	79.9	99.2
zshearsine71216b	509.5	13.4	168.8	37.4	55.7	117.1
zshearsine71216c	561.2	86.9	185.1	15.3	78.6	86.8
zshearsine71216d	558.9	153.3	225.1	44.5	20.3	23.6
zshearsine71216e	595.5	90.5	209.3	26.1	26.0	68.5
zshearsine71416a	608.4	124.2	199.9	22.5	55.7	213.5
zshearsine71416b	920.5	211.5	363.1	79.2	74.9	26.5
zshearsine71416c	608.8	39.5	234.2	32.7	43.3	122.7
zshearsine71416d	536.3	47.9	184.3	12.3	63.9	103.9
zshearsine71416e	678.5	128.6	199.6	52.8	66.0	118.5
zshearsine71416f	695.4	250.3	252.1	52.9	40.2	25.8
zshearsine71416g	534.8	78.4	201.5	12.5	37.3	78.3
zshearsine71416h	511.0	57.2	165.1	49.1	59.4	117.5
zshearsine71816a	662.2	135.8	221.9	17.5	61.2	105.8
zshearsine71816b	675.8	111.6	261.4	41.2	46.9	68.3
AVG	**630.7**	**114.1**	**224.5**	**37.1**	**54.5**	**93.4**
SD	**123.4**	**68.3**	**57.9**	**20.9**	**18.7**	**49.7**

Table 100: Magnitude of frequency components at a cycle in the steady state region (cycle 20) within the last 50 cycles at input frequency of 60 Hz under and 10% displacement.

Test Name	Magnitude at Significant Harmonics					
	1	2	3	5	7	9
zshearsine71216a	852.9	141.1	346.7	60.9	47.7	106.0
zshearsine71216b	495.6	20.1	182.1	50.6	67.4	111.8
zshearsine71216c	556.5	66.7	198.1	25.8	74.4	102.9
zshearsine71216d	556.3	109.8	227.9	35.1	23.7	26.2
zshearsine71216e	608.6	61.9	237.6	35.5	38.5	64.2
zshearsine71416a	595.7	80.0	220.9	30.5	51.8	164.9
zshearsine71416b	893.5	161.0	380.1	61.9	49.6	50.6
zshearsine71416c	697.7	13.1	274.7	25.6	60.4	120.2
zshearsine71416d	564.4	31.7	211.1	6.8	62.9	104.4
zshearsine71416e	681.2	66.3	194.7	87.8	112.6	106.2
zshearsine71416f	731.0	223.7	263.9	32.6	7.7	52.5
zshearsine71416g	584.3	58.1	239.9	20.7	52.7	104.8
zshearsine71416h	501.6	29.2	175.9	56.9	67.8	109.5
zshearsine71816a	665.2	102.2	237.1	44.5	64.8	99.5
zshearsine71816b	641.9	55.5	250.7	35.3	29.9	48.3
AVG	**641.8**	**81.4**	**242.8**	**40.7**	**54.1**	**91.5**
SD	**116.3**	**57.9**	**56.9**	**20.2**	**24.5**	**35.8**

Table 101: Magnitude of frequency components at a cycle in the steady state region (cycle 20) within the first 50 cycles at input frequency of 60 Hz under and 25% displacement.

Test Name	Magnitude at Significant Harmonics						
	1	2	3	5	7	8	9
zshearsine61416a	983.1	357.2	545.7	123.1	153.9	182.1	532.8
zshearsine61416b	746.4	119.8	461.7	123.5	64.1	12.6	286.4
zshearsine61416c	765.8	54.1	493.8	222.6	128.9	19.6	236.1
zshearsine61416d	906.3	62.8	569.5	122.8	131.5	62.8	544.5
zshearsine61416e	998.7	22.7	628.2	288.7	303.0	117.2	924.1
zshearsine61416g	594.9	73.4	269.5	85.9	38.1	23.1	86.5
zshearsine61416h	830.2	33.4	562.6	356.3	279.9	135.6	590.7
zshearsine61616a	890.6	55.9	665.1	263.8	277.2	44.8	785.0
zshearsine61616b	1180.5	478.5	735.5	247.3	278.0	97.7	258.6
zshearsine61616c	473.9	84.1	299.4	53.8	82.9	13.0	167.7
zshearsine61616d	826.0	18.8	601.2	254.9	261.4	52.4	700.7
zshearsine61616e	608.7	56.6	228.2	76.6	56.3	125.9	86.3
zshearsine61616f	645.5	26.2	292.0	67.3	14.7	28.2	91.6
zshearsine61616g	711.6	227.1	288.9	33.9	46.5	26.8	104.9
zshearsine61616h	633.8	152.7	224.6	23.1	58.1	2.0	74.1
AVG	**786.4**	**121.5**	**457.7**	**156.2**	**144.9**	**62.9**	**364.7**
SD	**186.0**	**134.3**	**174.4**	**105.9**	**105.7**	**55.3**	**288.9**

Table 102: Magnitude of frequency components at a cycle in the steady state region (cycle 20) within the last 50 cycles at input frequency of 60 Hz under and 25% displacement.

Test Name	Magnitude at Significant Harmonics						
	1	2	3	5	7	8	9
zshearsine61416a	838.7	236.7	454.1	140.5	193.6	199.8	415.1
zshearsine61416b	920.4	66.9	629.7	138.6	151.4	48.6	529.5
zshearsine61416c	787.7	73.5	503.0	136.4	151.2	78.1	342.7
zshearsine61416d	841.8	60.8	514.4	117.3	119.2	35.1	404.9
zshearsine61416e	1030.4	23.7	610.0	264.8	250.9	188.2	741.1
zshearsine61416g	1031.6	102.1	700.4	157.5	91.6	62.0	379.3
zshearsine61416h	782.3	48.6	506.1	317.3	254.2	146.8	410.7
zshearsine61616a	836.8	56.6	569.2	232.8	336.3	73.6	750.5
zshearsine61616b	939.6	258.2	648.8	186.6	194.5	20.8	283.8
zshearsine61616c	794.9	96.3	587.0	92.1	162.9	81.6	431.9
zshearsine61616d	777.4	19.7	543.9	261.8	281.3	75.8	600.9
zshearsine61616e	538.8	20.6	349.9	114.9	149.4	49.1	280.7
zshearsine61616f	625.2	16.1	307.7	82.2	32.9	16.1	57.7
zshearsine61616g	671.9	203.2	294.4	66.7	28.6	30.1	89.2
zshearsine61616h	579.1	89.9	205.9	18.2	66.4	29.8	55.9
AVG	**799.8**	**91.5**	**494.9**	**155.2**	**164.3**	**75.7**	**384.9**
SD	**148.9**	**78.8**	**145.3**	**83.0**	**90.1**	**58.1**	**216.8**

Table 103: Magnitude of frequency components at a cycle in the steady state region (cycle 20) within the first 50 cycles at input frequency of 75 Hz under and 10% displacement.

Test Name	Magnitude at Significant Harmonics					
	1	2	3	5	7	9
zshearsine61316c	305.8	143.6	370.9	179.9	1409.6	19.8
zshearsine61316d	333.3	292.8	396.8	123.0	1780.0	56.3
zshearsine61316e	165.0	174.8	393.6	145.8	1257.8	28.8
zshearsine61316f	472.1	211.8	456.5	154.7	1608.0	45.3
zshearsine61316g	261.0	110.1	371.5	166.0	1300.0	24.0
zshearsine61316h	61.3	73.3	284.9	130.8	881.6	11.7
J75H32416a	414.8	131.3	402.8	130.6	405.7	8.7
J75H32416b	389.2	36.9	378.1	103.0	270.5	6.9
J75H32416c	374.9	6.9	426.8	103.3	90.6	26.4
J75H32416d	426.5	148.3	387.6	47.3	423.7	36.6
J75H32416e	536.6	167.3	430.9	106.9	444.1	34.7
J75H32416f	526.5	39.6	488.2	159.1	108.7	212.2
J75H32416g	438.5	33.3	392.2	101.8	41.1	433.7
J75H32416h	607.6	40.3	305.4	87.9	95.6	573.8
AVG	**379.5**	**115.0**	**391.9**	**124.3**	**722.6**	**108.5**
SD	**147.5**	**81.8**	**52.9**	**35.6**	**627.9**	**177.2**

Table 104: Magnitude of frequency components at a cycle in the steady state region (cycle 20) within the first 50 cycles at input frequency of 75 Hz under and 25% displacement.

Test Name	Magnitude at Significant Harmonics					
	1	2	3	5	7	9
zshearsine72516a	1776.5	608.6	1083.2	803.2	2386.7	565.0
zshearsine72516b	2047.1	511.8	1039.7	509.6	6629.4	541.8
zshearsine72516c	297.3	228.6	995.2	593.6	2898.7	70.8
zshearsine72516d	193.3	267.9	764.9	416.7	1074.4	32.1
zshearsine72516e	233.6	357.0	980.6	858.9	3746.4	153.9
zshearsine72516f	420.8	202.3	422.7	165.9	643.1	21.2
zshearsine72516g	219.9	236.2	557.9	374.8	1275.6	39.8
zshearsine72516h	126.4	270.3	775.8	549.5	1807.1	92.9
zshearsine72616a	416.5	363.8	1083.5	577.2	2848.0	134.4
zshearsine72616b	1272.4	523.5	605.4	545.2	5577.9	283.7
AVG	**700.4**	**357**	**830.9**	**539.5**	**2888.7**	**193.6**
SD	**719.2**	**143.6**	**240.3**	**199.6**	**1952.8**	**204.7**

Table 105: Magnitude of frequency components at a cycle in the steady state region (cycle 20) within the last 50 cycles at input frequency of 75 Hz under and 10% displacement.

Test Name	Magnitude at Significant Harmonics					
	1	2	3	5	7	9
zshearsine61316c	266.6	168.3	364.7	186.4	1426.5	42.6
zshearsine61316d	293.2	276.7	339.4	107.5	1915.4	38.0
zshearsine61316e	185.9	200.8	357.1	99.4	1202.9	21.5
zshearsine61316f	385.9	153.4	525.7	199.1	2084.9	54.8
zshearsine61316g	331.5	119.7	421.1	187.3	1747.5	22.4
zshearsine61316h	87.5	81.7	284.2	94.6	946.2	36.6
J75H32416a	388.7	140.4	398.9	149.7	411.8	17.2
J75H32416b	367.1	39.8	373.9	106.3	258.1	8.7
J75H32416c	405.0	73.1	411.9	56.8	201.4	32.8
J75H32416d	445.6	145.4	394.1	37.2	446.7	36.9
J75H32416e	494.8	156.0	430.9	96.1	415.5	39.3
J75H32416f	439.0	26.5	486.8	162.9	61.9	275.1
J75H32416g	343.9	71.7	433.7	118.1	30.7	343.5
J75H32416h	538.5	29.1	246.4	114.8	64.2	513.8
AVG	**355.2**	**120.2**	**390.6**	**122.6**	**800.9**	**105.9**
SD	**119.5**	**71.4**	**72.9**	**48.6**	**740.2**	**155.3**

Table 106: Magnitude of frequency components at a cycle in the steady state region (cycle 20) within the last 50 cycles at input frequency of 75 Hz under and 25% displacement.

Test Name	Magnitude at Significant Harmonics					
	1	2	3	5	7	9
zshearsine72516a	1528.9	640.2	200.2	335.9	2521.5	441.9
zshearsine72516b	1995.9	565.5	893.2	581.6	5604.3	51.6
zshearsine72516c	399.2	303.1	856.1	454.8	2011.1	89.3
zshearsine72516d	156.7	204.2	661.4	372.5	755.5	28.1
zshearsine72516e	113.4	312.8	592.2	518.9	1816.4	63.9
zshearsine72516f	229.3	250.6	495.7	301.9	1359.0	65.2
zshearsine72516g	40.7	215.3	712.2	444.1	1675.5	71.3
zshearsine72516h	37.3	216.7	624.3	301.1	854.8	54.6
zshearsine72616a	347.7	426.6	946.3	348.5	2192.3	59.0
zshearsine72616b	1960.5	643.7	825.4	587.9	5836.4	397.3
AVG	**680.9**	**377.9**	**680.7**	**424.7**	**2462.7**	**132.2**
SD	**809.7**	**178.2**	**222.3**	**109.6**	**1803.9**	**152.6**

Table 107: Magnitude of frequency components at a cycle in the steady state region (cycle 20) within the first 50 cycles at input frequency of 100 Hz under and 10% displacement.

Test Name	Magnitude at Significant Harmonics						
	1	2	3	5	6	7	9
zshearsine80216b	424.4	87.2	684.2	1092.7	42.4	16.3	111.6
zshearsine80216c	25.1	60.6	472.3	777.2	10.7	14.9	9.5
zshearsine80216d	253.8	105.6	612.2	1100.0	28.3	20.6	43.9
zshearsine80216e	82.2	65.8	529.6	841.3	6.9	18.5	15.0
zshearsine80216f	131.3	15.6	588.4	1050.9	23.4	26.3	35.1
zshearsine80216g	384.5	54.4	758.9	1355.9	42.0	29.5	51.8
zshearsine80216h	229.8	129.7	532.9	861.6	26.8	11.2	28.9
zshearsine80316a	125.5	105.9	525.3	1082.4	1.5	34.6	81.4
zshearsine80316b	103.7	34.6	604.8	1159.7	12.9	41.0	42.4
AVG	**195.6**	**73.3**	**589.8**	**1035.7**	**21.7**	**23.6**	**46.6**
SD	**137.8**	**36.9**	**88.8**	**181.2**	**14.7**	**9.9**	**32.2**

Table 108: Magnitude of frequency components at a cycle in the steady state region (cycle 20) within the first 50 cycles at input frequency of 100 Hz under and 25% displacement.

Test Name	Magnitude at Significant Harmonics						
	1	2	3	5	6	7	9
J100H41416a	1783.5	529.3	677.2	1065.5	2519.1	319.7	383.1
J100H41416b	425.1	73.6	920.5	1005.9	1752.2	282.2	49.5
J100H41416c	257.6	86.8	734.1	918.6	962.6	246.9	39.7
J100H41416d	210.1	157.1	693.1	650.0	717.5	154.9	15.2
J100H41416e	124.2	114.6	733.2	791.5	876.1	198.4	34.2
J100H41416f	144.9	78.5	671.1	691.1	367.5	149.8	18.3
J100H41416g	198.1	130.5	722.9	725.1	670.8	164.4	6.5
zshearsine42116a	320.5	66.7	601.2	674.5	610.3	207.6	27.2
zshearsine42116b	174.8	33.2	700.9	650.9	2130.5	153.0	20.9
zshearsine42116c	152.7	74.5	729.7	797.2	377.3	192.7	4.6
zshearsine42116d	231.3	110.4	644.8	564.8	676.7	92.5	6.3
AVG	**365.7**	**132.3**	**711.7**	**775.9**	**1060.1**	**196.6**	**55.0**
SD	**478.2**	**135.9**	**80.6**	**159.3**	**732.2**	**65.5**	**109.8**

Table 109: Magnitude of frequency components at a cycle in the steady state region (cycle 20) within the last 50 cycles at input frequency of 100 Hz under and 10% displacement.

Test Name	Magnitude at Significant Harmonics						
	1	2	3	5	6	7	9
zshearsine80216b	346.9	99.3	638.5	998.4	38.5	25.6	80.5
zshearsine80216c	38.9	84.7	434.2	833.6	51.5	35.9	57.8
zshearsine80216d	294.0	77.8	588.1	1041.7	24.2	40.0	53.0
zshearsine80216e	57.9	53.4	521.5	913.2	28.4	16.8	40.5
zshearsine80216f	68.3	59.2	505.5	1084.7	73.4	55.1	65.7
zshearsine80216g	394.4	36.4	717.3	1366.0	37.9	14.6	82.3
zshearsine80216h	179.7	118.6	516.9	781.8	11.4	17.4	53.0
zshearsine80316a	78.5	82.1	528.0	1102.4	9.0	35.3	75.0
zshearsine80316b	182.3	43.1	583.9	1198.1	30.1	25.2	103.0
AVG	**182.3**	**72.7**	**559.3**	**1035.5**	**33.8**	**29.5**	**67.9**
SD	**134.3**	**26.9**	**83.2**	**181.7**	**19.9**	**13.2**	**19.2**

Table 110: Magnitude of frequency components at a cycle in the steady state region (cycle 20) within the last 50 cycles at input frequency of 100 Hz under and 25% displacement.

Test Name	Magnitude at Significant Harmonics						
	1	2	3	5	6	7	9
J100H41416a	1657.8	765.0	499.8	331.1	3089.3	375.8	255.2
J100H41416b	444.7	108.9	836.1	905.0	2083.9	147.0	82.9
J100H41416c	335.8	142.8	741.3	818.9	983.4	238.3	30.3
J100H41416d	272.2	64.1	577.8	404.2	443.2	84.8	25.6
J100H41416e	96.1	44.3	737.2	744.6	1049.1	236.7	59.4
J100H41416f	227.0	44.7	572.7	527.9	426.2	133.3	7.4
J100H41416g	262.0	108.0	657.2	634.9	685.3	158.0	18.6
zshearsine42116a	385.1	95.1	569.1	636.0	829.5	236.4	30.4
zshearsine42116b	157.3	43.5	707.9	617.2	1632.3	136.6	15.6
zshearsine42116c	240.9	71.9	733.4	718.0	464.6	202.9	19.9
zshearsine42116d	222.0	93.6	617.5	515.4	590.2	142.3	14.9
AVG	**390.9**	**143.8**	**659.1**	**623.1**	**1116.1**	**190.2**	**50.9**
SD	**431.4**	**208.5**	**100.7**	**171.9**	**837.6**	**79.8**	**71.2**

Table 111: Magnitude of frequency components at a cycle in the steady state region (cycle 20) within the first 50 cycles at input frequency of 125 Hz under and 10% displacement.

Test Name	Magnitude at Significant Harmonics						
	1	2	3	4	5	6	7	9
zshearsine82216b	2192.8	462.8	1238.5	3760.8	702.8	1056.6	857.0	159.7
zshearsine82216c	2316.3	339.0	1480.2	3447.8	1757.0	1632.2	1971.8	172.5
zshearsine82216d	1982.2	334.4	1334.7	3951.7	1336.0	1590.8	1030.4	241.6
zshearsine82216e	2073.1	237.8	1232.6	3244.1	1182.9	891.2	353.0	106.0
zshearsine82216f	2191.3	302.0	1537.0	4290.0	1019.8	1175.1	1195.0	149.0
zshearsine82216g	2297.3	281.3	1550.0	4984.8	1218.7	2302.0	1976.9	252.5
zshearsine82216h	2150.3	361.4	1348.8	3550.7	991.9	846.6	248.9	99.3
zshearsine82316a	2029.8	434.1	1225.8	3500.1	877.9	1116.9	524.3	155.7
zshearsine82316b	2243.4	294.8	1363.8	3969.9	1072.4	1207.9	1035.4	172.8
zshearsine82316c	2079.8	259.0	1258.1	3567.8	841.2	1509.1	1811.6	198.6
AVG	**2155.6**	**330.6**	**1356.9**	**3826.8**	**1100.1**	**1332.9**	**1100.4**	**170.8**
SD	**112.9**	**72.6**	**125.6**	**508.7**	**298.4**	**437.3**	**643.5**	**50.1**

Table 112: Magnitude of frequency components at a cycle in the steady state region (cycle 20) within the last 50 cycles at input frequency of 125 Hz under and 10% displacement.

Test Name	Magnitude at Significant Harmonics							
	1	2	3	4	5	6	7	9
zshearsine82216b	2102.8	122.2	873.1	4431.1	1018.7	521.9	360.9	260.6
zshearsine82216c	2155.0	154.5	948.8	3940.3	1920.2	972.3	807.4	190.8
zshearsine82216d	2180.2	461.3	822.2	4674.3	1964.7	1017.8	1042.9	169.8
zshearsine82216e	1882.1	339.9	1304.5	2847.0	903.5	341.9	518.7	142.5
zshearsine82216f	2179.4	606.8	1077.9	4967.1	1359.4	873.5	638.3	519.6
zshearsine82216g	2497.8	346.2	1408.4	5715.9	2016.5	1882.8	763.9	217.0
zshearsine82216h	2072.2	351.7	1168.4	3039.0	1065.5	483.8	469.6	14.4
zshearsine82316a	1958.4	470.3	864.6	4196.7	1152.3	701.2	350.2	129.4
zshearsine82316b	2223.8	331.8	1191.1	3463.9	927.4	554.4	983.8	33.1
zshearsine82316c	2158.7	297.3	1201.4	3947.1	1198.3	1699.4	743.4	197.9
AVG	**2141.0**	**348.2**	**1086.1**	**4122.2**	**1352.7**	**904.9**	**667.9**	**187.5**
SD	**164.7**	**143.8**	**201.6**	**879.1**	**444.5**	**517.6**	**243.2**	**139.9**

Appendix C   Length of Transient Region

The length of the transient region at all deformation frequencies, displacement amplitudes, and set of 50 cycles is provided in Tables 113 through 118.

Table 113: Length of transient region in the first and second set of 50 cycles at 10% and 25% displacement a deformation frequency of 25 Hz.

Length of Transient Region (number of cycles)					
10% displacement			25% displacement		
Test Name	First 50	Last 50	Test Name	First 50	Last 50
zshearsine60116a	3	1	zshearsine20816a	7	5
zshearsine60116b	3	1	zshearsine20816b	10	5
zshearsine60116c	3	1	zshearsine20816e	5	5
zshearsine60116d	4	1	zshearsine20816g	8	6
zshearsine60116e	4	1	zshearsine20816h	10	3
zshearsine60116f	4	1	zshearsine21016a	5	3
zshearsine60116g	4	1	zshearsine21016b	7	5
zshearsine60716a	3	1	zshearsine21016c	7	3
zshearsine60716b	4	2	zshearsine21016d	7	3
zshearsine60716c	4	1	zshearsine21016e	7	4
zshearsine60716d	3	1	zshearsine60716g	6	4
zshearsine60716e	3	2	zshearsine60716h	11	2
zshearsine60716f	3	1	zshearsine60716i	8	2
			zshearsine60716j	6	3
AVG	3.5	1.2		7.4	3.8
SD	0.5	0.4		1.8	1.3
k Range					
First 50 Cycles	j-level	Transient Region	First 50 Cycles	j-level	Transient Region
	5	0 to 3		5	0 to 6
	6	0 to 6		6	0 to 12
Last 50 Cycles	j-level	Transient Region	Last 50 Cycles	j-level	Transient Region
	5	0 to 1		5	0 to 4
	6	0 to 2		6	0 to 7

Table 114: Length of transient region in the first and second set of 50 cycles at 10% and 25% displacement a deformation frequency of 50 Hz.

Length of Transient Region (number of cycles)					
10% displacement			25% displacement		
Test Name	First 50	Last 50	Test Name	First 50	Last 50
zshearsine60916a	4	1	zshearsine31016a	3	2
zshearsine60916b	4	1	zshearsine31016b	6	3
zshearsine60916c	6	1	zshearsine31016c	20	9
zshearsine60916d	4	1	zshearsine31016d	13	4
zshearsine60916e	5	3	zshearsine31016e	10	2
zshearsine60916f	5	1	zshearsine31016f	16	5
zshearsine60916g	4	1	zshearsine31016g	5	1
zshearsine60916h	4	1	zshearsine31016h	19	5
zshearsine61316a	4	1	zshearsine32116a	21	9
zshearsine61316b	5	1	zshearsine32116b	18	12
			zshearsine32116c	19	8
			zshearsine32116d	21	1
AVG	4.5	1.2	AVG	14.3	5.1
SD	0.7	0.6	SD	6.6	3.6
k Range					
First 50 Cycles	j-level	Transient Region	First 50 Cycles	j-level	Transient Region
	5	0 to 4		5	0 to 12
	6	0 to 7		6	0 to 24
Last 50 Cycles	j-level	Transient Region	Last 50 Cycles	j-level	Transient Region
	5	0 to 1		5	0 to 4
	6	0 to 2		6	0 to 8

Table 115: Length of transient region in the first and second set of 50 cycles at 10% and 25% displacement a deformation frequency of 60 Hz.

Length of Transient Region (number of cycles)					
10% displacement			25% displacement		
Test Name	First 50	Last 50	Test Name	First 50	Last 50
zshearsine71216a	4	3	zshearsine61416a	13	1
zshearsine71216b	4	1	zshearsine61416b	14	1
zshearsine71216c	3	1	zshearsine61416c	15	1
zshearsine71216d	4	1	zshearsine61416d	13	1
zshearsine71216e	6	1	zshearsine61416e	9	6
zshearsine71416a	7	1	zshearsine61416g	11	1
zshearsine71416b	9	4	zshearsine61416h	8	1
zshearsine71416c	5	4	zshearsine61616a	12	1
zshearsine71416d	5	1	zshearsine61616b	24	13
zshearsine71416e	6	3	zshearsine61616c	10	4
zshearsine71416f	9	5	zshearsine61616d	12	1
zshearsine71416g	4	1	zshearsine61616e	14	1
zshearsine71416h	4	1	zshearsine61616f	6	4
zshearsine71816a	7	4	zshearsine61616g	9	3
zshearsine71816b	8	1	zshearsine61616h	6	1
AVG	5.6	2.1	AVG	11.7	2.7
SD	1.9	1.5	SD	4.4	3.3
k Range					
First 50 Cycles	j-level	Transient Region	First 50 Cycles	j-level	Transient Region
	5	0 to 4		5	0 to 8
	7	0 to 15		8	0 to 61
Last 50 Cycles	j-level	Transient Region	Last 50 Cycles	j-level	Transient Region
	5	0 to 2		5	0 to 2
	7	0 to 6		7	0 to 7
				8	0 to 14

Table 116: Length of transient region in the first and second set of 50 cycles at 10% and 25% displacement a deformation frequency of 75 Hz.

Length of Transient Region (number of cycles)					
10% displacement			25% displacement		
Test Name	First 50	Last 50	Test Name	First 50	Last 50
zshearsine61316c	7	2	zshearsine72516a	25	1
zshearsine61316d	9	1	zshearsine72516b	17	11
zshearsine61316e	8	1	zshearsine72516c	16	1
zshearsine61316f	7	1	zshearsine72516d	18	4
zshearsine61316g	7	1	zshearsine72516e	22	1
zshearsine61316h	8	1	zshearsine72516f	8	6
J75H32416a	5	1	zshearsine72516g	16	1
J75H32416b	3	1	zshearsine72516h	12	1
J75H32416c	12	2	zshearsine72616a	12	4
J75H32416d	5	1	zshearsine72616b	15	9
J75H32416e	5	1			
J75H32416f	5	1			
J75H32416g	9	1			
J75H32416h	4	1			
AVG	6.7	1.1	AVG	16.1	3.9
SD	2.4	0.4	SD	4.9	3.7
k Range					
First 50 Cycles	j-level	Transient Region	First 50 Cycles	j-level	Transient Region
	4	0 to 4		4	0 to 9
	5	0 to 7		5	0 to 18
	6	0 to 14		6	0 to 35
	7	0 to 28		7	0 to 70
Last 50 Cycles	j-level	Transient Region	Last 50 Cycles	j-level	Transient Region
	4	0 to 1		4	0 to 2
	5	0 to 2		5	0 to 5
	6	0 to 3		6	0 to 9
	7	0 to 5		7	0 to 17

Table 117: Length of transient region in the first and second set of 50 cycles at 10% and 25% displacement a deformation frequency of 100 Hz.

Length of Transient Region (number of cycles)					
10% displacement			25% displacement		
Test Name	First 50	Last 50	Test Name	First 50	Last 50
zshearsine80216b	7	1	J100H41416a	20	3
zshearsine80216c	7	1	J100H41416b	14	1
zshearsine80216d	6	5	J100H41416c	7	1
zshearsine80216e	7	1	J100H41416d	13	1
zshearsine80216f	7	1	J100H41416e	10	4
zshearsine80216g	7	4	J100H41416f	10	1
zshearsine80216h	6	1	J100H41416g	8	1
zshearsine80316a	10	1	zshearsine42116a	18	7
zshearsine80316b	6	1	zshearsine42116b	10	9
			zshearsine42116c	19	7
			zshearsine42116d	18	6
AVG	7	1.8	AVG	13.4	3.7
SD	1.2	1.6	SD	4.7	3.0
k Range					
First 50 Cycles	j-level	Transient Region	First 50 Cycles	j-level	Transient Region
	5	0 to 6		5	0 to 11
	6	0 to 11		6	0 to 21
	7	0 to 22		7	0 to 42
	8	0 to 44		8	0 to 84
Last 50 Cycles	j-level	Transient Region	Last 50 Cycles	j-level	Transient Region
	5	0 to 2		5	0 to 3
	6	0 to 3		6	0 to 6
	7	0 to 6		7	0 to 12
	8	0 to 12		8	0 to 24

Table 118: Length of transient region in the first and second set of 50 cycles at 10% and 25% displacement a deformation frequency of 125 Hz.

Length of Transient Region (number of cycles)		
10% displacement		
Test Name	First 50	Last 50
zshearsine82216b	16	2
zshearsine82216c	23	8
zshearsine82216d	16	1
zshearsine82216e	20	16
zshearsine82216f	20	8
zshearsine82216g	17	14
zshearsine82216h	19	1
zshearsine82316a	16	15
zshearsine82316b	18	4
AVG	18.3	7.7
SD	2.4	6.1
k Range		
First 50 Cycles	j-level	Transient Region
	6	0 to 46
	7	0 to 92
Last 50 Cycles	j-level	Transient Region
	6	0 to 19
	7	0 to 38

Appendix D   Example of Fourier Transform

A simple example is the Fourier transform of the time function

$$h(t) = \begin{cases} 0 & t < 0 \\ e^{-at} & t \geq 0 \end{cases}$$

into frequency space, by (1).

$$H(f) \;=\; \int_{-\infty}^{\infty} h(t) e^{2\pi i f t}\, \mathrm{d}t \tag{29}$$

$$=\; \int_{0}^{\infty} e^{-at} e^{2\pi i f t}\, \mathrm{d}t \tag{30}$$

$$=\; \int_{0}^{\infty} e^{-(a+2\pi f i)t}\, \mathrm{d}t \tag{31}$$

$$=\; \lim_{x\to\infty} \frac{-1}{a+2\pi f i} e^{-(a+2\pi f i)t} \Big|_{t=0}^{t=x} \tag{32}$$

$$=\; \frac{-1}{a+2\pi f i}\left(\lim_{x\to\infty} e^{-(a+2\pi f i)x} - e^{-(a+2\pi f i)0}\right) \tag{33}$$

$$=\; \frac{-1}{a+2\pi f i}(0 - 1) \tag{34}$$

$$=\; \frac{1}{a+2\pi f i} \tag{35}$$

$$=\; \frac{a-2\pi f i}{a^2 - (2\pi f i)^2} \tag{36}$$

$$=\; \frac{a-2\pi f i}{a^2 + (2\pi f)^2} \tag{37}$$

which has a magnitude equal to $(a^2 + (2\pi f)^2)^{-1/2}$.

Appendix E Proof of Discrete Inverse Fourier Transform

To prove that (3) and (4) are inverses, substitute (3) into (4).

$$\frac{1}{N}\sum_{n=0}^{N-1}\left(\sum_{k=0}^{N-1}h_r e^{2\pi irn/N}\right)e^{-2\pi ikn/N} \tag{38}$$

$$=\sum_{n=0}^{N-1}\sum_{k=0}^{N-1}\frac{1}{N}h_r e^{-i(2\pi n/N)(k-r)} \tag{39}$$

$$=\sum_{k=0}^{N-1}\left(\sum_{n=0}^{N-1}e^{-i(2\pi n/N)(k-r)}\right)\frac{1}{N}h_r. \tag{40}$$

The magnitude of

$$e^{i2\pi k/N}=\cos(2\pi k/N)+i\sin(2\pi k/N) \tag{41}$$

is one, therefore $e^{i2\pi k/N}$ lies on the unit circle in the complex plane. Equation (42) always sums to zero. Figure (48) helps to visualize that $e^{i2\pi n/N}=-e^{i2\pi(1/2+n/N)}=e^{i(\pi+n2\pi/N)}$ for $1\le n\le N-1$ since $e^{i\pi}$ is -1. The $(k-r)2\pi$ term is always some multiple of 2π, since $k-r$ is an integer.

$$\left(\sum_{n=0}^{N-1}e^{-i(2\pi n/N)(k-r)}\right)=0 \quad\text{for}\quad k\ne r. \tag{42}$$

When $k=r$, equation (43) sums to N. Equation (43) is equal to N because e^0 is equal to 1, which is summed N times.

$$\left(\sum_{n=0}^{N-1}e^{-i(2\pi n/N)(k-r)}\right)=N \quad\text{for}\quad k=r. \tag{43}$$

Therefore, the sum in (40) equals h_k.

An alternative proof of the discrete Fourier transform inverses is shown by equation (44). The range of the transform is an n-dimensional complex vector space with basis vectors of $e^{2\pi ikn/N}$ $(n=0,1,\ldots,N-1)$ with each H_n being represented by a sum of constants times those complex numbers. In order for the basis vectors to be orthonormal, the dot product must equal one, however, in this case, the dot product is equal to N. Therefore, it is necessary to divide the inverse Fourier transform by $1/N$ to normalize the basis vectors.

$$u_k^T u_k^* = \sum_{n=0}^{N-1}\left(e^{2\pi ikn/N}\right)\left(e^{2\pi i(-k)n/N}\right)=N\delta_{kk} \tag{44}$$

where u_k^* is the complex conjugate $H(-f)$. Equation (44) shows why it is necessary to have the $1/N$ factor before the summation in (4) to define the inverse Fourier
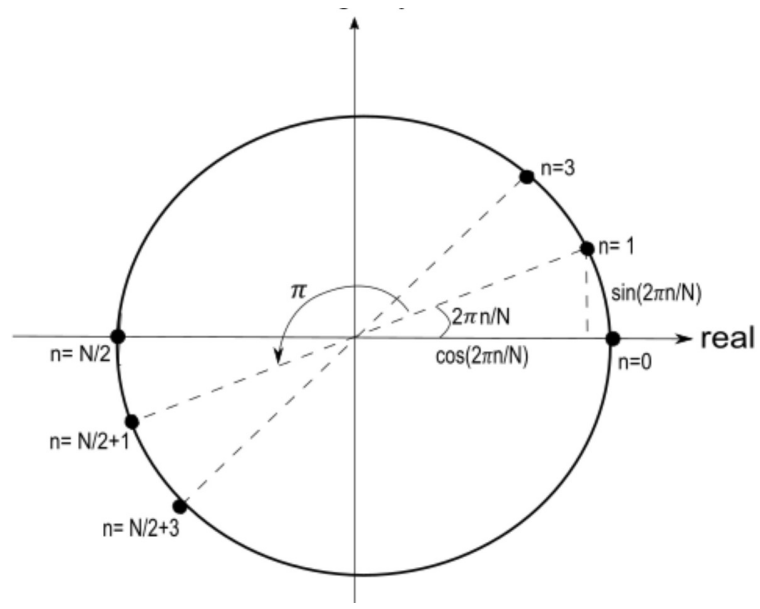
Figure 48: Graph of the unit circle in a complex plane. $e^{-2\pi n/N}$ is plotted to show geometrically that $e^{2\pi n/N} = e^{i(\pi+2\pi n/N)}$.

transform.

References

[1] O'Neil, M. E., Carlson, K., and Storzbach, D. (2013). Complications of Mild Traumatic Brain Injury in Veterans and Military Personnel: A Systematic Review. Washington DC: Department of Veterans Affairs (US).

[2] Whittall, K. P., Mackay, A. L., Graeb, D. A., Nugent, R. A., Li, D. K., and Paty, D. W. (1997). In vivo measurement ofT2 distributions and water contents in normal human brain. *Magnetic Resonance in Medicine*, 37(1), 34-43. doi:10.1002/mrm.1910370107

[3] Przekwas, A., Somayaji, M. R., and Gupta, R. K. (2016). Synaptic Mechanisms of Blast-Induced Brain Injury. *Frontiers in Neurology*, 7, 2. http://doi.org/10.3389/fneur.2016.00002

[4] Haslach, H. W., Jr., Gipple, J. M., and Leahy, L. N. (2017). Influence of high deformation rate, brain region, transverse compression, and specimen size on rat brain shear stress morphology and magnitude. *Journal of the Mechanical Behavior of Biomedical Materials*, 68, 88-102. doi:10.1016/j.jmbbm.2017.01.036

[5] Haslach, H. W., Jr., Leahy, L. N., Riley, P., Gullapalli, R., Xu, S., and Hsieh, A. H. (2014). Solid-extracellular fluid interaction and damage in the mechanical response of rat brain tissue under confined compression. *Journal of the Mechanical Behavior of Biomedical Materials*, 29, 138-150. doi:10.1016/j.jmbbm.2013.08.027

[6] Haslach, H. W., Leahy, L. N., and Hsieh, A. H. (2015). Transient solidfluid interactions in rat brain tissue under combined translational shear and fixed compression. *Journal of the Mechanical Behavior of Biomedical Materials*, 48, 12-27. doi:10.1016/j.jmbbm.2015.04.003

[7] Rodriguez, U. A., Zeng, Y., Deyo, D., Parsley, M. A., Hawkins, B. E., Prough, D. S., and Dewitt, D. S. (2018). Effects of Mild Blast Traumatic Brain Injury on

Cerebral Vascular, Histopathological, and Behavioral Outcomes in Rats. Journal of Neurotrauma, 35(2), 375-392. doi:10.1089/neu.2017.5256

[8] Iliff, J., Wang, M., Liao, Y., Plogg, B., Peng, W., Gundersen, G., Benveniste, H., Vates, G., Deane, R., Goldman, S., Nagelhus, E., and Nedergaard, M. (2012). A paravascular pathway facilitates CSF flow through the brain parenchyma and the clearance of interstitial solutes, including Amyloid Beta. *Science Translational Medicine*, 4, 1-10.

[9] Press, W. H., Flannery, B. P., Teukolsky, S. A., and Vetterling, W. T. (1986). Numerical recipes (2nd ed., Vol. 1). Cambridge: Cambridge Univ. Pr.

[10] Newland, D.E. (1994). Wavelet Analysis of Vibration, Part I: Theory and Part II: Wavelet Maps. *Journal of Vibration and Acoustics*, 116, 409-425.

[11] Gao, R. X., and Yan, R. (2011). *Wavelets theory and applications for manufacturing.* New York: Springer. doi:10.1007/978-1-4419-1545-0-2.

[12] Dremin, I. M., Ivanov, O. V., and Nechitailo, V. A. (2001). Wavelets and their uses. *Physics-Uspekhi*, 44(5), 447-478. doi:10.1070/pu2001v044n05abeh000918

[13] Kozachenko, Y., Olenko, A., and Polosmak, O. (2014). Uniform Convergence of Compactly Supported Wavelet Expansions of Gaussian Random Processes. *Communications in Statistics - Theory and Methods*, 43(10-12), 2549-2562. doi:10.1080/03610926.2013.784338

[14] Strang, G., and Nguyen, T. (2009). *Wavelets and filter banks.* Wellesley, MA: Wellesley-Cambridge.

[15] Lee, D. T., and Yamamoto, A. (1994). Wavelet Analysis and Its Applications. *Wavelets: Theory, Algorithms, and Applications Wavelet Analysis and Its Applications*, 44-52. doi:10.1016/b978-0-08-052084-1.50001-6

[16] Newland, D. E. (1993). Harmonic Wavelet Analysis. *Proceedings of the Royal Society A: Mathematical, Physical and Engineering Sciences*, 443, 203-225.

[17] Bonel-Cerdan, J. I., and Nikolajsen, J. L. (1997). An Introduction to Harmonic Wavelet Analysis of Machine Vibrations. *Manufacturing Materials and Metallurgy; Ceramics; Structures and Dynamics; Controls, Diagnostics and Instrumentation*, 4. doi:10.1115/97-gt-058

[18] Kim, D. S., Choi, H. J., Yang, J. S., Cho, Y. J., and Kang, S. H. (2015). Radiologic Determination of Corpus Callosum Injury in Patients with Mild Traumatic Brain Injury and Associated Clinical Characteristics. *Journal of Korean Neurosurgical Society*, 58(2), 131136. http://doi.org/10.3340/jkns.2015.58.2.131

[19] Morell, P., and Quarles, R. H. (1999). Characteristic Composition of Myelin. In *Basic Neurochemistry: Molecular, Cellular and Medical Aspects* (6th ed.). Philadelphia: Lippincott-Raven. Available from: https://www.ncbi.nlm.nih.gov/books/NBK28221/

[20] University of Utah: Health Sciences (2105). Animal Models for Addiction Research. Retrieved November 10, 2017, from http://learn.genetics.utah.edu/content/addiction/mice/

[21] Ouyang, H., Nauman, E., and Shi, R. (2013). Contribution of cytoskeletal elements to the axonal mechanical properties. *Journal of Biological Engineering*, 7(1), 21. doi:10.1186/1754-1611-7-21

[22] The Effects of Psilocybin On Empathy. (n.d.). Retrieved February 16, 2018, from https://www.macalester.edu/projects/UBNRP/Website The Effects Of Psilocybin On Empathy/part1.html

[23] Reddy, L. V., Koirala, S., Sugiura, Y., Herrera, A. A., and Ko, C. (2003). Glial Cells Maintain Synaptic Structure and Function and Promote Development of

the Neuromuscular Junction In Vivo. *Neuron*, 40(3), 563-580. doi:10.1016/s0896-6273(03)00682-2

[24] Von Batheld, C. S., Bahney, J., and Herculano-Houzel, S. (2016). The search for true numbers of neurons and glial cells in the human brain: A review of 150 years of cell counting. *Journal of Comparative Neurology*, 524(18), 3865-3895. doi:10.1002/cne.24040

[25] Araque, A., and Navarrete, M. (2010). Glial cells in neuronal network function. *Philosophical Transactions of the Royal Society B: Biological Sciences*, 365(1551), 23752381. http://doi.org/10.1098/rstb.2009.0313

[26] Brain Anatomy. (n.d.). Retrieved from http://www.nxdomain.nl/ anja/brains/he rsenen.html

[27] Assi, H., Candolfi, M., Lowenstein, P. R., and Castro, M. G. (2012). Rodent Glioma Models: Intracranial Stereotactic Allografts and Xenografts. In *Animal Models of Brain Tumors* (Vol. 77). Totowa, NJ: Humana Press.

[28] Verkman, A. S. (2013). Diffusion in the extracellular space in brain and tumors. *Physical Biology*, 10(4), 045003. doi:10.1088/1478-3975/10/4/045003

[29] Jessen, N. A., Munk, A. S. F., Lundgaard, I., and Nedergaard, M. (2015). The Glymphatic System A Beginners Guide. *Neurochemical Research*, 40(12), 25832599. http://doi.org/10.1007/s11064-015-1581-6

[30] Iliff, J. J., Wang, M., Liao, Y., Plogg, B. A., Peng, W., Gundersen, G. A., Benveniste, H., Vates, G.E., Deane, R., Goldman, S.A., Nagelhus, E.A., and Nedergaard, M. (2012). A Paravascular Pathway Facilitates CSF Flow Through the Brain Parenchyma and the Clearance of Interstitial Solutes, Including Amyloid Beta. *Science Translational Medicine*, 4(147), 147ra111. http://doi.org/10.1126/scitranslmed.3003748

[31] Iliff, J. J., Wang, M., Zeppenfeld, D. M., Venkataraman, A., Plog, B. A., Liao, Y., Deane, R., and Nedergaard, M. (2013). Cerebral Arterial Pulsation Drives Paravascular CSF-Interstitial Fluid Exchange in the Murine Brain. *Journal of Neuroscience*, 33(46), 18190-18199. doi:10.1523/jneurosci.1592-13.2013

[32] Leahy, L. N., and Haslach, H. W. (2018). Time-frequency analyses of fluidsolid interaction under sinusoidal translational shear deformation of the viscoelastic rat cerebrum. *Mechanics of Time-Dependent Materials*, 22(1). doi:10.1007/s11043-017-9348-x

[33] Hocke, L. M., Duszynski, C. C., Debert, C. T., Dleikan, D., and Dunn, J. F. (2018). Reduced Functional Connectivity in Adults with Persistent Post-Concussion Symptoms: A Functional Near-Infrared Spectroscopy Study. *Journal of Neurotrauma*, 35(11), 1224-1232. doi:10.1089/neu.2017.5365

[34] Hughes, D., Jackson, A., Mason, D., Berry, E., Hollis, S., and Yates, D. (2004). Abnormalities on magnetic resonance imaging seen acutely following mild traumatic brain injury: Correlation with neuropsychological tests and delayed recovery. *Neuroradiology*, 46(7). doi:10.1007/s00234-004-1227-x

[35] Lannsjo, M., Backheden, M., Johansson, U., Geijerstam, J. L., and Borg, J. (2012). Does head CT scan pathology predict outcome after mild traumatic brain injury? *European Journal of Neurology*, 20(1), 124-129. doi:10.1111/j.1468-1331.2012.03813.x

[36] Sosa, M. A., Gasperi, R. D., Paulino, A. J., Pricop, P. E., Shaughness, M. C., Maudlin-Jeronimo, E., Hall, A.A., Janssen, W.G/M., Yuk, F.J., Dorr, N.P., Dickstein, D.L., Mccarror, R.M., Chavko, M., Hof, P.R., Ahlers, S.T., and Elder, G. A. (2013). Blast overpressure induces shear-related injuries in the brain

of rats exposed to a mild traumatic brain injury. *Acta Neuropathologica Communications*, 1(1), 51. doi:10.1186/2051-5960-1-51

[37] Girgis, F., Pace, J., Sweet, J., and Miller, J. P. (2016). Hippocampal Neurophysiologic Changes after Mild Traumatic Brain Injury and Potential Neuromodulation Treatment Approaches. *Frontiers in Systems Neuroscience*, 10, 8. http://doi.org/10.3389/fnsys.2016.00008

[38] Traub, R. D., Miles, R., Muller, R. U., and Gulyas, A. I. (1992). Functional organization of the hippocampal CA3 region: Implications for epilepsy, brain waves and spatial behaviour. *Network: Computation in Neural Systems*, 3(4), 465-488. doi:10.1088/0954-898x34009

[39] Hjornevik, T., Leergaard, T. B., Darine, D., Moldestad, O., Dale, A. M., Willoch, F., and Bjaalie, J. G. (2007). Three-dimensional atlas system for mouse and rat brain imaging data. *Frontiers in Neuroinformatics*, 1. doi:10.3389/neuro.11.004.2007

[40] Anand, K. S., and Dhikav, V. (2012). Hippocampus in health and disease: An overview. Annals of Indian Academy of Neurology, 15(4), 239246. http://doi.org/10.4103/0972-2327.104323

[41] Ouyang, Y., Ning, S., Adler, J.R., Maciver, B., Knox, S.J., and Giffard, R.G. (2017). Alteration of Interneuron Immunoreactivity and Autophagic Activity in Rat Hippocampus after Single High-Dose Whole-Brain Irradiation. *Cureus*, 9(6). doi:10.7759/cureus.1414

[42] What are Brainwaves? (n.d.). Retrieved October 3, 2017, from http://www.brainworksneurotherapy.com/what-are-brainwaves

[43] Buzsaki, G. (2002). Theta Oscillations in the Hippocampus. *Neuron*, 33(3), 325-340. doi:10.1016/s0896-6273(02)00586-x

[44] Ranade, S., Syeda, R., and Patapoutian, A. (2015). Mechanically Activated Ion Channels. *Neuron*, 88(2), 433. doi:10.1016/j.neuron.2015.10.016

[45] Tufail, Y., Matyushov, A., Baldwin, N., Tauchmann, M. L., Georges, J., Yoshihiro, A., Tillery, S.I.H., and Tyler, W. J. (2010). Transcranial Pulsed Ultrasound Stimulates Intact Brain Circuits. *Neuron*, 66(5), 681-694. doi:10.1016/j.neuron.2010.05.008

[46] Dommelen, J. V., Sande, T. V., Hrapko, M., and Peters, G. (2010). Mechanical properties of brain tissue by indentation: Interregional variation. *Journal of the Mechanical Behavior of Biomedical Materials*, 3(2), 158-166. doi:10.1016/j.jmbbm.2009.09.001

[47] Arbogast, K. B., and Margulies, S. S. (1998). Material characterization of the brainstem from oscillatory shear tests. *Journal of Biomechanics*, 31(9), 801-807. doi:10.1016/s0021-9290(98)00068-2

[48] Johnson, C. L., Mcgarry, M. D., Gharibans, A. A., Weaver, J. B., Paulsen, K. D., Wang, H., and Georgiadis, J. G. (2013). Local mechanical properties of white matter structures in the human brain. *NeuroImage*, 79, 145-152. doi:10.1016/j.neuroimage.2013.04.089

[49] Haldar, K., and Pal, C. (2018). Rate dependent anisotropic constitutive modeling of brain tissue undergoing large deformation. *Journal of the Mechanical Behavior of Biomedical Materials*, 81, 178-194. doi:10.1016/j.jmbbm.2017.12.021

[50] Panzer, M. B., Myers, B. S., Capehart, B. P., and Bass, C. R. (2012). Development of a Finite Element Model for Blast Brain Injury and the Effects of CSF Cavitation. *Annals of Biomedical Engineering*, 40(7), 1530-1544. doi:10.1007/s10439-012-0519-2

[51] Diani, J., Brieu, M., and Vacherand, J. (2006). A damage directional constitutive model for Mullins effect with permanent set and induced anisotropy. *European Journal of Mechanics - A/Solids*, 25(3), 483-496. doi:10.1016/j.euromechsol.2005.09.011

[52] Blanchard, A. F., and Parkinson, D. (1952). Breakage of Carbon-Rubber Networks by Applied Stress. *Rubber Chemistry and Technology*, 25(4), 808-842. doi:10.5254/1.3543444

[53] Essen, D. C. (1997). A tension-based theory of morphogenesis and compact wiring in the central nervous system. *Nature*, 385(6614), 313-318. doi:10.1038/385313a0

[54] Catheline, S., Gennisson, J., Tanter, M., and Fink, M. (2003). Observation of Shock Transverse Waves in Elastic Media. *Physical Review Letters*, 91(16). doi:10.1103/physrevlett.91.164301